

# PNAS

[www.pnas.org](http://www.pnas.org)

Supplementary Information for

**A de novo strategy to develop NIR precipitating fluorochrome for long-term in situ cell membrane bioimaging**

Ke Li<sup>a</sup>, Yifan Lyu<sup>a</sup>, Yan Huang<sup>a</sup>, Shuai Xu<sup>a</sup>, Hong-Wen Liu<sup>a</sup>, Lanlan Chen<sup>b</sup>, Tian-Bing Ren<sup>a</sup>, Mengyi Xiong<sup>a</sup>, Shuangyan Huan<sup>a</sup>, Lin Yuan<sup>a</sup>, Xiao-Bing Zhang<sup>a,\*</sup>, and Weihong Tan<sup>a</sup>

Email: [xbzhang@hnu.edu.cn](mailto:xbzhang@hnu.edu.cn)

**This PDF file includes:**

- Experimental section
- Synthesis section
- Schemes S1 to S4
- Figures S1 to S83
- Tables S1 to S21
- SI References

## Experimental Section

**Materials and instruments.** Solvents and reagents of the best grade available were supplied by Qingdao Ocean Chemicals (Qingdao, China), Beyotime Biotechnology, Sigma-Aldrich, Bide Pharmaceutical Technology, Abcam, and SANTA CRUZ BIOTECHNOLOGY INC, and were used without further purification unless noted otherwise. Column chromatography was employed over silica gel (100-200 mesh), and thin-layer chromatography (TLC) was executed using silica gel 60 F254 plates. Water was purified and doubly distilled by a Milli-Q system (Millipore, USA). Fluorescence measurements were conducted at room temperature on a Hitachi F-4600 spectrofluorometer (Tokyo, Japan) with both excitation and emission slit set at 10.0 nm. NMR spectra were recorded on a Bruker DRX-400 spectrometer at 100 MHz for  $^{13}\text{C}$  NMR and 400 MHz for  $^1\text{H}$  NMR, using TMS as an internal standard. Mass spectra were performed using a Matrix Assisted Laser Desorption Ionization Time of Flight Mass Spectrometry (ultrafleXtreme). DAPI (D4055) was obtained from US. Everbright® Inc. Bcy-GGT was obtained from Jiang's group (1). L-Glutamic acid  $\gamma$ -(7-amido-4-methylcoumarin) (AMCG) was purchased from Sigma-Aldrich (G7261). Folate-PEG5000-CY 5.5 was purchased from Tanshui Biotechnology. Synthesis of all new compounds is described in Scheme S1-S4.

**DFT Calculations.** To describe the excited state of the fluorophores 2-(2-hydroxyphenyl)quinazolin-4(3H)-one (HPQ-H), HPQ1, HPQ-N and HPQ2, TD-DFT (time-dependent density functional theory) calculations were performed. All calculations and DFT-optimized structures were carried out using the Gaussian 09 program package. All geometries of these fluorophores were optimized at B3LYP/6-31+G level using a CPCM solvation model with water as the solvent. Molecular orbital (MO) plots and MO energy levels were computed at the same theoretical level.

**Spectrophotometric Experiments.** Fluorescence measurement experiments were carried out in 10 mM Tris-buffered saline (1% glycerol, TBS; 10 mM Tris-HCl and 0.15 M NaCl, pH 7.4) buffer solution containing 5% DMSO as the co-solvent. UV-Vis absorption experiments were carried out in DMSO or glycerol: PBS = 1:1. Fluorescence emission spectra were recorded at an excitation wavelength of 450 nm with emission wavelength ranging from 550 to 800 nm. Solutions of various species were prepared from L-lysine, L-glutamate, L-valine, L-isoleucine, L-threonine, L-tyrosine, L-tryptophan, phenylalanine, arginine, glucose,  $\text{CaCl}_2$ , BSA, NaClO,  $\text{H}_2\text{O}_2$ ,  $\text{Zn}(\text{NO}_3)_2$ ,  $\text{FeSO}_4$ ,  $\text{FeCl}_3$ ,  $\text{MgCl}_2$ , GSH, cathepsin B, monoamine oxidase, alkaline phosphatase, leucine aminopeptidase, and sulfatase in deionized water. The test solution was composed of HYPQG (5  $\mu\text{M}$ ) in 1 mL of 10 mM TBS buffer. The resulting solutions were cultured at 37  $^\circ\text{C}$  for 40 min, followed by measurement of fluorescence spectra. All the filtration experiments were performed by using 0.22  $\mu\text{m}$  filter.

**Kinetics Assay of Probe HYPQG.** The enzyme reaction for kinetics study of HYPQG was performed at a series of the final concentrations (2-20  $\mu\text{M}$ ) and hydrolyzed by GGT (80 U/L). The reaction was monitored by measuring fluorescence change at 650 nm (excited at 450 nm) at 37  $^\circ\text{C}$  for 40 min. Initial velocity was calculated from the slope of each progress curve. The parameters  $V_{\text{max}}$  and  $K_m$  with GGT for HYPQG was determined by Lineweaver-Burk plot as shown in Fig. S13. The results were fitted to the Michaelis-Menten equation for calculating the apparent kinetics parameters, as

$$V = V_{\text{max}}[\text{S}]/(K_m + [\text{S}]),$$

where  $[\text{S}]$  = substrate concentration and  $V$  = initial velocity.

**Single crystal.** Crystallization of HPQ from DMF. Crystallization of HPQ4 from dichloromethane (DCM) and hexane.

**Determination of the fluorescence quantum yield.** Fluorescence quantum yield for HYPQ was determined by using cresol purple as reference ( $\Phi_r = 0.58$  in ethanol). The quantum yield was calculated using the following equation:

$$\Phi_s = \Phi_r (A_r F_s / A_s F_r) (n_s^2 / n_r^2)$$

Where, *s* and *r* denote sample and reference, respectively. *A* is the absorbance at the excitation wavelength. *F* is the relative integrated fluorescence intensity and *n* is the refractive index of the solvent.  $\Phi$  is the fluorescence quantum yield. The solid-state fluorescence quantum yield of HYPQ was determined in an integrating sphere.

**Molecule docking.** Docking simulation was operated by using SYBYL (X-2.1). Here, the X-ray crystallographic structure of Alkaline Phosphatase (PDB entry 3tg0) (2) and Glutamyl Transpeptidase 1 (PDB entry 4zcg) (3) were selected for docking analysis. The structure of the probe HYPQG, AMCG and HTPQG was assigned with Gasteiger-Huckel charges. Other parameters were set at default values.

**Cytotoxicity Study.** To study cytotoxicity, A2780, OVCAR3, NIH3T3 and HepG2 cells were seeded onto 96-well plates ( $6 \times 10^3$  cells per well per 200  $\mu$ L of medium), respectively, and incubated for 24 h before treatment, followed by exposure to different concentrations (0-30  $\mu$ M, 1% DMSO) of the HYPQG probe for 6 h, followed by washing with Dulbecco's Phosphate Buffered Saline (DPBS) and incubating for an additional 24 h. Finally, cell viability was measured by 3-(4,5-dimethylthiazol-2-yl)-5-(3-carboxymethoxyphenyl)-2-(4-sulfophenyl)-2H-tetrazolium (MTS) assay, and the absorbance value was measured at 490 nm using a microplate reader.

As shown in Fig. S21, the fluorescence signal gradually reached a plateau within 70 s under 365 nm irradiation, which indicated that the probe was highly sensitive in light. In view of the phototoxicity of UV-light in cell experiments, we also measured the response time of the probe in living cells under blue light (450 nm ~ 470 nm, 18 W) irradiation. The fluorescence signal in cells gradually increased and reached a plateau under blue light irradiation for 2 min, which suggested that we could test the HYPQ toxicity by using this HYPQ-photoactivatable probe.

To study cytotoxicity, A2780, OVCAR3, NIH3T3 and HepG2 cells were seeded in 96-well plates ( $6 \times 10^3$  cells per well per 200  $\mu$ L of medium), respectively, and incubated the HYPQ-photoactivatable probe (0-30  $\mu$ M, 1% DMSO) for 1 h and then washed with Dulbecco's Phosphate Buffered Saline (DPBS), followed by irradiating under blue light for 2 min and incubating for additional 24 h. Finally, cell viability was measured by 3-(4,5-dimethylthiazol-2-yl)-5-(3-carboxymethoxyphenyl)-2-(4-sulfophenyl)-2H-tetrazolium (MTS) assay, and the absorbance value was measured at 490 nm using a microplate reader.

**Flow Cytometry Analysis.** Flow cytometry (BD FACS Calibur) was employed to determine endogenous GGT with the HYPQG probe. A2780, OVCAR3 and NIH3T3 cells in a 6-well plate were precultured for 24 h, respectively, and then treated with HYPQG (5  $\mu$ M) for 40 min. A2780 cells in a 6-well plate were precultured for 24 h and treated with 1 mM of 6-Diazo-5-oxo-L-norleucine (DON) for 1 h, followed by incubation with the HYPQG probe for 40 min. After incubation, the cells were treated with trypsin, washed with DPBS and subjected to flow cytometry analysis. The fluorescence signal was determined by counting 10,000 events in an FL-7 detector by flow cytometry.

**Immunofluorescence Assays.** A2780 and OVCAR3 cells were incubated on a 25 mm Petri dish for 24 h, respectively. The medium was removed, and the cells were washed twice with DPBS (1 mL each). Then, the cells were fixed with 4% paraformaldehyde (500  $\mu$ L per well) for 15 min at room temperature. The 4% paraformaldehyde was removed, and the cells were washed three times with DPBS. Proteins were blocked with 5% BSA in DPBS for 4 h at room temperature. GGT was detected by a 1 mL of GGT antibody (Anti-GGT/GGT antibody, ab55138, obtained from Abcam; dilution 1:500) in 1% BSA in DPBS for 1 h at room temperature. The cells were washed three times with DPBS and labeled with 0.5 mL of secondary antibody (m-IgGk BP-CFL 488, sc-516176, obtained from SANTA CRUZ BIOTECHNOLOGY, INC; dilution 1:100) in DPBS for 2 h at room temperature. Cells were then treated with DAPI (D4055, obtained from U.S. Everbright® Inc.) in DPBS for 0.5 h at room temperature. Finally, the cells were washed three times with DPBS, and the immunofluorescence imaging was performed on a laser confocal microscope (Nikon, Japan). All images and channels were placed at the same settings.

**Western Blotting Analysis.** A2780, OVCAR3 and HepG2 cells were placed in a 25 cm<sup>2</sup> flask and cultured for 24 h, respectively. The medium was removed, and the cells were washed twice with DPBS (1mL each). After that, the cells were treated with M-PER buffer (no.78501, Thermo Fisher Scientific) containing protease inhibitors (no. B14001, Biotool) and lysed for 30 min at 0 °C. The lysates were gathered and centrifuged for 15 min to collect the supernatant (500 × g). The protein concentration of supernatant was measured by a NanoDrop 2000/2000c (Thermo). All proteins were separated by SDS-PAGE and then transferred to a nitrocellulose membrane. The membrane was divided into two parts and then treated with GGT antibodies and GAPDH antibodies (sc-47724, obtained from SANTA CRUZ BIOTECHNOLOGY, INC.; dilution 1:10000) for 12 hours at 4 °C, respectively, followed by incubating with a secondary antibody for 2 hours at room temperature. Finally, the GGT was visualized on ChemiDoc XRS+ with Image Lab software (Bio-RAD).

**Fluorescence microscopy imaging in live cells.** To investigate the capability of HYPQG probe for detection of GGT activity in living cells, cells were first cultured in 1640 medium supplemented with 100 U/mL penicillin, 100 U/mL streptomycin and 10% fetal bovine serum at 37 °C with 5 wt %/vol CO<sub>2</sub> for 24 h before the experiment. Then the media were removed from each well, and cells were washed with DPBS. After that, the cells were cultured with 5 μM of HYPQG in DPBS buffer for 40 min (1% DMSO) at 37 °C, washed with DPBS, and imaged. To confirm that fluorescence enhancement was triggered by the catalysis of GGT, cells were cultured in DPBS buffer containing 1 mM of DON for 1 hour and then treated with HYPQG (5 μM) for another 40 min. Confocal fluorescence imaging of cells was obtained on a confocal laser scanning microscope (Nikon, Japan). Image analysis was performed by using ImageJ.

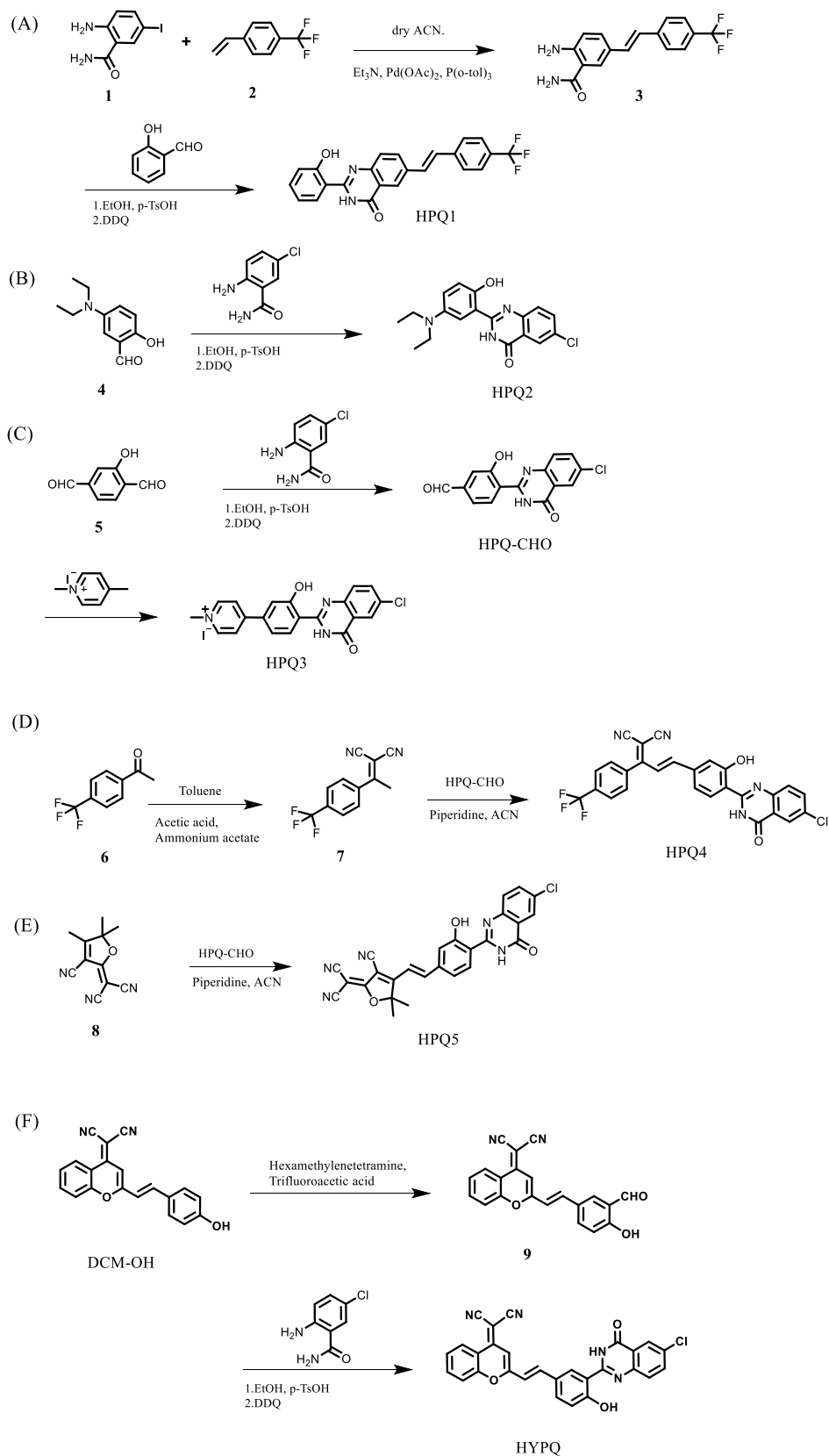
**Long-term imaging experiments.** A2780 cells were plated in 24 Petri dishes (25 mm) and cultured for 24 h, respectively. The medium was removed, and the cells were washed with DPBS (1mL each). After that, the cells were treated with 5 μM of HYPQG in DPBS buffer for 40 min, 70 min, 100 min, 160 min, 220 min, 280 min, 340 min and 400 min (1% DMSO) at 37 °C, respectively, and then washed with DPBS and imaged. Cells were treated with 5 μM of Memb-Tracker Green or Memb-Tracker Red for 10 min, 40 min, 70 min, 130 min, 190 min, 250 min, 310 min and 370 min (1% DMSO) at 37 °C and then washed with DPBS and imaged. HepG2 cells were plated in 8 Petri dishes (25 mm) and cultured for 24 h, respectively. The medium was removed, and the cells were washed with TBS (1mL each). After that, the cells were treated with 5 μM of HTPQA in TBS buffer for 40 min, 70 min, 100 min, 160 min, 220 min, 280 min, 340 min and 400 min (1% DMSO) at 37 °C, respectively, and then washed with TBS and imaged. All “0 h” fluorescence images were obtained when the fluorescence signal had reached a plateau for each probe, thus ensuring that the long-term imaging experiments were performed under the same conditions.

**Animal model.** Animal procedures were performed in accordance with protocol No. SYXK (Xiang) 2008-0001 approved by the Laboratory Animal Center of Hunan. Male BALB/c homozygous athymic mice (~3 weeks old, 16~18 g) were obtained from Hunan SJA Laboratory Animal Co., Ltd. and used under protocols approved by Hunan University Laboratory Animal Center. Nude mice were kept in a pathogen-free environment and housed in sterile cages with airflow hoods.

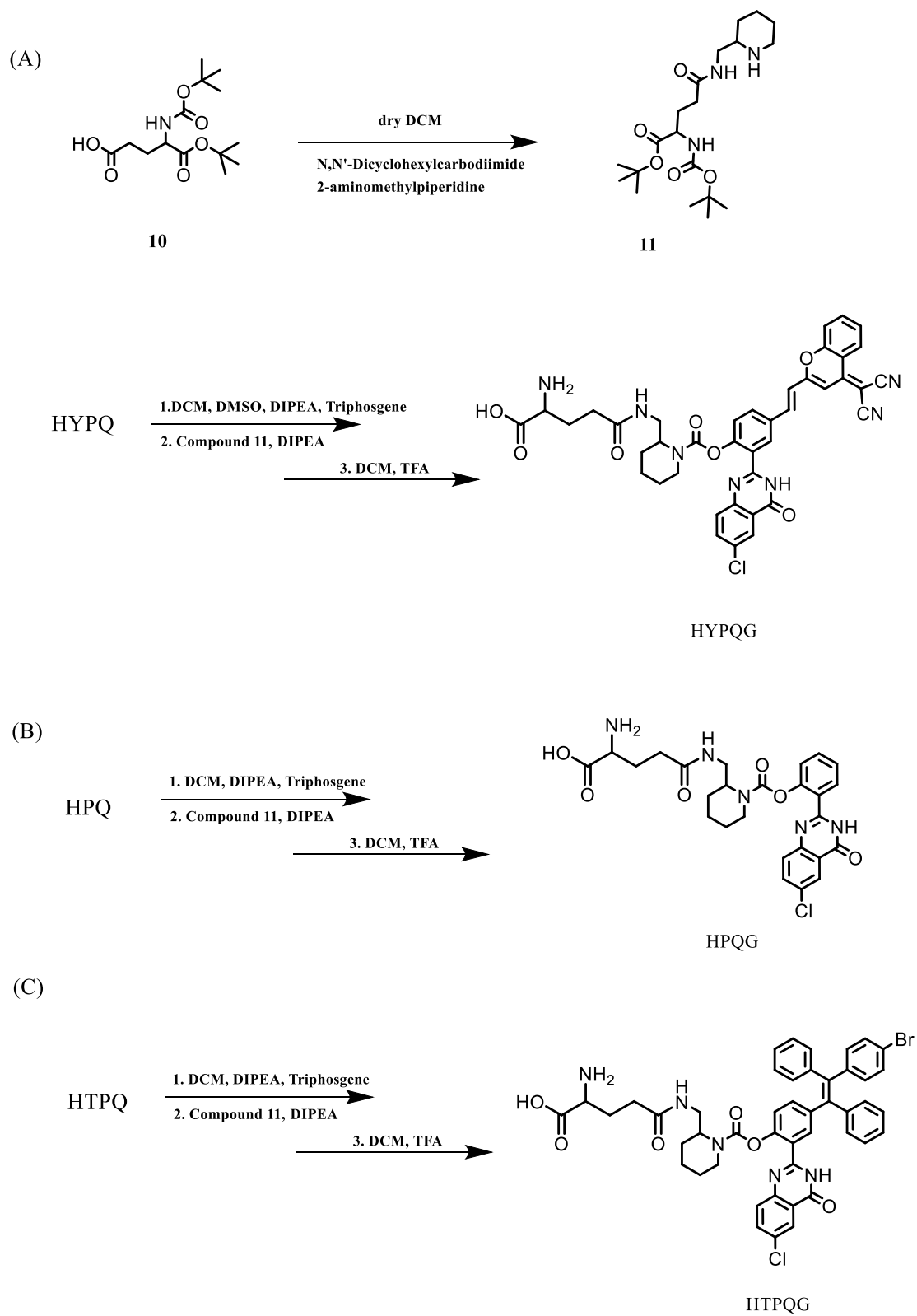
To generate the A2780 murine tumor model, 5×10<sup>7</sup> A2780 cells in 100 μL DPBS were subcutaneously injected in the right flanks of each mouse. Diameter of tumors is ca. 5 mm.

**In vivo imaging.** Before *in vivo* imaging, mice were anesthetized by inhalation of 5% isoflurane in 100% oxygen. Nude mice were imaged using a Caliper VIS Lumina XR small animal optical *in vivo* imaging system. The concentration of the injected solution was 20 μM (25 μL, PBS/DMSO = 8:2, pH = 7.4). For *in vivo* imaging: HYPQ and DCMG: λ<sub>ex</sub> = 535 nm, Bcy-GGT and Folate-PEG5000-CY 5.5: λ<sub>ex</sub> = 640 nm, and Cy5.5 filter was chosen as the all emission channel.

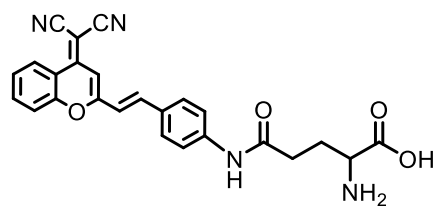
## Synthesis Section



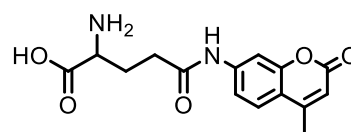
**Scheme S1.** Synthetic routes of HPQ1, HPQ2, HPQ3, HPQ4, HPQ5 and HYPQ.



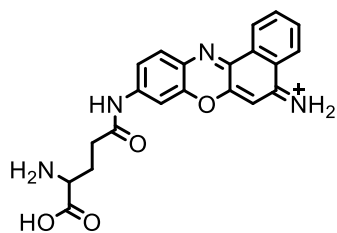
**Scheme S2.** Preparation of probe HYPQG, HPQG and HTPQG.



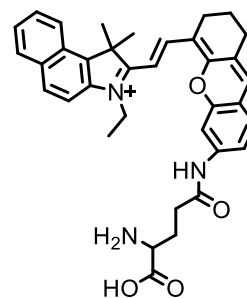
DCMG



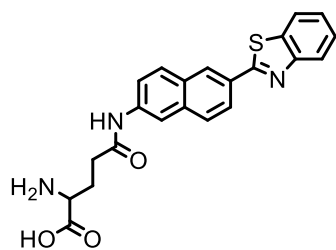
AMCG



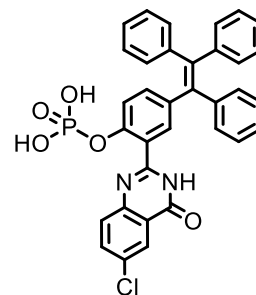
Cv-Glu



Bey-GGT

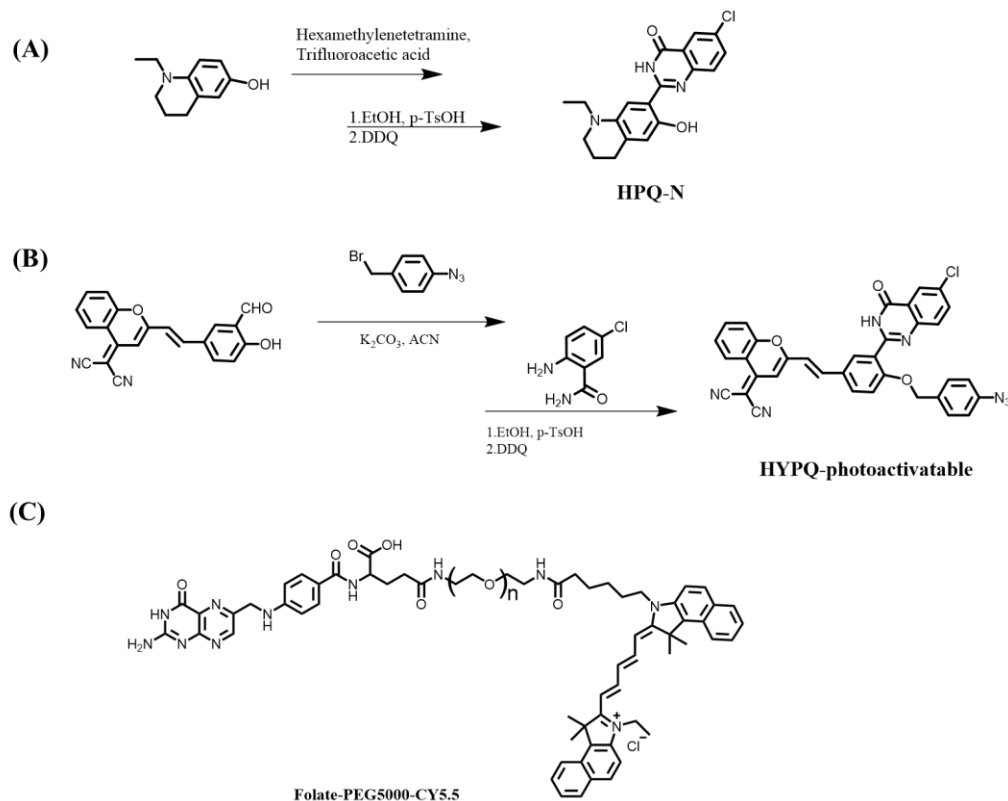


Np-Glu



HTPQA

**Scheme S3.** Preparation of the control probes.



**Scheme S4.** Preparation of the control fluorophore (A) or probes (B) and (C).

**(E)-2-amino-5-(4-(trifluoromethyl) styryl) benzamide (3).**

2-amino-5-iodobenzamide (131.0 mg, 0.5 mmol), 1-(trifluoromethyl)-4-vinylbenzene (258.0 mg, 1.5 mmol) and Et<sub>3</sub>N (255.0 mg, 2.5 mmol) were dissolved in 10 mL of anhydrous ACN. Then Pd(OAc)<sub>2</sub> (12.6 mg, 0.05 mmol) and P(o-tol)<sub>3</sub> (46.0 mg, 0.1 mmol) were added. The flask was sealed, and the solution was stirred at 120 °C for 5 hours. Reaction was monitored by TLC (DCM: EtOH 40:1). Upon completion, the reaction mixture was diluted with DCM and washed with saturated NH<sub>4</sub>Cl. The organic phase was dried over Na<sub>2</sub>SO<sub>4</sub> and concentrated under reduced pressure. The residue was purified by column chromatography on silica gel (DCM: EtOH 50:1). The product was obtained as a white solid (78.0 mg, 51% yield). <sup>1</sup>H NMR (400 MHz, Methanol-*d*<sub>4</sub>) δ 7.8 (s, 1H), 7.7 (d, *J* = 8.2 Hz, 2H), 7.6 (d, *J* = 8.3 Hz, 2H), 7.5 (d, *J* = 7.5 Hz, 1H), 7.2 (d, *J* = 6.4 Hz, 1H), 7.1 (d, *J* = 6.4 Hz, 1H), 6.8 (d, *J* = 8.6 Hz, 1H). <sup>13</sup>C NMR (101 MHz, Chloroform-*d*) δ 171.3, 141.2, 136.3, 130.9, 130.3, 128.5, 127.2, 126.1, 125.6, 125.2, 123.9, 119.4, 117.8. MALDI-TOF/MS, *m/z*: calcd for [C<sub>16</sub>H<sub>13</sub>F<sub>3</sub>N<sub>2</sub>O+H<sup>+</sup>] 307.1, found 307.8.

**(E)-2-(2-hydroxyphenyl)-6-(4-(trifluoromethyl) styryl) quinazolin-4(3H)-one (HPQ1).**

Compound 3 (52.0 mg, 0.17 mmol) was dissolved in absolute EtOH to give a red solution to which salicylaldehyde (18 μL, 0.17 mmol) was added at room temperature. This reaction mixture was heated to reflux for 30 min, and then *p*-TsOH monohydrate (0.02 equiv.) was added, and reflux was continued for 2 h. The yellow suspension was cooled to room temperature, and then 2,3-dichloro-5,6-dicyano-1,4-benzoquinone (DDQ, 1.01 equiv.) was added in several portions, and the reaction mixture was further stirred overnight at room temperature. The precipitate was filtered, washed three times with absolute EtOH, and then twice with diethyl ether. It was finally air dried to yield a beige powder showing strong green fluorescence under a UV lamp (56.9 mg, 82% yield). <sup>1</sup>H NMR (400 MHz, DMSO-*d*<sub>6</sub>) δ 13.7 (s, 1H), 12.5 (s, 1H), 8.3 (s, 1H), 8.2 (s, 1H), 8.2 (d, *J* = 8.3 Hz, 1H), 7.9 (d, *J* = 7.7 Hz, 2H), 7.8 – 7.7 (m, 3H), 7.6 (q, *J* = 6.5 Hz, 2H), 7.5 (d, *J* = 7.6 Hz, 1H), 7.0 (d, *J* = 8.2 Hz, 1H), 6.9 (d, *J* = 7.5 Hz, 1H). <sup>13</sup>C NMR (101 MHz, DMSO-*d*<sub>6</sub>) δ 161.7, 160.4, 153.7, 148.1, 146.4, 141.4, 135.7, 134.2, 133.2, 130.4, 128.7, 128.1, 128.0, 127.6, 127.1, 126.0, 124.8, 121.5,



119.3, 118.4, 114.3, 113.8, 83.1. MALDI-TOF/MS, *m/z*: calcd for [C<sub>23</sub>H<sub>15</sub>F<sub>3</sub>N<sub>2</sub>O<sub>2</sub>+H<sup>+</sup>] 409.1, found 409.3.

**6-chloro-2-(5-(diethylamino)-2-hydroxyphenyl) quinazolin-4(3H)-one (HPQ2).**

Compound HPQ2 was synthesized following a procedure similar to that of HPQ1. The crude product was recrystallized in EtOH to yield compound HPQ2 as a yellow solid (230.0 mg, 0.67 mmol) in 92% yield. <sup>1</sup>H NMR (400 MHz, DMSO-*d*<sub>6</sub>) δ 10.2 (s, 1H), 8.1 – 8.0 (m, 1H), 7.8 (dd, *J* = 8.8, 2.5 Hz, 1H), 7.6 (d, *J* = 8.7 Hz, 1H), 7.2 (s, 1H), 6.6 (s, 1H), 6.5 – 6.3 (m, 1H), 6.1 (d, *J* = 2.5 Hz, 1H), 3.5 (s, 4H), 1.1 (d, *J* = 6.5 Hz, 6H). <sup>13</sup>C NMR (101 MHz, DMSO-*d*<sub>6</sub>) δ 163.0, 154.9, 143.6, 135.3, 131.8, 130.6, 129.9, 129.2, 125.5, 121.3, 114.8, 112.8, 104.3, 100.8, 98.2, 44.3, 13.0, 11.2. MALDI-TOF/MS, *m/z*: calcd for [C<sub>18</sub>H<sub>18</sub>ClN<sub>3</sub>O<sub>2</sub>+H<sup>+</sup>] 344.1, found 344.1.

**4-(4-(6-chloro-4-oxo-3,4-dihydroquinazolin-2-yl)-3-hydroxyphenyl)-1-methylpyridin-1-ium iodide (HPQ3).**

HPQ-CHO (150.0 mg, 0.50 mmol), 1,4-dimethylpyridin-1-ium iodide (235.0 mg, 1.0 mmol) and piperidine (0.8 mL) were dissolved in ACN (20 mL) under nitrogen protection. The resultant mixture was refluxed for 6 h, followed by extraction with DCM. The organic layers were dried over Na<sub>2</sub>SO<sub>4</sub> and concentrated under reduced pressure. The crude product was recrystallized in EtOH and then purified by column chromatography on silica gel (DCM: EtOH 20:1) to yield compound HPQ3 as a yellow solid (88.4 mg, 36% yield). <sup>1</sup>H NMR (400 MHz, DMSO-*d*<sub>6</sub>) δ 9.9 (s, 1H), 8.9 (d, *J* = 6.2 Hz, 2H), 8.8 (s, 1H), 8.2 (d, *J* = 6.1 Hz, 2H), 8.1 (d, *J* = 5.6 Hz, 2H), 8.0 (d, *J* = 6.3 Hz, 1H), 7.8 (dd, *J* = 8.2, 14.2 Hz, 5H), 7.2 (d, *J* = 8.5 Hz, 1H), 4.3 (s, 3H). <sup>13</sup>C NMR (101 MHz, DMSO-*d*<sub>6</sub>) δ 190.6, 179.1, 153.3, 145.2, 140.4, 135.3, 134.2, 132.6, 128.5, 128.1, 125.3, 123.4, 122.4, 121.5, 120.0, 118.9, 98.5, 89.1, 68.2, 27.0. MALDI-TOF/MS, *m/z*: calcd for C<sub>20</sub>H<sub>15</sub>ClN<sub>3</sub>O<sub>2</sub> 390.8, found 390.4.

**2-(1-(4-(trifluoromethyl) phenyl) ethylidene) malononitrile (7).**

1-(4-(trifluoromethyl) phenyl) ethan-1-one (90.0 mg, 0.50 mmol) and dicyanopropane (132.0 mg, 2.0 mmol) were dissolved in toluene (20 mL) with acetic acid (0.20 mL) and ammonium acetate (154.0 mg, 2.0 mmol) under nitrogen protection. The resultant mixture was refluxed for 5 h, followed by extraction with DCM. The organic layers were dried over Na<sub>2</sub>SO<sub>4</sub> and concentrated under reduced pressure. The crude product was purified by column chromatography on silica gel (PE: DCM 5:1) to yield compound **7** as a white solid (43.7 mg, 37% yield). <sup>1</sup>H NMR (400 MHz, Chloroform-*d*) δ 7.8 (d, *J* = 8.1 Hz, 2H), 7.7 (d, *J* = 8.0 Hz, 2H), 2.7 (s, 3H). <sup>13</sup>C NMR (101 MHz, CDCl<sub>3</sub>) δ 173.8, 139.2, 133.8, 133.5, 127.7, 126.2, 124.6, 121.9, 112.0, 86.7, 68.2, 31.9, 30.3, 29.7, 24.4, 22.7, 14.1. ESI/MS, *m/z*: calcd for [C<sub>12</sub>H<sub>7</sub>F<sub>3</sub>N<sub>2</sub>-H] 235.1, found 235.1.

**(E)-2-(3-(4-(6-chloro-4-oxo-3,4-dihydroquinazolin-2-yl)-3-hydroxyphenyl)-1-(4-(trifluoromethyl) phenyl) allylidene) malononitrile (HPQ4).**

HPQ-CHO (150.0 mg, 0.50 mmol) and 2-(1-(4-(trifluoromethyl) phenyl) ethylidene) malononitrile (236.0 mg, 1.0 mmol) were dissolved in ACN (20 mL) with piperidine (0.8 mL) under nitrogen protection. The resultant mixture was refluxed for 8 h, followed by extraction with DCM. The organic layers were dried over Na<sub>2</sub>SO<sub>4</sub> and concentrated under reduced pressure. The crude product was purified by column chromatography on silica gel (DCM: EtOH 80:1) to yield compound HPQ4 as a yellow solid (101 mg, 39% yield). <sup>1</sup>H NMR (400 MHz, DMSO-*d*<sub>6</sub>) δ 8.51 (s, 1H), 8.0 (d, *J* = 8.6 Hz, 2H), 7.8 (d, *J* = 8.0 Hz, 3H), 7.8 (d, *J* = 8.5 Hz, 3H), 7.5 (d, *J* = 9.2 Hz, 1H), 7.2 (s, 1H), 7.0 (s, 1H), 6.8 (d, *J* = 5.8 Hz, 1H), 6.7 (s, 1H). <sup>13</sup>C NMR (101 MHz, DMSO-*d*<sub>6</sub>) δ 170.1, 160.9, 153.9, 149.2, 135.5, 134.5, 131.8, 130.5, 130.1, 128.7, 126.4, 125.5, 122.9, 122.5, 119.9, 114.7, 114.4, 113.5, 35.6, 31.7, 29.5, 29.5, 29.1, 29.0, 27.0, 25.6, 22.5, 14.4. MALDI-TOF/MS, *m/z*: calcd for C<sub>27</sub>H<sub>14</sub>ClF<sub>3</sub>N<sub>4</sub>O<sub>2</sub> 518.1, found 518.1.

**(E)-2-(4-(4-(6-chloro-4-oxo-3,4-dihydroquinazolin-2-yl)-3-hydroxystyryl)-3-cyano-5,5-dimethylfuran-2(5H)-ylidene) malononitrile (HPQ5).**

2-(3-cyano-4,5,5-trimethylfuran-2(5H)-ylidene) malononitrile was synthesized following the procedure previously described (5). HPQ5 was synthesized following the same procedure as that for HPQ4. The crude product was recrystallized in EtOH to yield compound HPQ5 as a yellow solid

(46.5 mg, 26% yield). <sup>1</sup>H NMR (400 MHz, DMSO-*d*<sub>6</sub>) δ 8.1 (dd, *J* = 4.1, 2.2 Hz, 1H), 7.9 – 7.9 (m, 1H), 7.7 (d, *J* = 8.8 Hz, 2H), 7.5 (d, *J* = 8.0 Hz, 3H), 7.1 (d, *J* = 7.7 Hz, 3H), 2.3 (s, 6H). <sup>13</sup>C NMR (101 MHz, DMSO-*d*<sub>6</sub>) δ 159.7, 159.3, 141.2, 138.3, 136.1, 132.3, 128.5 (m), 125.9, 124.6, 121.5, 99.9, 21.2, 20.1. MALDI-TOF/MS, *m/z*: calcd for C<sub>26</sub>H<sub>16</sub>ClN<sub>5</sub>O<sub>3</sub> 481.1, found 481.0.

**(E)-2-(2-(3-formyl-4-hydroxystyryl)-4H-chromen-4-ylidene) malononitrile (9).**

DCM-OH was synthesized following the previously described procedure (6). DCM-OH (156.0 mg, 0.50 mmol) and hexamethylenetetramine (84.0 mg, 0.60 mmol) were dissolved in trifluoroacetic acid (5.0 mL) under nitrogen protection. The resultant mixture was refluxed for 5 h, followed by hydrolysis with 4 mol HCl for 2 h at 100 °C. The precipitate was filtered, washed three times with diethyl ether and finally air dried to yield a black powder. The black solid was purified by column chromatography on silica gel (DCM: EA 100:1) to yield compound **9** as a yellow solid (34 mg, 20% yield). <sup>1</sup>H NMR (400 MHz, Chloroform-*d*) δ 11.3 (s, 1H), 10.2 (s, 1H), 9.0 – 8.9 (m, 1H), 7.8 (s, 2H), 7.7 (d, *J* = 7.2 Hz, 1H), 7.6 – 7.5 (m, 2H), 7.5 (t, *J* = 7.3 Hz, 1H), 7.1 (d, *J* = 9.3 Hz, 1H), 6.9 (s, 1H), 6.8 (d, *J* = 5.9 Hz, 1H). <sup>13</sup>C NMR (101 MHz, DMSO-*d*<sub>6</sub>) δ 190.4, 168.6, 163.3, 158.9, 155.0, 153.4, 152.5, 138.5, 135.8, 129.1, 126.8, 125.0, 123.3, 119.5, 118.8, 118.1, 117.7, 117.5, 116.3, 106.7, 60.2. MALDI-TOF/MS, *m/z*: calcd for [C<sub>21</sub>H<sub>12</sub>N<sub>2</sub>O<sub>3</sub>+H<sup>+</sup>] 341.1, found 341.9.

**(E)-2-(2-(3-(6-chloro-4-oxo-3,4-dihydroquinazolin-2-yl)-4-hydroxystyryl)-4H-chromen-4-ylidene) malononitrile (HYPQ).**

Compound **9** (34.0 mg, 0.1 mmol) was dissolved in EtOH (15 mL) and DCM (5 mL) to give a yellow solution to which 2-amino-5-chlorobenzamide (25.0 mg, 0.15 mmol) was added at room temperature. This reaction mixture was heated to reflux for 30 min, then *p*-TsOH monohydrate (0.02 equiv.) was added, and reflux was continued for 2 h. The red suspension was cooled to room temperature, and then DDQ (1.01 equiv.) was added in several portions. The reaction mixture was further stirred overnight at room temperature. The precipitate was filtered, washed three times with absolute EtOH, then twice with DCM, and finally air dried to yield a dark red powder showing strong red fluorescence under a UV lamp. (14.2 mg, 29% yield). <sup>1</sup>H NMR (400 MHz, DMSO-*d*<sub>6</sub>) δ 8.9 – 8.7 (m, 1H), 8.6 (s, 1H), 8.1 (s, 1H), 7.9 (s, 2H), 7.9 – 7.8 (m, 4H), 7.8 – 7.7 (m, 2H), 7.6 (d, *J* = 7.9 Hz, 1H), 7.4 (s, 1H), 7.1 (d, *J* = 8.8 Hz, 1H), 6.9 (s, 1H). <sup>13</sup>C NMR (101 MHz, DMSO-*d*<sub>6</sub> and pyridine-*d*<sub>5</sub>) δ 189.9, 182.4, 172.8, 161.2, 155.6, 147.6, 136.5, 135.4, 134.6, 134.2, 132.8, 130.0, 128.9, 125.4, 124.7, 124.2, 123.2, 122.7, 121.8, 115.4, 44.2. ESI/MS, *m/z*: calcd for [C<sub>28</sub>H<sub>15</sub>ClN<sub>4</sub>O<sub>3</sub>-H] 489.1, found 489.3.

**Tert-butyl N2-(tert-butoxycarbonyl)-N5-(piperidin-2-ylmethyl) glutamate (11).**

To an ice-cold suspension of Boc-Glu-OtBu (303.0 mg, 1 mmol) and hydroxybenzotriazole (150.0 mg, 1.1 mmol) in dry DCM (20 mL) was added dropwise a solution of N,N'-dicyclohexylcarbodiimide (227.0 mg, 1.1 mmol), and the mixture was stirred for 15 min. Then 2-aminomethylpiperidine (114.0 mg, 1mmol) was added dropwise to the reaction mixture. After 24 h stirring at room temperature, the colorless solid material 1,3-dicyclohexylurea was filtered off. The filtrate was washed with sat. NaHCO<sub>3</sub> and then extracted several times with a solution of HCl at pH = 3. DCM (100 mL) was added to the combined acidic aqueous layers which were then treated with an aqueous solution of 2 M NaOH to reach a pH of 12. This basic aqueous layer was washed twice with DCM, and organic layers were dried with anhydrous Na<sub>2</sub>SO<sub>4</sub> and evaporated under reduced pressure to a yield crude oil. The oil was left at 4 °C overnight, and the remaining crystallized 1,3-dicyclohexylurea was filtered off, as previously described. Column chromatography (DCM : MeOH = 40 : 1) gave compound **11** (164 mg, 41%) <sup>1</sup>H NMR (400 MHz, Chloroform-*d*) δ 6.7 (d, *J* = 7.3 Hz, 1H), 5.4 (d, *J* = 7.6 Hz, 1H), 4.1 (s, 1H), 3.3 (d, *J* = 8.5 Hz, 1H), 3.2 – 2.9 (m, 2H), 2.8 (s, 1H), 2.7 – 2.5 (m, 2H), 2.2 (t, *J* = 7.2 Hz, 3H), 1.8 (s, 2H), 1.6 (d, *J* = 7.9 Hz, 2H), 1.6 (s, 1H), 1.5 – 1.3 (m, 18H), 1.2 – 1.0 (m, 1H). <sup>13</sup>C NMR (101 MHz, CDCl<sub>3</sub>) δ 172.3, 171.5, 155.9, 123.9, 123.7, 118.6, 111.2, 82.2, 79.8, 55.9, 53.5, 46.5, 45.0, 32.5, 30.2, 29.9, 29.3, 28.3, 27.9, 26.2, 25.9, 24.0. MALDI-TOF/MS, *m/z*: calcd for [C<sub>20</sub>H<sub>37</sub>N<sub>3</sub>O<sub>5</sub>+H<sup>+</sup>] 400.3, found 400.3.

**(E)-N5-((1-((2-(6-chloro-4-oxo-3,4-dihydroquinazolin-2-yl)-4-(2-(4-(dicyanomethylene)-4H-chromen-2-yl) vinyl) phenoxy) carbonyl) piperidin-2-yl) methyl) glutamine (HYPQG).**

HYPQ (49.0 mg, 0.10 mmol) and DIPEA (1 mL) was dissolved in a mixture solution (10 mL dry DCM and 1 mL dry DMSO). The mixture was cooled in an ice bath, then solution of triphosgene (124.0 mg, 0.42 mmol) in dry DCM (1 mL) was injected with vigorous stirring, and the solution was stirred for 40 min at 0 °C, followed by removal of the ice bath. After 12 h stirring at room temperature, a solution of triphosgene (31.0 mg, 0.1 mmol) in dry DCM (1.0 mL) was injected with vigorous stirring, and the solution was stirred again for 12 h at room temperature. The resulting mixture was then evaporated to dryness under reduced pressure, and the volatiles were trapped in a liquid nitrogen trap. The resulting solution was resuspended in dry DCM and cooled to 0 °C before a solution of compound 4 (80.0 mg, 0.2 mmol) in dry DCM was added dropwise, followed by DIPEA (1 mL). The progression of the reaction was followed by TLC (DCM / MeOH, 40:1). The reaction mixture was then diluted with DCM and washed twice with brine and then treated with an aqueous solution of 1 M HCl to reach a pH of 4. The organic solvent was evaporated under reduced pressure to a yield crude solid. The solid was suspended in EtOH (2 mL), and the HYPQ was filtered off and rinsed with EtOH. The organic solvent was evaporated under reduced pressure to a yield crude solid. After that, the mixture was dissolved in TFA (3 mL) and DCM (3 mL) at 0 °C and stirred for 7 h at room temperature. After removal of the solvent from the reaction mixture under reduced pressure, the residue was washed with diethyl ether and dichloromethane, respectively, to obtain a crude yellowed solid. The crude product was purified by preparatory TLC (DCM: MeOH 10:1) to yield compound HYPQG as a yellow solid (9.1 mg, 12% yield). <sup>1</sup>H NMR (400 MHz, DMSO-*d*<sub>6</sub>) δ 8.7 (d, *J* = 8.3 Hz, 1H), 8.5 (s, 1H), 8.1 (s, 1H), 8.1 (s, 1H), 7.9 (t, *J* = 8.1 Hz, 3H), 7.9 – 7.8 (m, 1H), 7.8 – 7.8 (m, 1H), 7.7 (d, *J* = 8.7 Hz, 1H), 7.8 – 7.5 (m, 2H), 7.4 (s, 1H), 7.0 (s, 1H), 4.1 – 3.9 (m, 1H), 3.8 (s, 1H), 3.7 (s, 1H), 3.6 (s, 1H), 3.5 (s, 1H), 2.9 (s, 3H), 2.2 (s, 2H), 1.9 (s, 2H), 1.5 (s, 4H), 1.5 (s, 2H). <sup>13</sup>C NMR (101 MHz, DMSO-*d*<sub>6</sub>) δ 158.2, 153.4, 152.5, 150.6, 137.4, 136.0, 135.1, 132.5, 131.7, 130.3, 128.2, 126.7, 125.4, 125.1, 124.4, 122.7, 120.9, 119.5, 117.5, 116.2, 107.5, 83.4, 70.2, 61.2, 49.3, 29.5, 27.9, 20.5, 19.0, 15.4, 11.60. HRMS, *m/z*: calcd for [C<sub>40</sub>H<sub>34</sub>CIN<sub>7</sub>O<sub>7</sub>+H<sup>+</sup>] 760.2286, found 760.2287.

**N5-((1-((2-(6-chloro-4-oxo-3,4-dihydroquinazolin-2-yl) phenoxy) carbonyl) piperidin-2-yl) methyl) glutamine (HPQG).**

HPQ was synthesized following a previously described procedure (7, 8). To HPQ (65.0 mg, 0.24 mmol) in a two-neck flask under argon were added dry DCM (10 mL) and DIPEA (1 mL), and the mixture was left to cool in an ice bath. A solution of triphosgene (212.0 mg, 0.72 mmol) in dry DCM (3.0 mL) was injected with vigorous stirring, and the solution was stirred for 40 min at 0 °C, followed by removal of the ice bath. The resulting mixture was then evaporated to dryness under reduced pressure, and the volatiles were trapped in a liquid nitrogen trap. The resulting solution was resuspended in dry DCM and cooled to 0 °C before a solution of compound 4 (83.0 mg, 0.24 mmol) in dry DCM was added dropwise, followed by DIPEA (1.0 mL). The progression of the reaction was followed by TLC (DCM / MeOH, 40:1). The reaction mixture was then diluted with DCM and washed twice with brine and then treated with an aqueous solution of 1 M HCl to reach a pH of 4. The organic solvent was evaporated under reduced pressure to a yield a crude solid. The solid was suspended in EtOH (2 mL), and the HPQ was filtered off and rinsed with EtOH. The organic solvent was evaporated under reduced pressure to yield a crude solid. After that, the mixture was dissolved in TFA (5 mL) and DCM (5 mL) at 0 °C and stirred for 7 h at room temperature. After removal of the solvent from the reaction mixture under reduced pressure, the residue was washed with diethyl ether and dichloromethane, respectively, to obtain a crude solid. The crude product was purified by preparatory TLC (DCM: MeOH 10:1) to yield compound HPQG as a white solid (54.7 mg, 42% yield). <sup>1</sup>H NMR (400 MHz, Methanol-*d*<sub>4</sub>) δ 8.3 (d, *J* = 7.9 Hz, 1H), 7.9 (t, *J* = 7.6 Hz, 1H), 7.8 (d, *J* = 7.7 Hz, 1H), 7.8 (d, *J* = 8.2 Hz, 1H), 7.7 (d, *J* = 7.7 Hz, 1H), 7.6 (t, *J* = 7.6 Hz, 1H), 7.5 (t, *J* = 7.5 Hz, 1H), 7.4 (d, *J* = 8.0 Hz, 1H), 4.3 (s, 1H), 3.9 (t, *J* = 6.2 Hz, 1H), 3.8 (s, 1H), 3.5 (q, *J* = 7.0 Hz, 1H), 3.1 (t, *J* = 4.6 Hz, 1H), 2.4 (d, *J* = 6.9 Hz, 2H), 2.1 (d, *J* = 7.6 Hz, 2H), 1.6 – 1.5 (m, 4H), 1.4 (s, 1H), 1.2 (t, *J* = 7.0 Hz, 2H). <sup>13</sup>C NMR (101 MHz, MeOD) δ 172.9, 170.0, 162.9, 161.3, 152.3, 149.0, 134.7, 131.9, 129.8, 127.0, 126.4, 125.9, 125.6, 123.1, 120.5, 115.1, 65.5, 53.4, 52.2, 40.1, 38.1, 31.2, 25.6, 18.4, 14.0. HRMS, *m/z*: calcd for [C<sub>26</sub>H<sub>28</sub>CIN<sub>5</sub>O<sub>6</sub>+H<sup>+</sup>] 542.1806, found 542.1807.

**(E)-N5-((1-((4-(2-(4-bromophenyl)-1,2-diphenylvinyl)-2-(6-chloro-4-oxo-3,4-dihydroquinazolin-2-yl) phenoxy) carbonyl) piperidin-2-yl) methyl) glutamine (HTPQG).**

HTPQG was synthesized following a same procedure as that for HPQG. HTPQ was synthesized following a previously described procedure (9). The crude product was purified by preparatory TLC (DCM: MeOH 10:1) to yield compound HTPQG as a light yellow solid (43% yield). <sup>1</sup>H NMR (400 MHz, DMSO-*d*<sub>6</sub>) δ 12.5 (s, 1H), 8.6 (s, 3H), 8.0 (s, 3H), 7.7 (d, *J* = 7.1 Hz, 2H), 7.7 – 6.5 (m, 12H), 4.3 (s, 1H), 3.9 (s, 1H), 3.6 (s, 1H), 3.3 (s, 2H), 3.1 (s, 4H), 2.8 (m, 4H), 2.5 (s, 1H), 2.2 (s, 1H), 1.9 (s, 1H), 1.4 (m, 2H). <sup>13</sup>C NMR (101 MHz, DMSO-*d*<sub>6</sub>) δ 152.5, 147.8, 147.6, 142.8, 142.6, 140.6, 140.3, 140.16, 134.8, 134.1, 133.0, 132.4, 131.4, 131.0, 128.5, 128.3, 127.4, 126.9, 125.2, 123.1, 122.5, 120.4, 79.7, 79.4, 79.0, 65.3, 49.2, 39.4, 18.9, 15.5, 11.4. HRMS, *m/z*: calcd for [C<sub>46</sub>H<sub>41</sub>BrClN<sub>5</sub>O<sub>6</sub>+H<sup>+</sup>] 847.2009, found 847.2009.

**(E)-N5-(4-(2-(4-(dicyanomethylene)-4H-chromen-2-yl) vinyl) phenyl) glutamine (DCMG).**

DCMG was synthesized following a previously described procedure (10). <sup>1</sup>H NMR (400 MHz, DMSO-*d*<sub>6</sub>) δ 10.5 (s, 1H), 8.7 (d, *J* = 7.6 Hz, 1H), 8.5 (s, 3H), 7.9 (t, *J* = 7.4 Hz, 1H), 7.8 (d, *J* = 8.2 Hz, 1H), 7.7 (d, *J* = 4.5 Hz, 4H), 7.6 (s, 1H), 7.5 (t, *J* = 7.7 Hz, 1H), 7.4 (d, *J* = 6.1 Hz, 1H), 6.9 (s, 1H), 3.9 (t, *J* = 6.2 Hz, 1H), 2.7 – 2.5 (m, 2H), 2.2 – 2.1 (m, 2H). <sup>13</sup>C NMR (101 MHz, DMSO-*d*<sub>6</sub>) δ 171.1, 170.6, 158.8, 158.3, 153.3, 152.6, 141.6, 138.9, 135.8, 130.1, 129.6, 126.5, 125.0, 119.6, 119.1, 118.2, 117.7, 117.5, 116.4, 116.1, 106.7, 60.2, 51.9, 32.2, 26.1. HRMS, *m/z*: calcd for [C<sub>25</sub>H<sub>20</sub>N<sub>4</sub>O<sub>4</sub>+H<sup>+</sup>] 441.1563, found 441.1564.

**6-chloro-2-(1-ethyl-6-hydroxy-1,2,3,4-tetrahydroquinolin-7-yl) quinazolin-4(3H)-one (HPQ-N).**

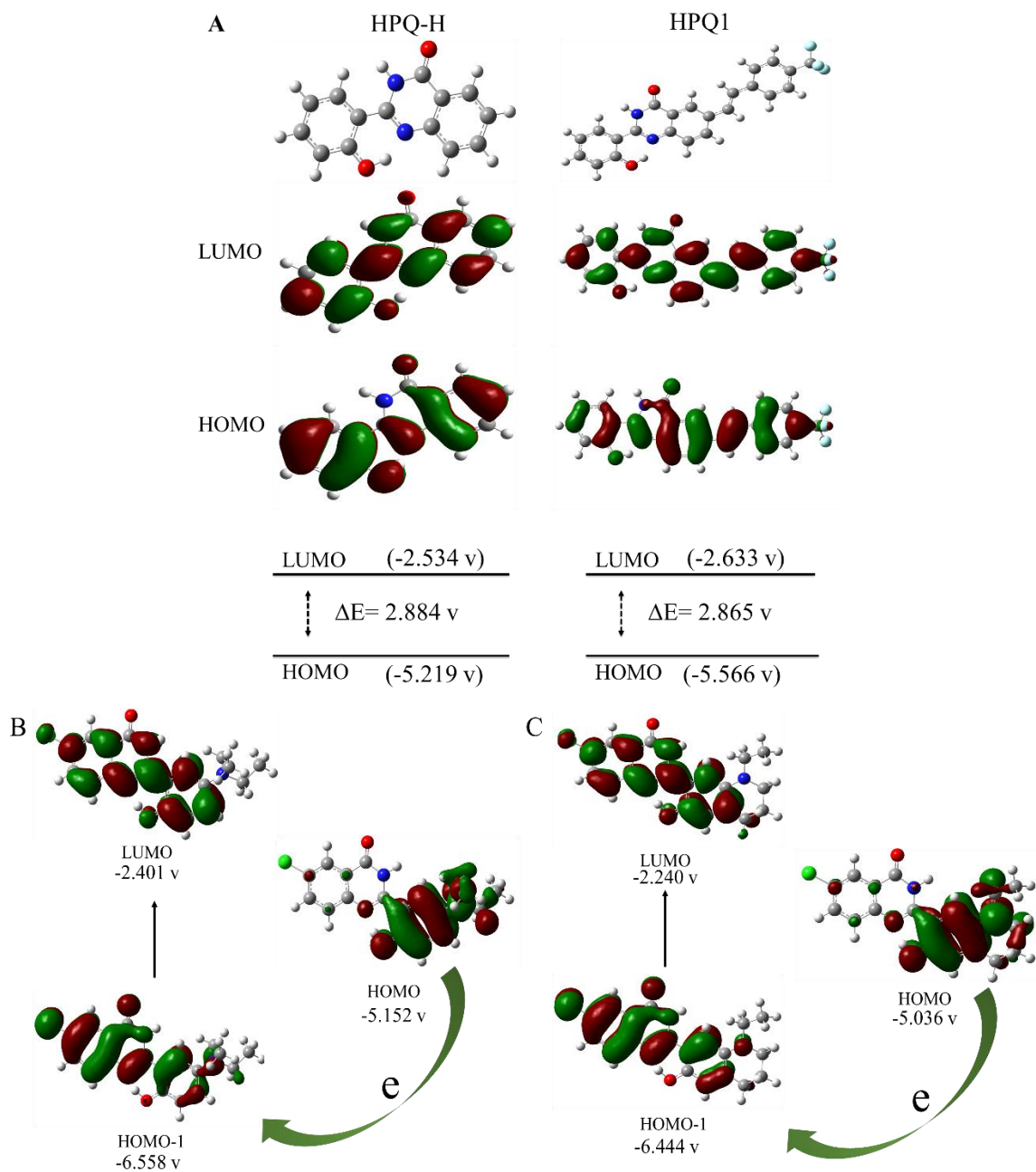
HPQ-N was synthesized following a same procedure as that for HYPQ. <sup>1</sup>H NMR (400 MHz, DMSO-*d*<sub>6</sub>) δ 8.3 (s, 1H), 8.1 (d, *J* = 11.4 Hz, 1H), 7.8 (s, 1H), 7.6 (s, 1H), 7.4 (s, 1H), 3.2 (s, 4H), 1.6 (d, *J* = 9.5 Hz, 4H), 1.3 – 1.2 (m, 3H), 0.9 (d, *J* = 1.6 Hz, 2H). HRMS, *m/z*: calcd for [C<sub>19</sub>H<sub>18</sub>ClN<sub>3</sub>O<sub>2</sub> +H<sup>+</sup>] 356.1166, found 356.1161.

**(E)-2-(2-(4-((4-azidobenzyl)oxy)-3-(6-chloro-4-oxo-3,4-dihydroquinazolin-2-yl)styryl)-4H-chromen-4-ylidene)malononitrile (HYPQ-photoactivatable).**

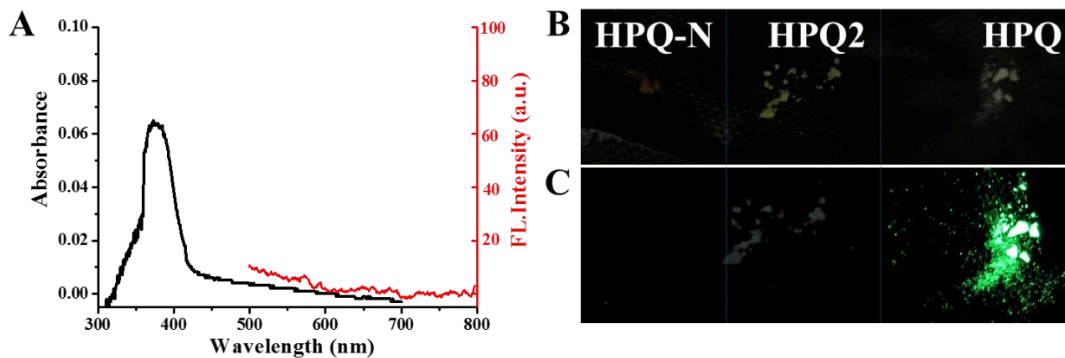
Compound 9 (170.0 mg, 0.5 mmol) was added to a 50 mL flask with a reflux condenser, followed by adding 20 mL acetonitrile. Meanwhile, 210 mg (1.0 mmol) 1-azido-4-(bromomethyl) benzene and 276 mg (2.0 mmol) K<sub>2</sub>CO<sub>3</sub> were added. The resultant mixture was refluxed for 6 h, followed by extraction with DCM. The organic layers were dried over Na<sub>2</sub>SO<sub>4</sub> and concentrated under reduced pressure. Then the mixture was filtered and then diluted with DCM and washed twice with brine. The organic solvent was evaporated under reduced pressure to a yield a crude solid. The crude solid was re-dissolved in absolute EtOH (15 mL) and then 2-amino-5-chlorobenzamide (75.0 mg, 0.45 mmol) was added at room temperature. This reaction mixture was heated to reflux for 30 min, then *p*-TsOH monohydrate (0.02 equiv.) was added, and reflux was continued for 2 h. The suspension was cooled to room temperature, and then DDQ (1.01 equiv.) was added in several portions. The reaction mixture was further stirred overnight at room temperature. Next, the organic solvent was evaporated under reduced pressure to a yield a crude solid, followed by fast column chromatography to obtain the product (petroleum ether /ethyl acetate = 5:2, v / v). <sup>1</sup>H NMR (400 MHz, Chloroform-*d*) δ 8.9 (d, *J* = 8.3 Hz, 2H), 7.8 (t, *J* = 7.9 Hz, 2H), 7.6 (d, *J* = 10.3 Hz, 1H), 7.6 – 7.5 (m, 4H), 6.9 (s, 2H), 6.5 (dd, *J* = 17.4, 10.7 Hz, 2H), 6.4 (d, *J* = 17.3 Hz, 2H), 5.8 (d, *J* = 10.8 Hz, 2H), 5.4 (s, 1H), 4.7 (s, 1H). HRMS, *m/z*: calcd for [C<sub>35</sub>H<sub>20</sub>ClN<sub>7</sub>O<sub>3</sub> +H<sup>+</sup>] 622.1394, found 622.1390.

CV-Glu was synthesized following a previously described procedure (11).

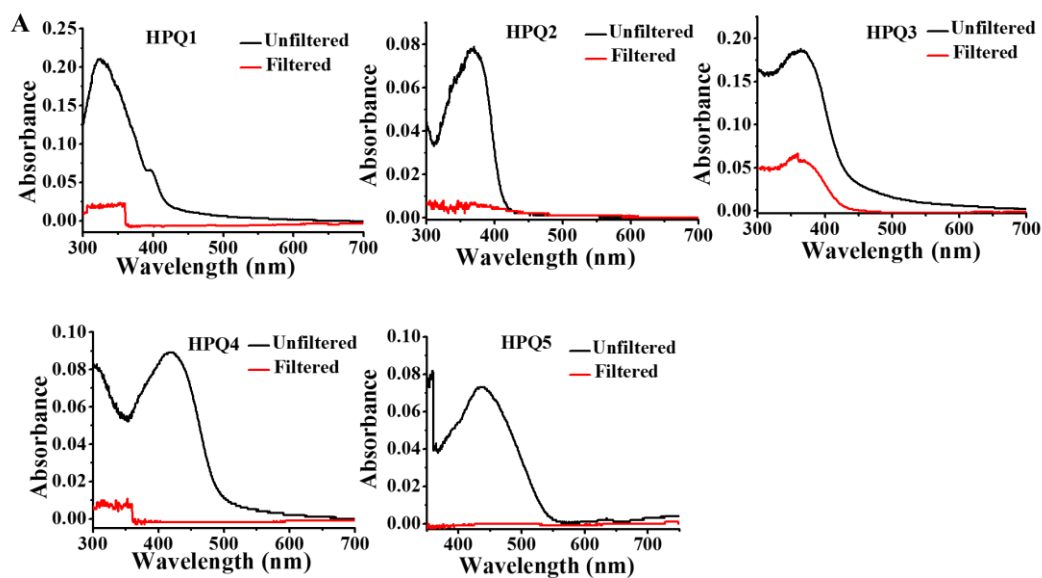
Np-Glu and HTPQA were obtained from our group (12).

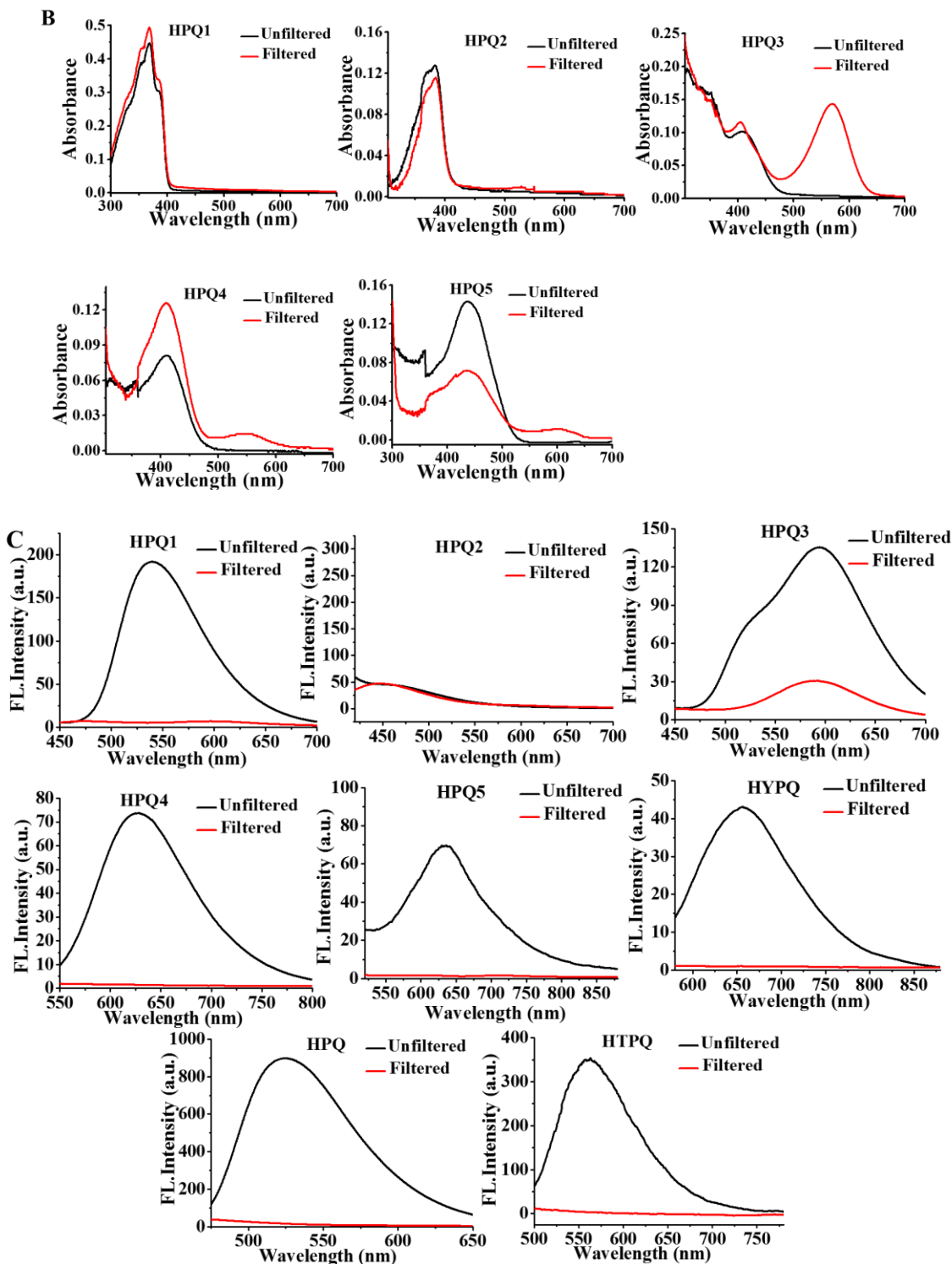


**Fig. S1.** (A) DFT-optimized structures and HOMO/LUMO energy gaps of HPQ-H and HPQ1. Frontier orbitals (LUMO/HOMO) of HPQ2 (B) and HPQ-N (C).



**Fig. S2.** (A) The absorbance/emission spectra of HPQ-N (10  $\mu$ M) in PBS containing 1% DMSO and 10% glycerol. The solid-state fluorescence of HPQ, HPQ2 and HPQ-N before (B) and after (C) under UV lamp at 365 nm irradiation.

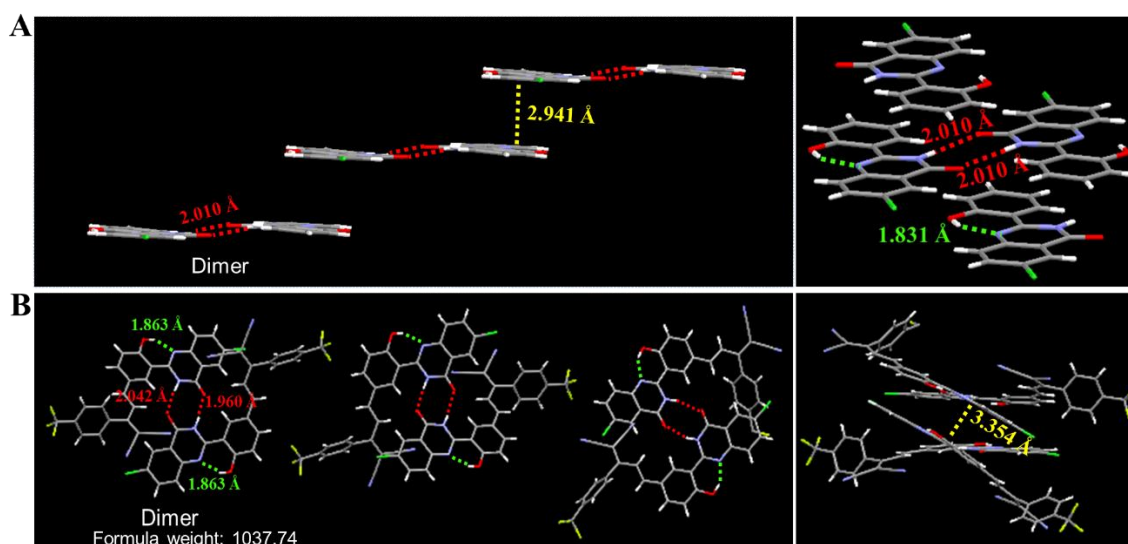




**Fig. S3.** The absorbance spectra of all 10  $\mu\text{M}$  compounds (HPQ1, HPQ2, HPQ3, HPQ4, HPQ5,) in PBS containing 1% DMSO and 10% glycerol (A) or in DCM (B). The fluorescence spectra of all 10  $\mu\text{M}$  compounds (HPQ1, HPQ2, HPQ3, HPQ4, HPQ5, HYPQ, HPQ, HTPQ) in PBS containing 1% DMSO and 10% glycerol. The black lines and red lines indicated the absorbance/fluorescence spectra intensity change of these compounds before and after filtration.


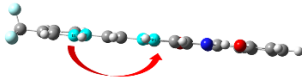
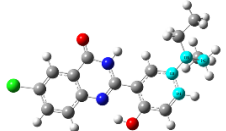
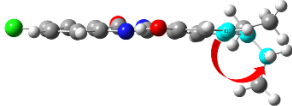
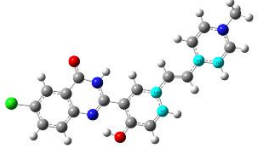
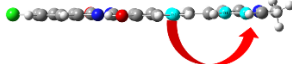
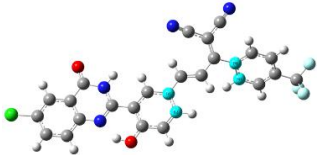
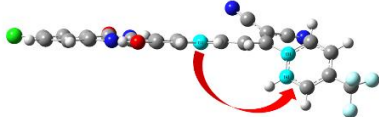
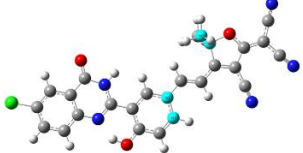
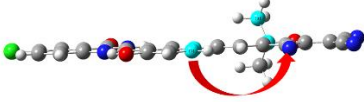
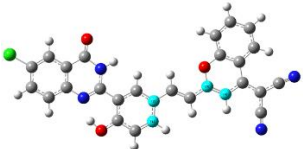
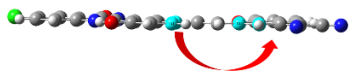
	$\lambda_{\text{Abs/nm}}$	$\lambda_{\text{Em/nm}}$	Stokes shift/nm
HPQ	355	515	160
HPQ1	395	535	140
HPQ2	370	/	/
HPQ3	385	590	205
HPQ4	409	625	216
HPQ5	445	636	191
HYPQ	450	650	200

**Table S1:** The data analysis of absorption/emission of these solid-state fluorophores.

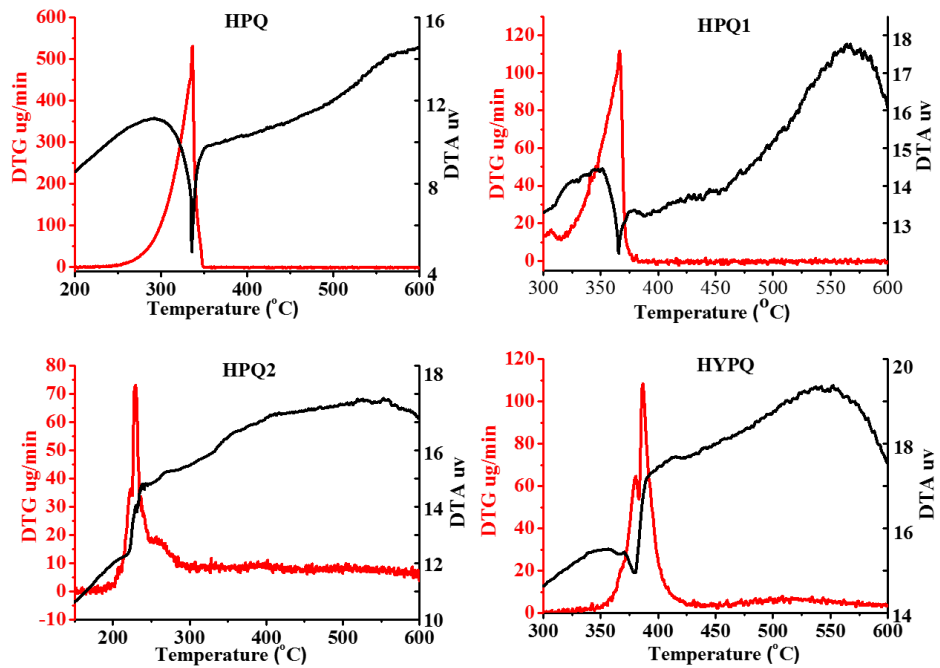


**Fig. S4.** Crystal structures of HPQ (CCDC: 2045408) (A) and HPQ4 (CCDC: 2045423) (B). The green dotted lines indicated the intramolecular hydrogen bond, and the red dotted lines indicated intermolecular H-bonding interactions. The yellow dotted lines indicated the distance between the two dimers in crystals respectively.



Solid-state fluorochrome	Optimized structure	The graphical presentation of the twisted angle between substituted groups and HPQ structure	Twist angle
HPQ1			6.51°
HPQ2			55.96°
HPQ3			1.46°
HPQ4			62.34°
HPQ5			70.74°
HYPQ			0.02°

**Table S2:** The DFT-optimized structures of these solid-state fluorophores.



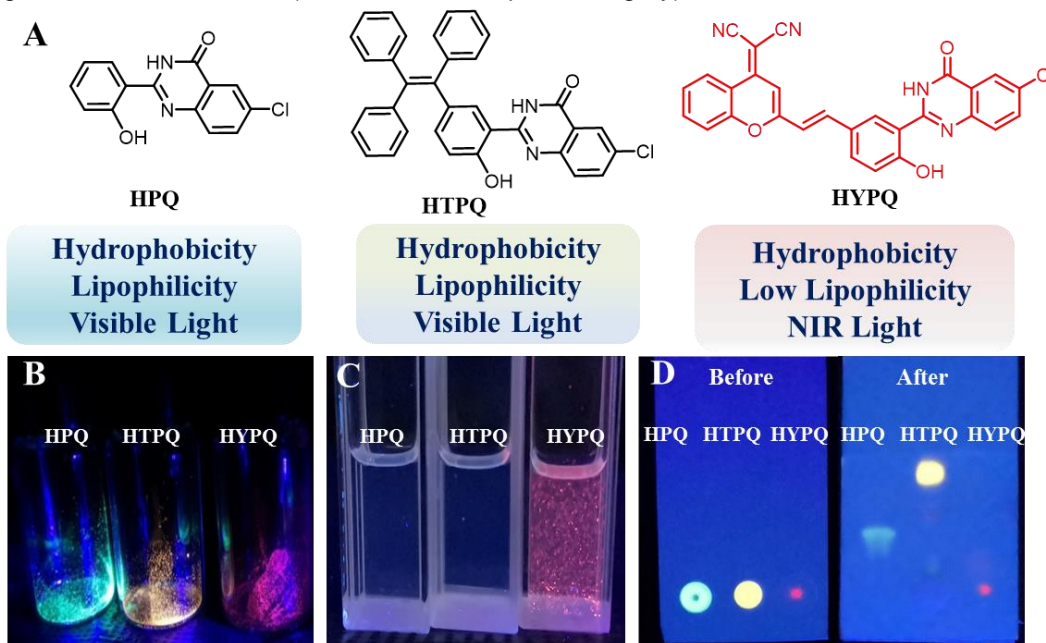
**Fig. S5.** The DTA (black) and TG (red) curves of compounds HPQ, HPQ1, HPQ2 and HYPQ. The DTA measurement was performed with a HENGJIU HCT-4 instrument.

	Chemical Structure	Melting point (°C)
HPQ		336.16
HPQ1		362.31
HPQ2		231.26
HPQ3		364.15
HPQ4		123.24
HPQ5		240.60
HYPQ		386.79

**Table S3:** The melting point of these solid-state fluorophores was obtained from the TG-DTA curves.

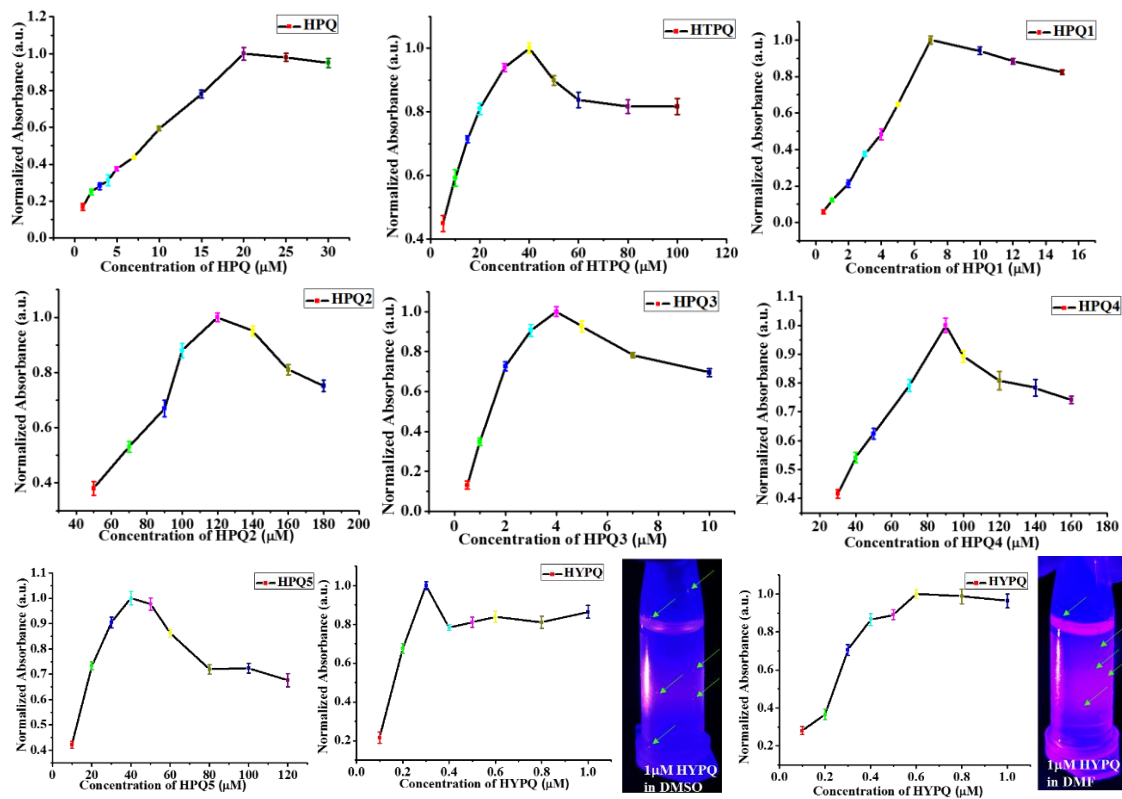
fluorophore	LogP
HPQ1	6.06
HPQ2	4.27
HPQ3	-0.07
HPQ4	6.57
HPQ5	3.98
HYPQ	5.38

**Table S4:** The distribution coefficient (logP) of these solid-state fluorophores was carried out using MarvinSketch 15.6.29 (ChemAxon, Budapest, Hungary).



**Fig. S6.** (A) Molecular structures of HPQ, HTPQ and HYPQ. Based on the traditional solid-state fluorophore HPQ, we developed a novel type of omni-insoluble NIR solid-state fluorochrome, HYPQ. (B) Solid-state fluorescent photographs of HPQ, HTPQ and HYPQ in powder samples. (C)

After HPQ, HTPQ and HYPQ were respectively dispersed in dichloromethane solutions (10  $\mu\text{M}$ ), solid-state fluorescent photos were obtained. HPQ and HTPQ were liposoluble, thereby dissolving absolutely without solid-state fluorescence. (D) HPQ, HTPQ and HYPQ were chromatographed by TLC with pure dichloromethane. By the omni-insoluble property of HYPQ, it could not be separated on silica gel plates.



**Fig. S7.** The measurement of the solubility of these solid-state fluorophores in DMSO solutions by using UV absorbance. Inset: Photos of HYPQ (1  $\mu\text{M}$ ) in DMSO and DMF solutions respectively under UV lamp at 365 nm excitation.

Planarity	HPQ5 HPQ4 HPQ2 HPQ1 HPQ3 HYPQ
	Bad <span style="float: right;">Good</span>
Melting point	HPQ4 HPQ2 HPQ5 HPQ1 HPQ3 HYPQ
	Low <span style="float: right;">High</span>
Solubility in DMSO	HPQ2 HPQ4 HPQ5 HPQ1 HPQ3 HYPQ
	High <span style="float: right;">Low</span>

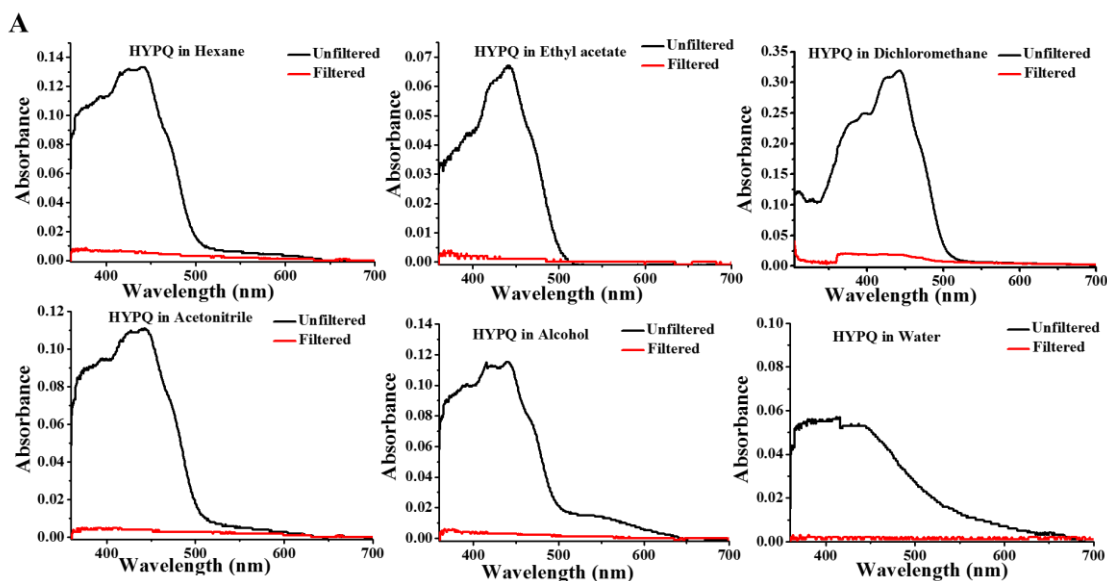
**Table S5:** The comparison of characters of these solid-state fluorochromes. The data analysis of planarity, melting point and solubility came from Table S2, Table S3 and Fig. S7 respectively.

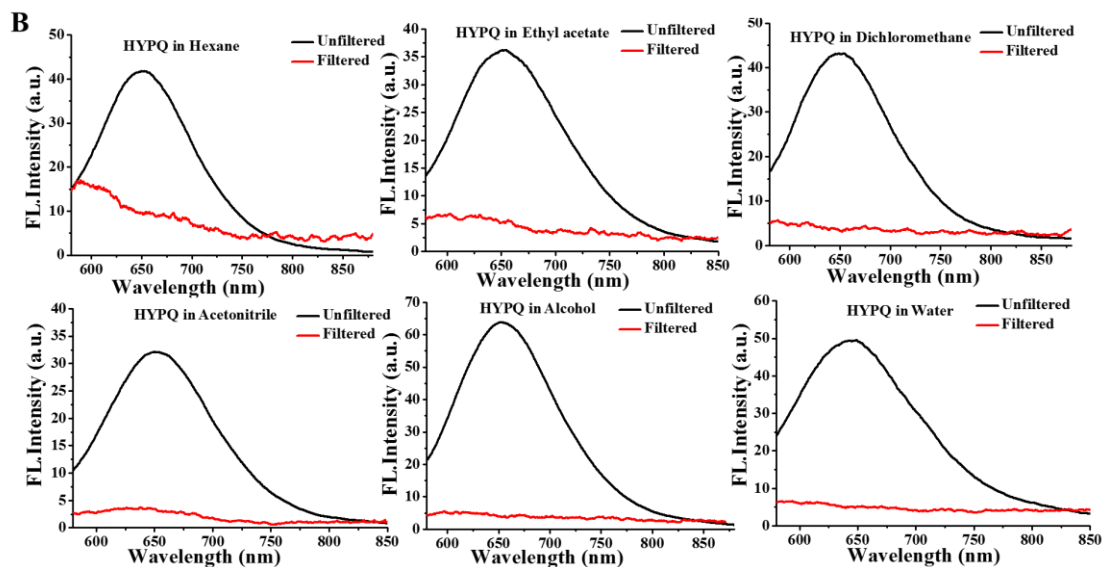
Solvent	$\lambda_{\text{Abs/nm}}$	$\epsilon(\text{M}^{-1} \text{cm}^{-1})$	$\lambda_{\text{Em/nm}}$	$\Phi_f$	Stokes shift/nm
DMSO	585	28000	650	0.10	65
glycerol	450	3000	650	0.19	200

The quantum yields were determined using cresol purple as reference ( $\Phi_f = 0.58$  in ethanol).

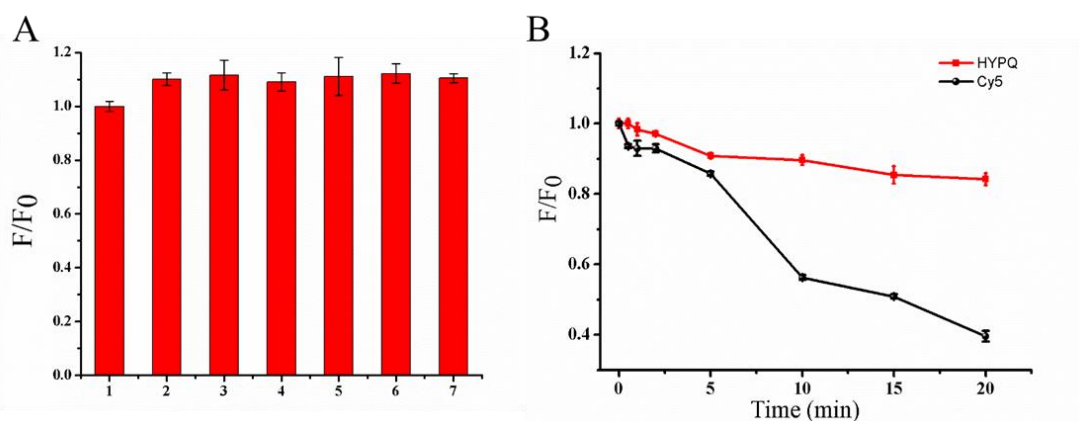
Solid-State	$\lambda_{\text{Abs/nm}}$	$\lambda_{\text{Em/nm}}$	$\Phi_f(\%)$	Stokes shift/nm	$\tau$ (ns)
Powder	450	650	0.38	200	0.62

**Table S6:** The photophysical characterization of HYPQ.

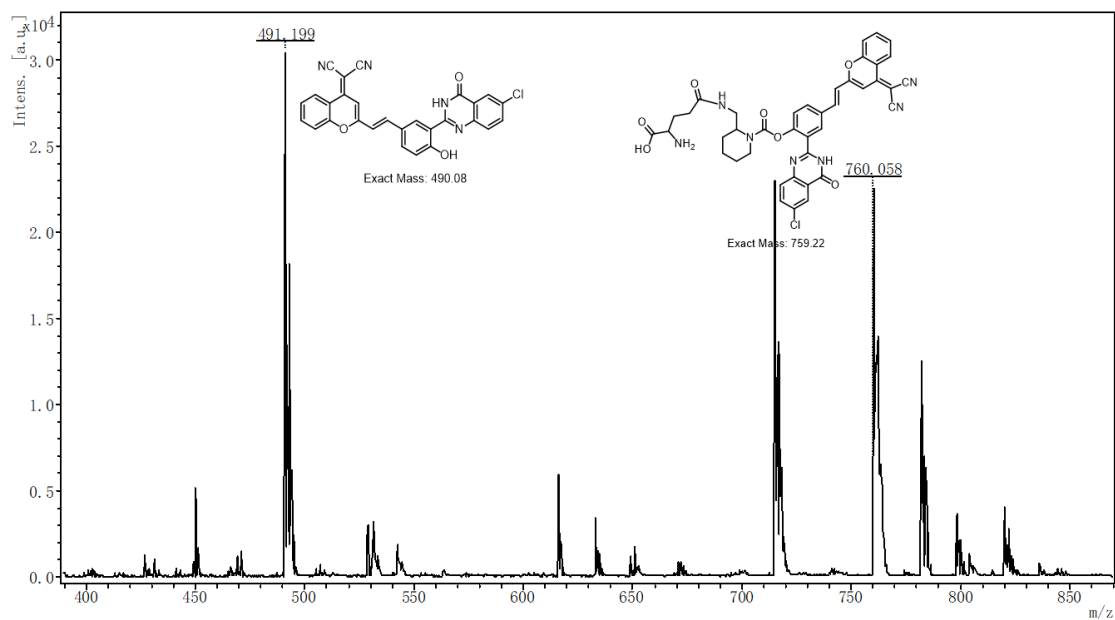




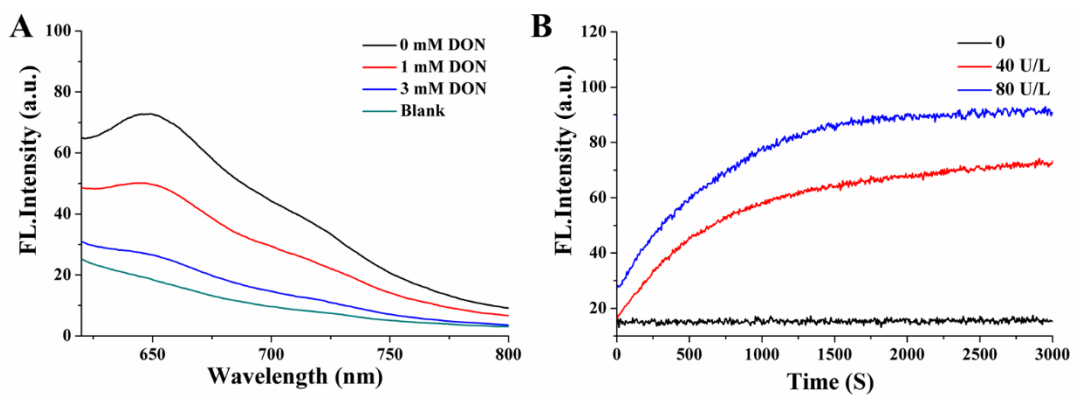
**Fig. S8.** The absorbance/fluorescence spectra of HYPQ (10 μM) in different solvents. The black lines and red lines indicated the absorbance/fluorescence spectra intensity change of these compounds before and after filtration.



**Fig. S9.** (A) Fluorescence responses of HYPQ upon treatment with various ROS/RNS (100 μM). 1. Blank, 2. O<sub>2</sub><sup>-</sup>, 3. H<sub>2</sub>O<sub>2</sub>, 4. ClO<sup>-</sup>, 5. S<sup>2-</sup>, 6. S<sub>2</sub><sup>2-</sup>, 7. SO<sub>3</sub><sup>2-</sup>. Fluorescence spectra were measured at 650 nm with an excitation at 450 nm. (B) Photostability of HYPQ and Cy5 in TBS buffer solution (pH 7.4, 1% glycerol). Samples were continuously irradiated by white light (50 W) in ice-bath condition.

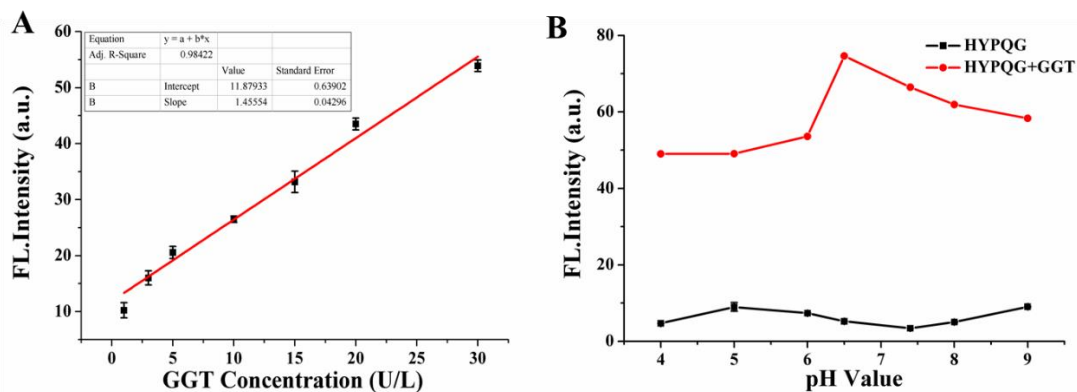


**Fig. S10.** The MALDI-TOF/MS spectrum of probe HYPQG in the presence of GGT.

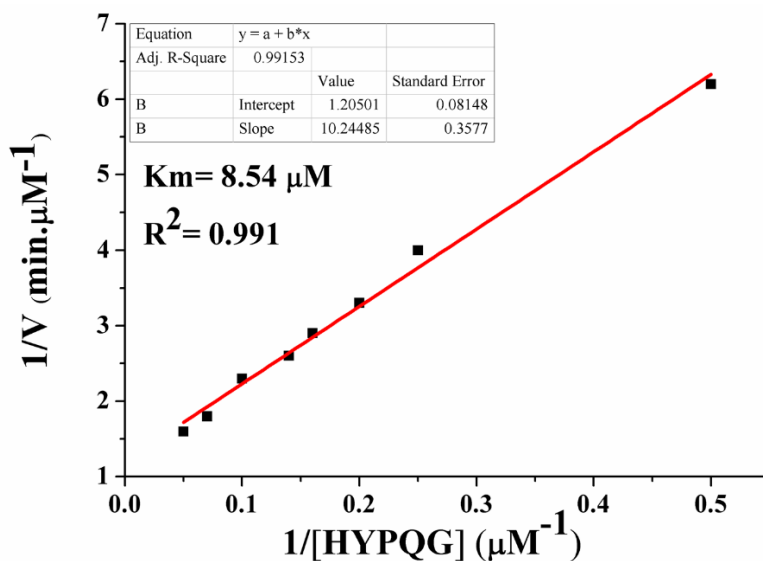


**Fig. S11.** (A). Fluorescence emission spectra of HYPQG (5 μM) in the presence of GGT and inhibitors (pH=7.4 TBS-buffered aqueous at 37 °C). DON was incubated for 30 min, and then HYPQG was added for another 40 min. (B). Fluorescence intensity of HYPQG (5 μM) vs. reaction time in the presence of various concentrations of GGT (0 U/L, 40 U/L, 80 U/L). The measurements were performed at 37 °C in 10 mM TBS (pH 7.4) with  $\lambda_{ex/em} = 450/650$  nm.

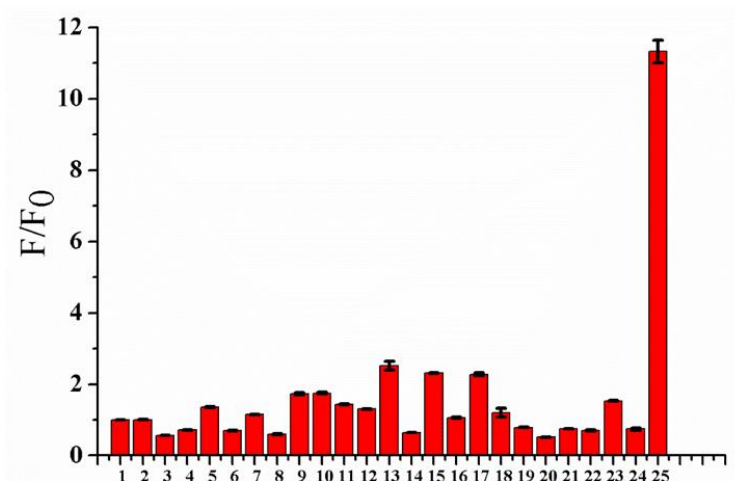




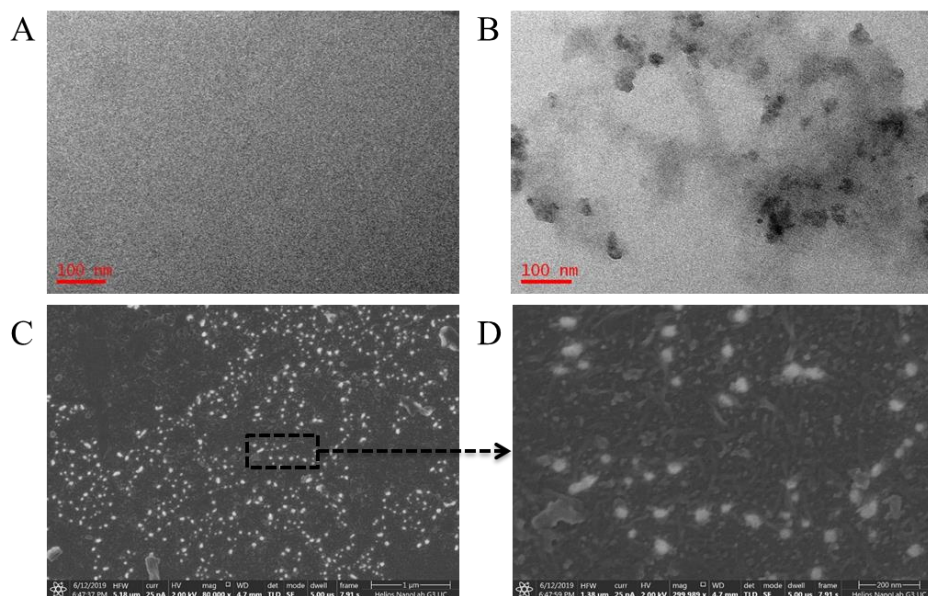
**Fig. S12.** (A) The linearity between fluorescence intensities at 650 nm and increasing concentrations of GGT (1-30 U/L). (B) Fluorescence intensity (650 nm) vs. pH value. Effect of pH on the fluorescence intensity of black line, HYPQG (5  $\mu$ M); red line, HYPQG (5  $\mu$ M) with GGT (80 U/L) in buffered/DMSO/glycerol (94/5/1, v/v/v, pH= 4.0 - 9.0, 10 mM).  $\lambda_{ex}$  =450 nm.



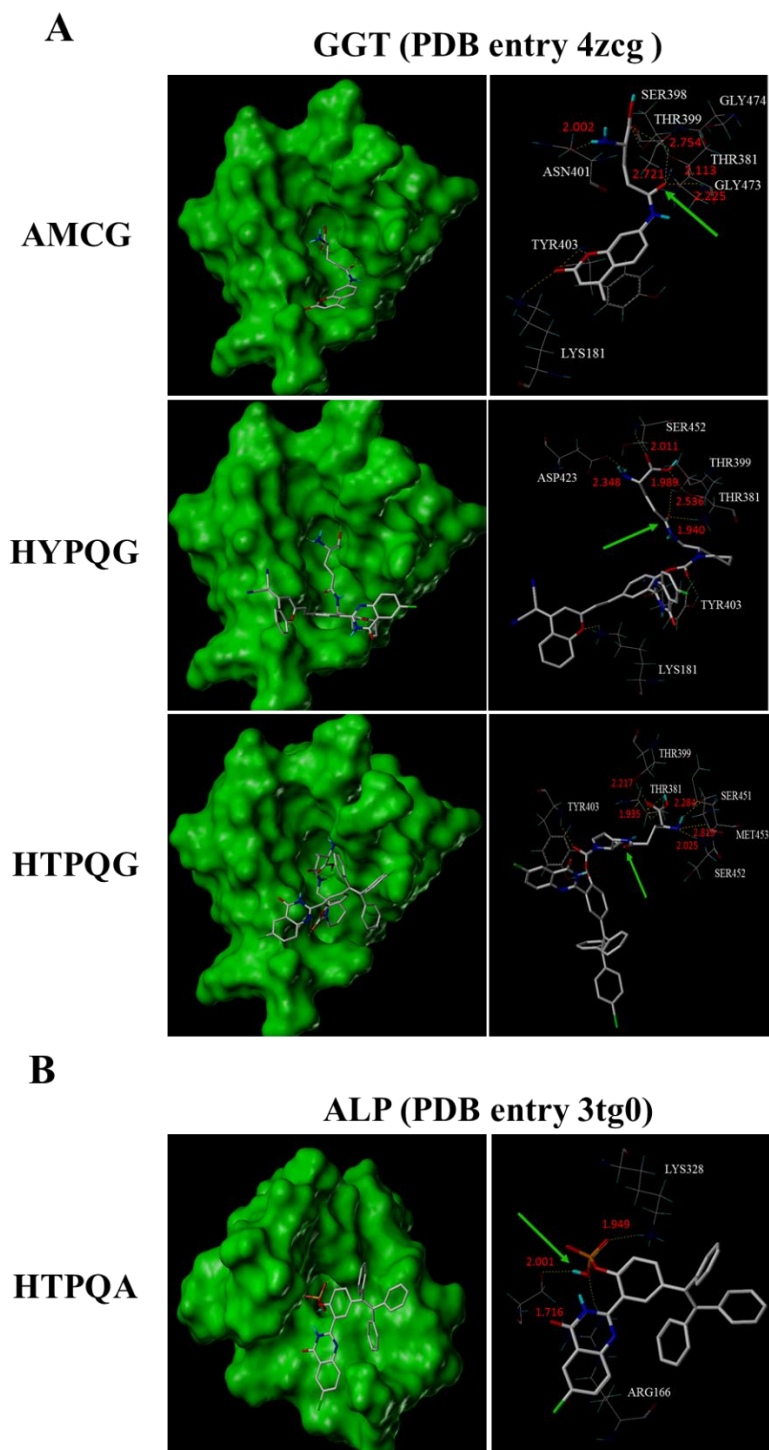
**Fig. S13.** Lineweaver-Burk plot for the enzyme-catalyzed reaction of HYPQG. The Michaelis-Menten equation was described as  $V = V_{max} [\text{probe}] / (K_m + [\text{probe}])$ , where V is the initial reaction rate, [probe] is the probe concentration (substrate), and  $K_m$  is the Michaelis constant. Conditions: 80 U/L GGT, 2-20  $\mu$ M of HYPQG. The measurements were performed at 37  $^{\circ}$ C with  $\lambda_{ex/em}$  = 450/650 nm.



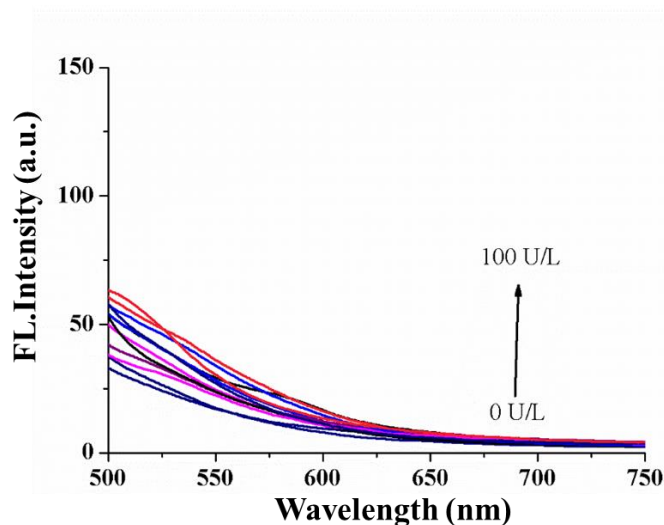
**Fig. S14.** Fluorescence responses of HYPQG (5  $\mu\text{M}$ ) toward other substances (100  $\mu\text{M}$  for 1-18): 1. L-lysine, 2. L-glutamate, 3. L-valine, 4. L-isoleucine, 5. L-threonine, 6. L-tyrosine, 7. L-tryptophan, 8. phenylalanine, 9. arginine, 10. glucose, 11.  $\text{CaCl}_2$ , 12. BSA, 13.  $\text{NaClO}$ , 14.  $\text{H}_2\text{O}_2$ , 15.  $\text{Zn}(\text{NO}_3)_2$ , 16.  $\text{FeSO}_4$ , 17.  $\text{FeCl}_3$ , 18.  $\text{MgCl}_2$ , 19. GSH (5 mM), 20. cathepsin B (100 U/L), 21. monoamine oxidase (10  $\mu\text{g}/\text{mL}$ ), 22. alkaline phosphatase (100 U/L), 23. leucine aminopeptidase (50 U/L), 24. sulfatase (1000 U/L), 25. GGT (80 U/L). The test solution was kept in TBS-buffered (10 mM,  $\text{pH}=7.4$ ) aqueous DMSO solution (94:5, v/v, 1% glycerol) at 37  $^\circ\text{C}$  for 40 min before measurement.  $\lambda_{\text{em}}=450$  nm.



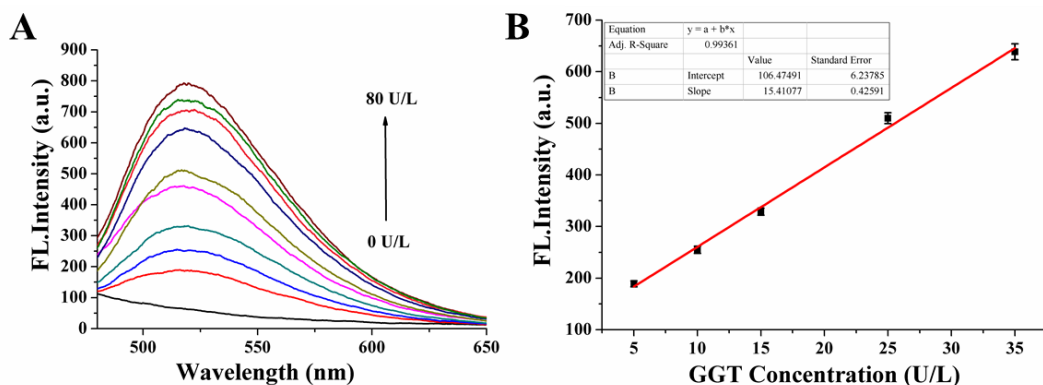
**Fig. S15.** TEM photos of HYPQG (10  $\mu\text{M}$ ) before (A) and after (B) reaction with GGT (150 U/L). SEM photos of HYPQG (10  $\mu\text{M}$ ) reaction with GGT at the scale of 1  $\mu\text{m}$  (C) and 200 nm (D).



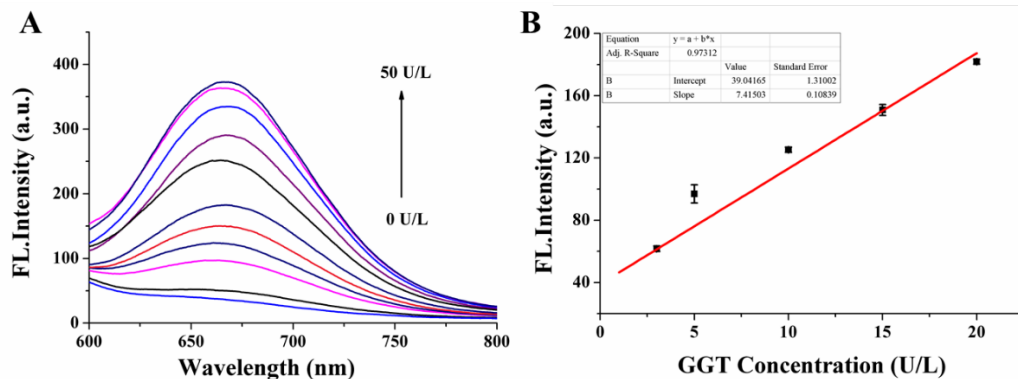
**Fig. S16.** (A) The molecular docking modes of AMCG, HYPQG and HTPQG in the ligand binding pocket of gamma glutamyltransferase (GGT). (B) The molecular docking mode of HTPQA in the ligand binding pocket of alkaline phosphatase (ALP). The interaction of hydrogen bonds between the probes and the protein structure was displayed as dotted lines. The hydrogen bond lengths were denoted in red and reaction sites were indicated by green arrows.



**Fig. S17.** Fluorescence emission spectra of HTPQG (5  $\mu$ M) in the presence of different concentrations of GGT (0, 3, 5, 10, 20, 30, 50, 60, 80, 90, and 100 U/L) in TBS-buffered (10 mM, pH=7.4) aqueous DMSO solution (5%) at 37  $^{\circ}$ C.

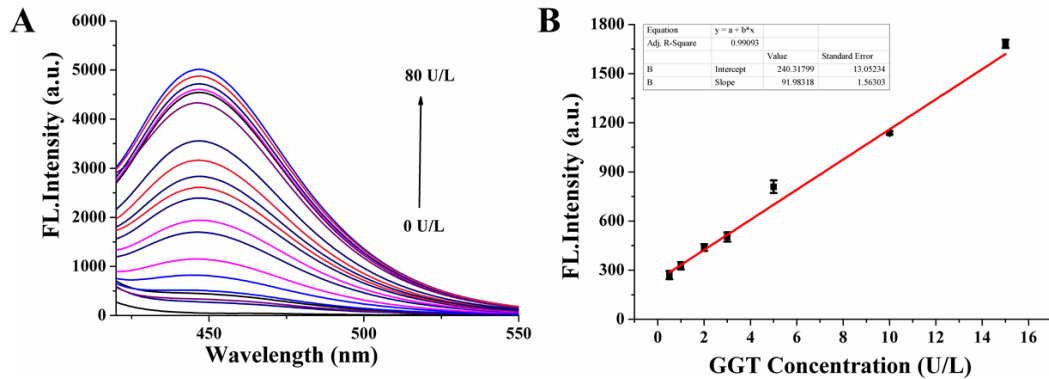


**Fig. S18.** (A) The fluorescence emission spectra of HPQG (5  $\mu$ M) in the presence of different concentrations of GGT (0, 1, 5, 10, 15, 25, 35, 50, 70, and 80 U/L) in TBS-buffered (10 mM, pH=7.4) aqueous DMSO solution (5%) at 37  $^{\circ}$ C. (B) The linearity between fluorescence intensities at 510 nm and increasing concentrations of GGT (5-35 U/L).

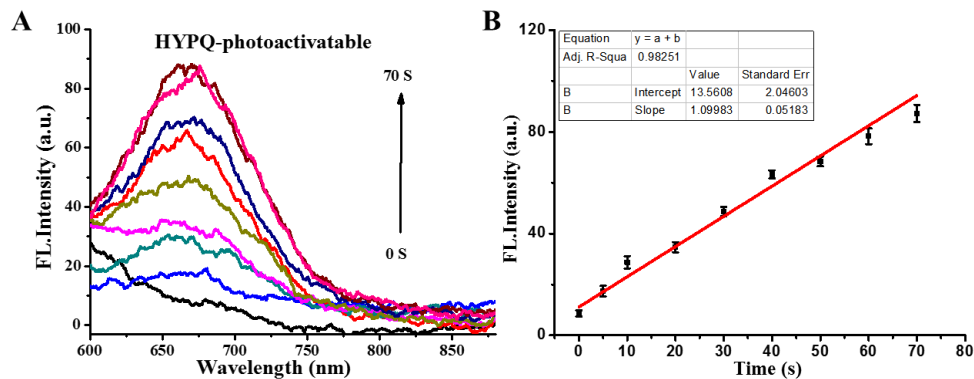


**Fig. S19.** (A) Fluorescence emission spectra of DCMG (5  $\mu$ M) in the presence of different concentrations of GGT (0, 3, 5, 10, 15, 20, 25, 30, 40, 45, and 50 U/L) in TBS-buffered (10 mM, pH=7.4) aqueous DMSO solution (5%) at 37  $^{\circ}$ C. (B) The linearity between fluorescence intensities at 650 nm and increasing concentrations of GGT (5-20 U/L).

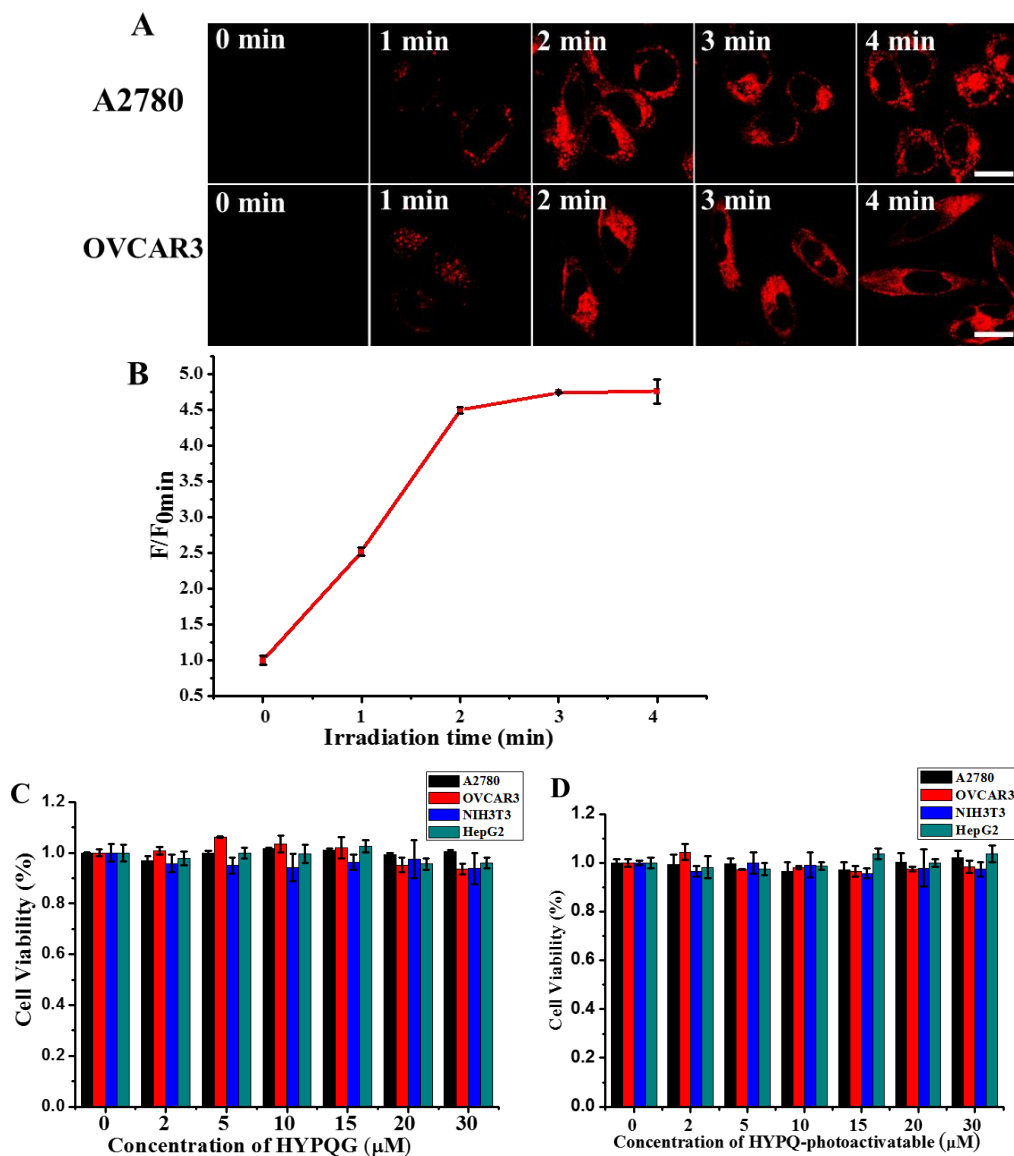
pH=7.4) aqueous DMSO solution (5%) at 37 °C. (B) The linearity between fluorescence intensities at 660 nm and increasing concentrations of GGT (3-20 U/L).



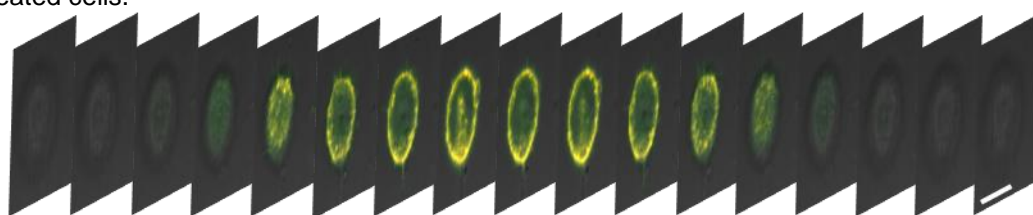
**Fig. S20.** (A) Fluorescence emission spectra of AMCG (5  $\mu$ M) in the presence of different concentrations of GGT (0, 0.5, 1, 2, 3, 5, 10, 15, 20, 25, 30, 35, 40, 45, 50, 55, 60, 70, and 80 U/L) in TBS-buffered (10 mM, pH=7.4) aqueous DMSO solution (5%) at 37 °C. (B) The linearity between fluorescence intensities at 450 nm and increasing concentrations of GGT (0.5-15 U/L).



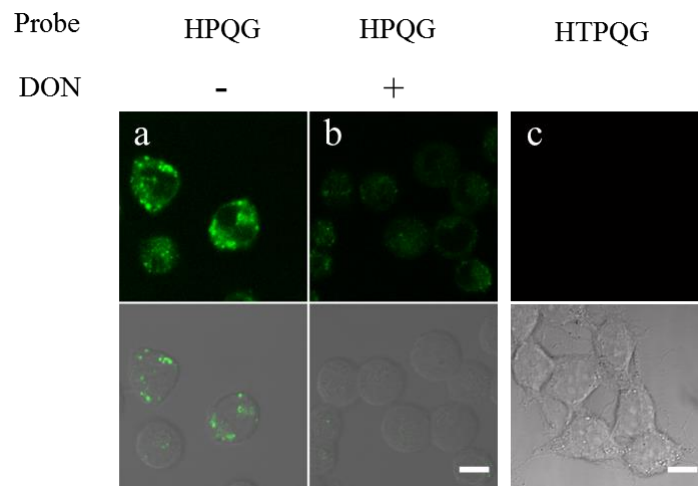
**Fig. S21.** (A) Fluorescence emission spectra of HYPQ-photoactivatable (10  $\mu$ M) after irradiation by 365 nm light for 5 S, 10 S, 20 S, 30 S, 40 S, 50 S, 60 S and 70 S in glycerol/ PBS/ DMSO = 5/4/1. (B) The linearity between fluorescence intensities at 650 nm and increasing irradiation time under 365 nm light.



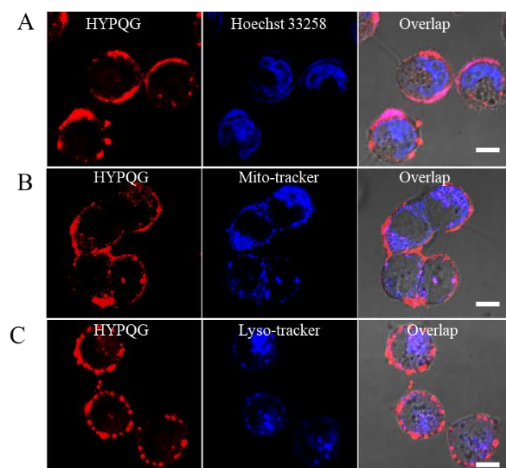
**Fig. S22.** (A) Real-time imaging of living cells incubated with HYPQ-photoactivatable (5  $\mu\text{M}$ ) in DPBS buffer after the different irradiation times under blue light (450 nm–470 nm). (B) Average intensity found in Fig. S22A; that of  $t=0$  min was defined as 1.0.  $\lambda_{\text{ex}} = 488$  nm,  $\lambda_{\text{em}} = 584\text{-}676$  nm. Scale bar = 20  $\mu\text{m}$ . (C) Cytotoxicity of HYPQG toward A2780, OVCAR3, NIH3T3 and HepG2 cells. (D) Cytotoxicity of HYPQ-photoactivatable toward A2780, OVCAR3, NIH3T3 and HepG2 cells. Cell viability was measured by MTS assay, and the results are reported as percentage relative to untreated cells.



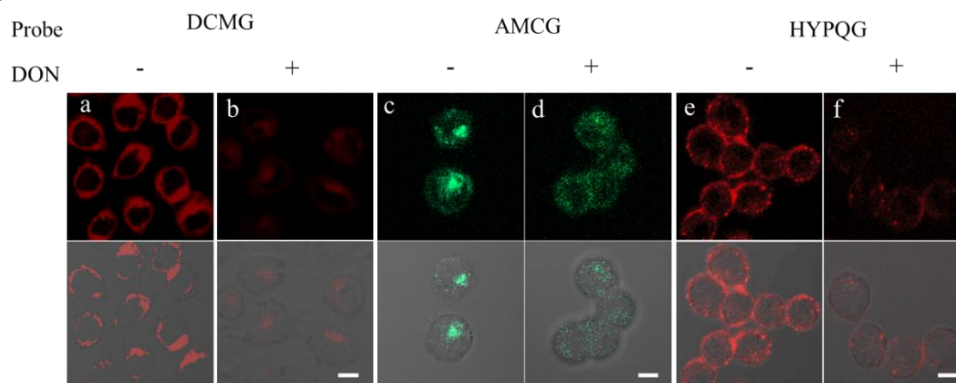
**Fig. S23.** Z-stack images of the 3-D spheroid from 0-60  $\mu\text{m}$  after A2780 cells were incubated with HYPQG and Memb-Tracker Green. Scale bar: 20  $\mu\text{m}$



**Fig. S24.** Confocal images of GGT in A2780 cells treated with the HPQG probe (a), and HTPQG (c) for 40 min. The cells were pretreated with DON (1 mM) for 1 h before incubation with HPQG for 40 min (b). Scale bar: 20  $\mu$ m

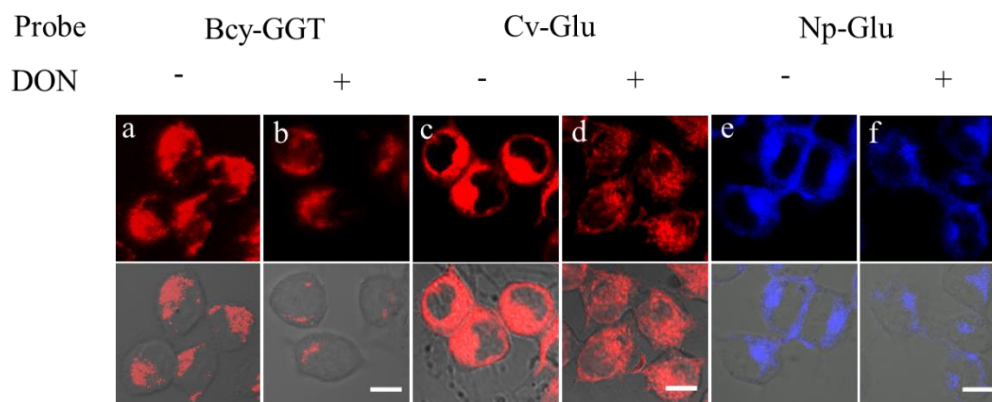


**Fig. S25.** Co-incubation with organelle trackers. A2780 cells were incubated with HYPQG (5  $\mu$ M) for 40 min and then co-stained with 5  $\mu$ M Hoechst33258, Mito-Tracker Blue and Lyso-Tracker for 10 min, respectively. (A) Nuclei staining: Hoechst33258,  $\lambda_{ex}$  = 405 nm,  $\lambda_{em}$  = 425-475 nm; (B) Mito-Tracker:  $\lambda_{ex}$  = 405 nm,  $\lambda_{em}$  = 425-475 nm; (C) Lyso-Tracker:  $\lambda_{ex}$  = 405 nm,  $\lambda_{em}$  = 425-475 nm. Scale bar: 20  $\mu$ m

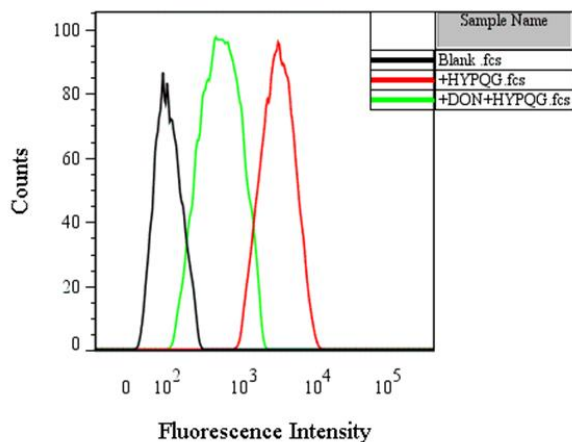


**Fig. S26.** Confocal images of GGT in A2780 cells treated with the DCMG (a), AMCG (c) and HYPQG (e) probes, or pretreated with DON (1 mM) for 1 h before incubation with DCMG (b), AMCG

(d) and HYPQG (f) for 40 min. (DCMG:  $\lambda_{ex}$  = 488 nm,  $\lambda_{em}$  = 663–738 nm; AMCG:  $\lambda_{ex}$  = 405 nm,  $\lambda_{em}$  = 425–475 nm; HYPQG:  $\lambda_{ex}$  = 488 nm,  $\lambda_{em}$  = 584–676 nm). Scale bar: 20  $\mu$ m

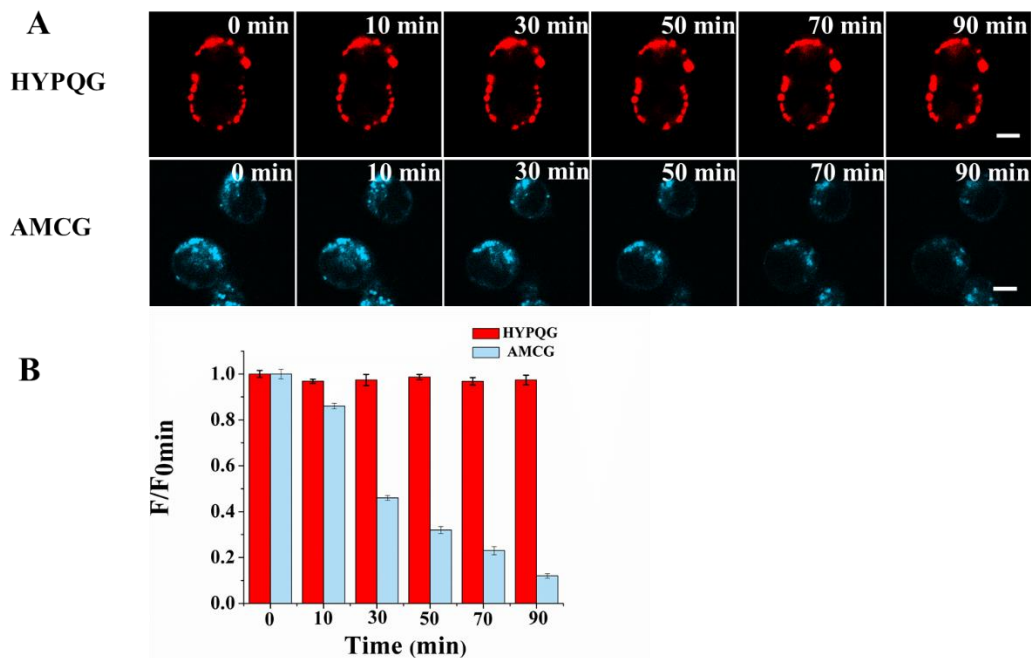


**Fig. S27.** Confocal images of GGT in A2780 cells treated with the Bcy-GGT (a), Cv-Glu (c) and Np-Glu (e) probes, or pretreated with DON (1 mM) for 1 h before incubation with Bcy-GGT (b), Cv-Glu (d) and Np-Glu (f) for 40 min. (Bcy-GGT:  $\lambda_{ex}$  = 640 nm,  $\lambda_{em}$  = 663–738 nm; Cv-Glu:  $\lambda_{ex}$  = 560 nm,  $\lambda_{em}$  = 584–676 nm; Np-Glu:  $\lambda_{ex}$  = 405 nm,  $\lambda_{em}$  = 425–475 nm). Scale bar: 20  $\mu$ m

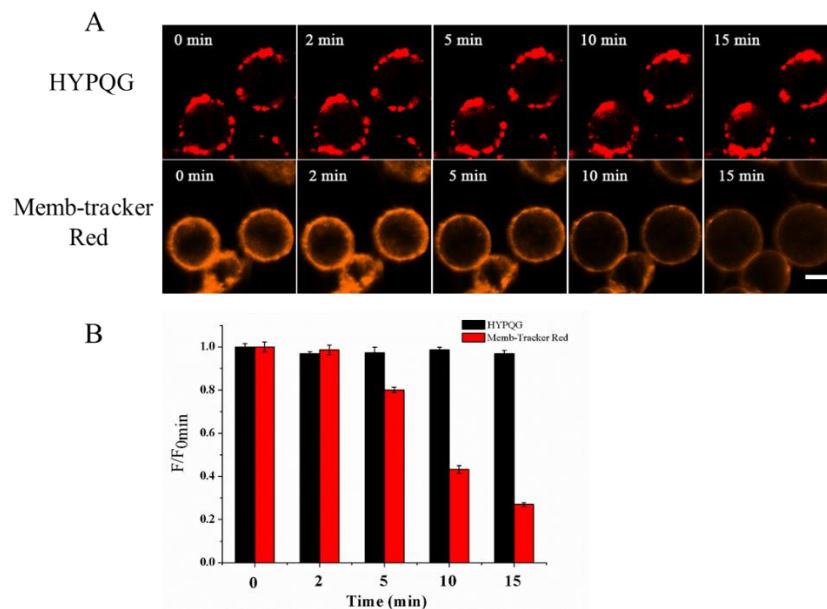


**Fig. S28.** Flow cytometric analysis of intact A2780 and A2780 loaded HYPQG treated with DON (1 mM). The X-axis is the Cy5 channel that captured the fluorescence of HYPQG ( $\lambda_{ex}$  = 488 nm).

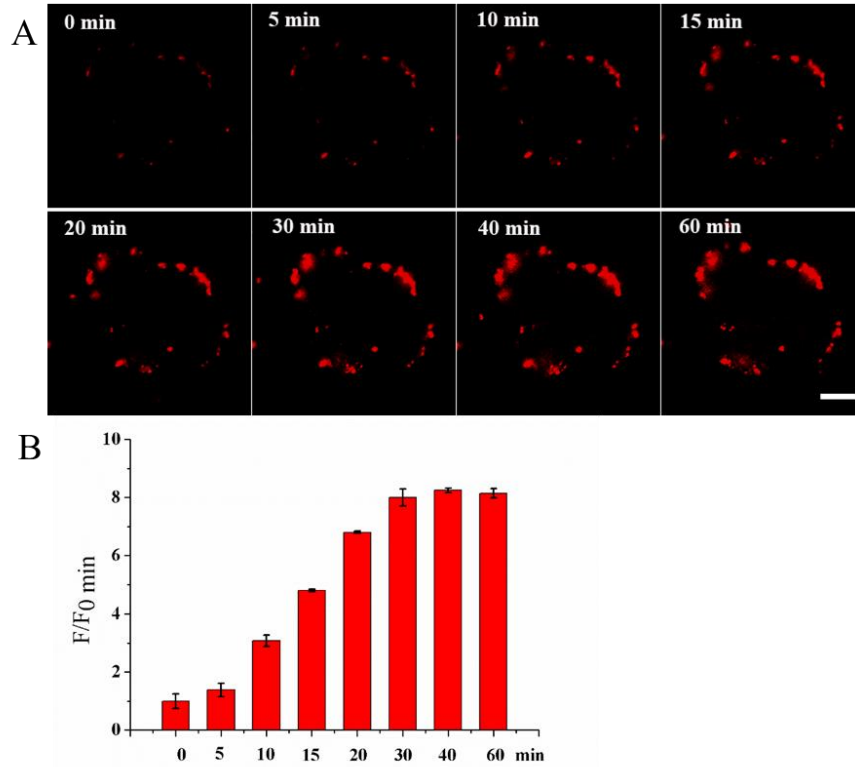




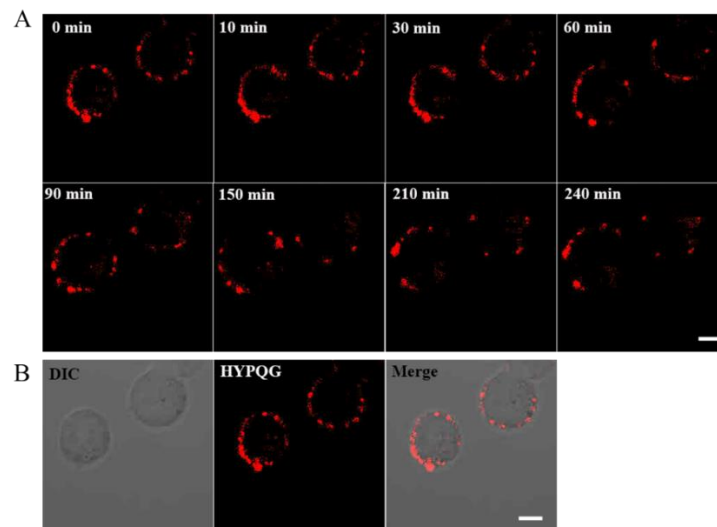
**Fig. S29.** Anti-diffusion performance of HYPQG was investigated by comparing with the commercially available AMCG probe. (A) A2780 cells were incubated with HYPQG (top) and AMCG (bottom) for 40 min, respectively, and then washed with DPBS, followed by real-time images obtained every 10 min for a total of 90 min. HYPQG:  $\lambda_{ex} = 488$  nm,  $\lambda_{em} = 584$ -676 nm; AMCG:  $\lambda_{ex} = 405$  nm,  $\lambda_{em} = 425$ -475 nm. (B) Average fluorescence intensity found in Fig. S29A; initial intensity was defined as 1.0. Scale bar = 20  $\mu$ m



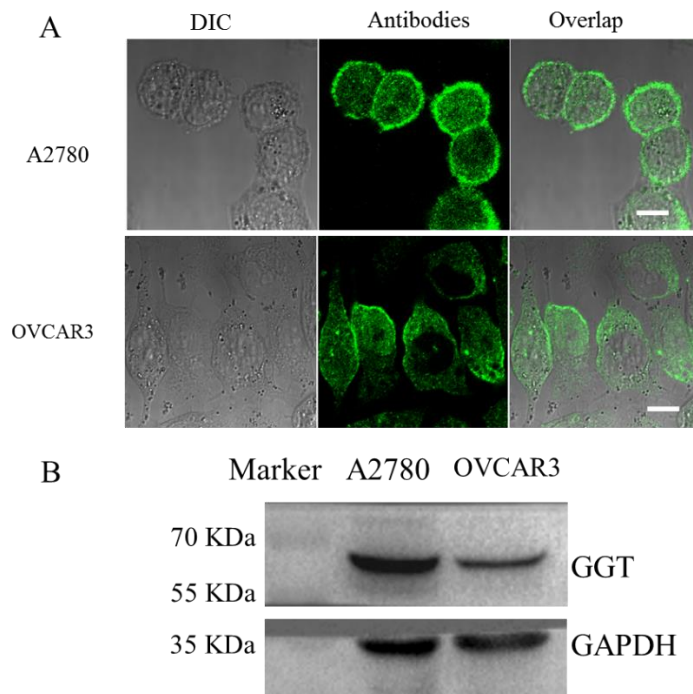
**Fig. S30.** (A) A2780 cells were incubated with HYPQG (5  $\mu$ M) for 40 min and Memb-Tracker Red (5  $\mu$ M) for 10 min, respectively, and then real-time fluorescence scanning was carried out. (B) Average intensity found in Fig. S30A; that of  $t = 0$  min was defined as 1.0. HYPQG:  $\lambda_{ex} = 488$  nm,  $\lambda_{em} = 584$ -676 nm; Memb-Tracker Red:  $\lambda_{ex} = 560$  nm,  $\lambda_{em} = 570$ -620 nm. Scale bar = 20  $\mu$ m



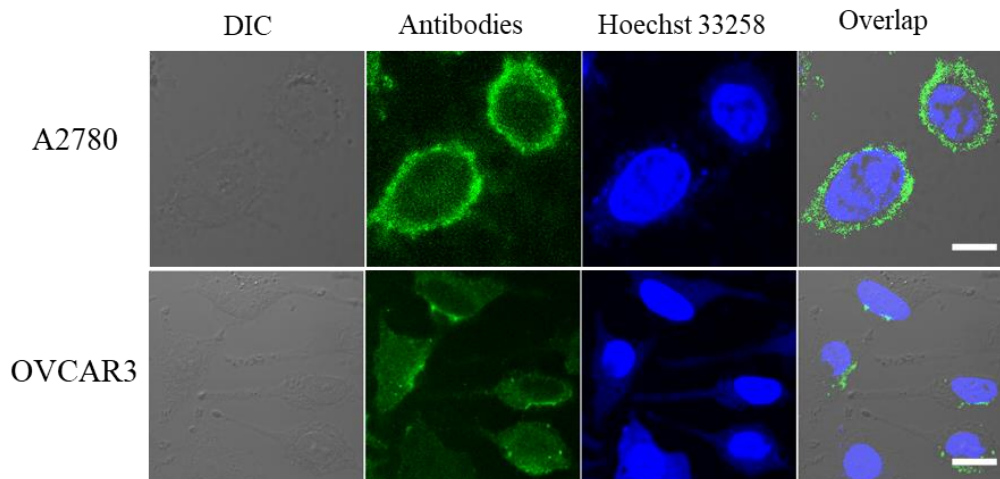
**Fig. S31.** Real-time imaging of A2780 cells incubated with HYPQG (5  $\mu$ M) in DPBS buffer in 5 min intervals. (A) Fluorescence micrographs covering a total of 60 min incubation time. (B) Average intensity found in Fig. S31A; that of  $t=0$  min was defined as 1.0.  $\lambda_{ex} = 488$  nm,  $\lambda_{em} = 584-676$  nm. Scale bar = 20  $\mu$ m



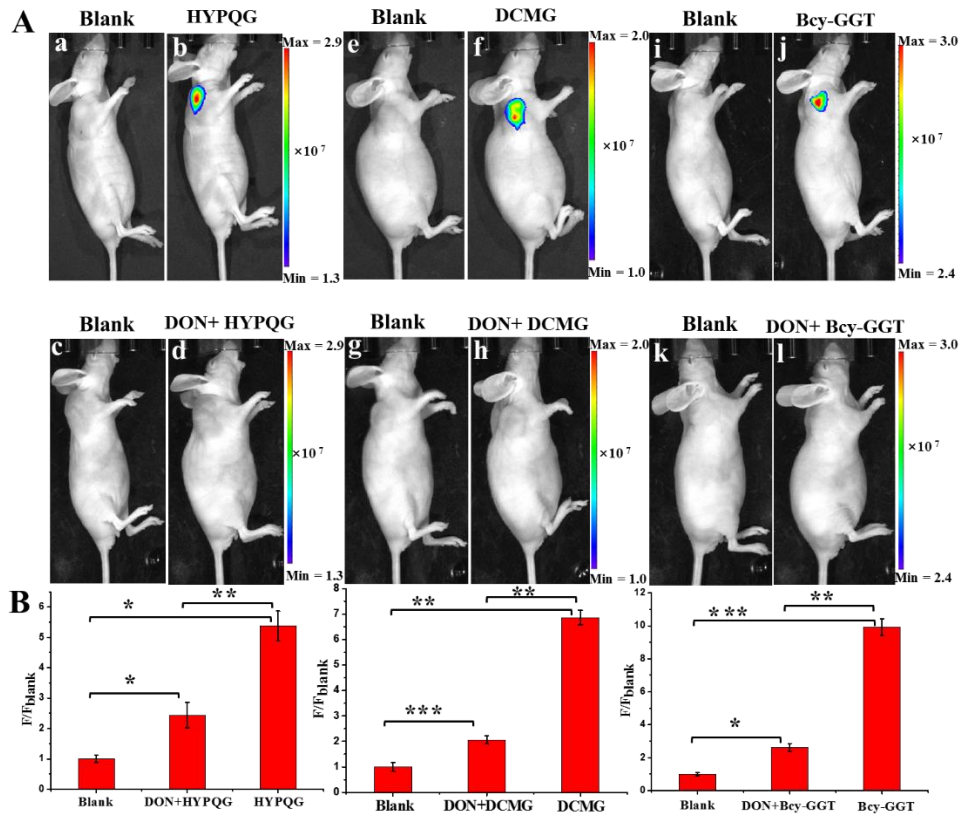
**Fig. S32.** (A) Long-term imaging of endogenous GGT in live A2780 cells. (B) Bright and overlap field.



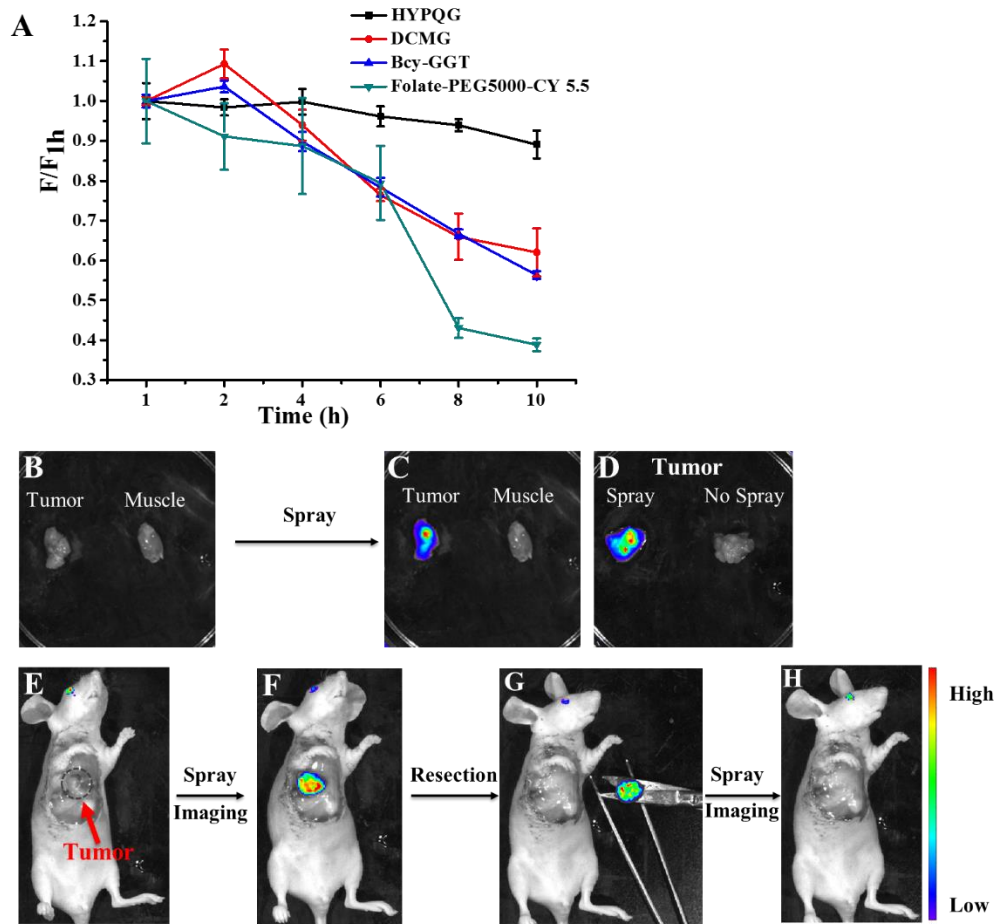
**Fig. S33.** (A) Immunofluorescence analysis with an anti-GGT antibody and a secondary fluorescent antibody in A2780 cells and OVCAR3 cells. The green channel (500-550 nm) shows the fluorescence signal of secondary antibodies excited at 488 nm. (C) Western blot analysis with antibodies against GGT. Results indicated that the GGT expression level in A2780 was higher than that of OVCAR3 cells. Scale bar = 20  $\mu$ m



**Fig. S34.** Immunofluorescence and colocalization analysis in A2780 and OVCAR3 cells with antibodies and nucleus trackers. Nuclei staining: DAPI,  $\lambda_{ex}$  = 405 nm,  $\lambda_{em}$  = 425-475 nm; antibodies:  $\lambda_{ex}$  = 488 nm,  $\lambda_{em}$  = 500-550 nm. Scale bar = 20  $\mu$ m



**Fig. S35.** (A) In vivo fluorescence imaging of endogenous GGT in A2780 cells tumor-bearing mice after intratumoral injection of 20  $\mu$ M HYPQG (b), DCMG (f) and Bcy-GGT (j) for 60 min respectively, or pretreated with DON (5 mM) for 1 h before incubation with HYPQG (d), DCMG (h) and Bcy-GGT (l) for 60 min. (B) Average fluorescence intensity found in Fig. S35A; blank intensity was defined as 1.0. Statistical significance p-values (\* p < 0.05, \*\* p < 0.01, \*\*\* p < 0.001) were determined using two-sided Student's t-test (n=3).



**Fig. S36.** (A) The quantitative analysis of long-term imaging experiments *in vivo*. Average fluorescence intensity found in Fig. 6; the fluorescence intensity of 1 h was defined as 1.0. In vitro imaging of cancer tissue and normal muscle tissue (B and C) through spraying HYPQG. Fluorescence imaging of tumor tissues via spraying or no spraying probe HYPQG (D) Image-guided resection by spraying probe HYPQG in nude mice bearing A2780 xenograft tumor: (E) fluorescence image; (F) spraying HYPQG for 1 hour, then fluorescence image; (G) surgical removal of tumor; (H) respraying HYPQG for 1 hour, then fluorescence image.

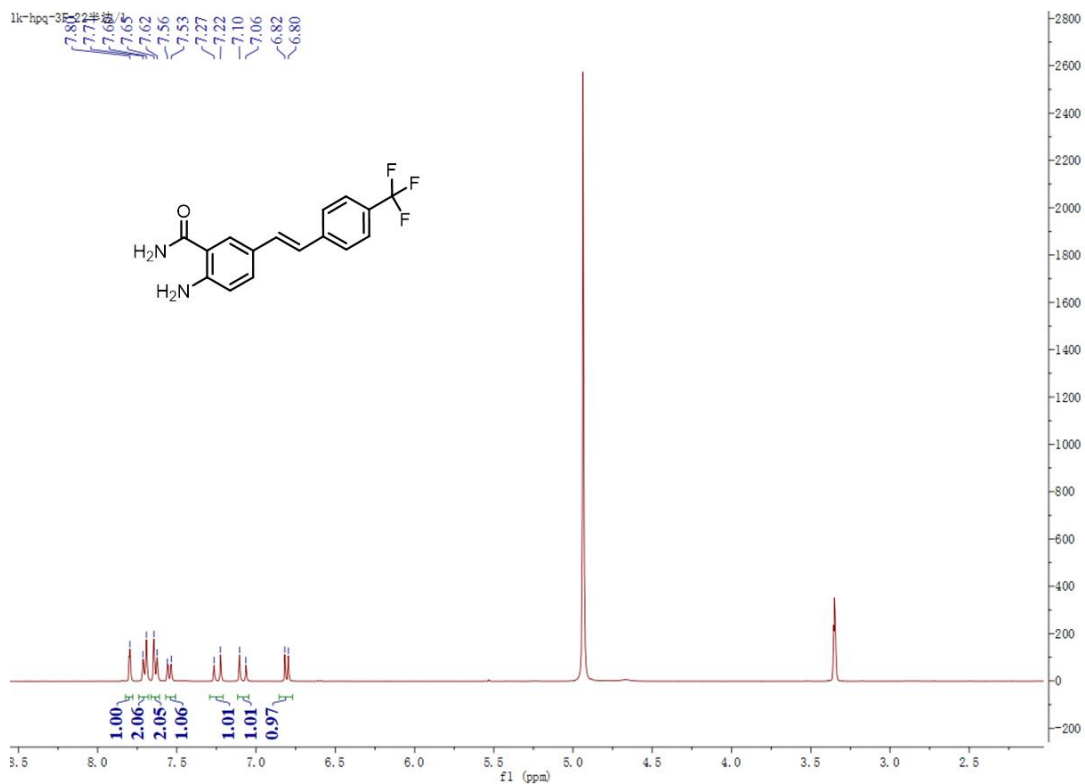


Fig. S37. <sup>1</sup>H NMR spectrum of compound 3.

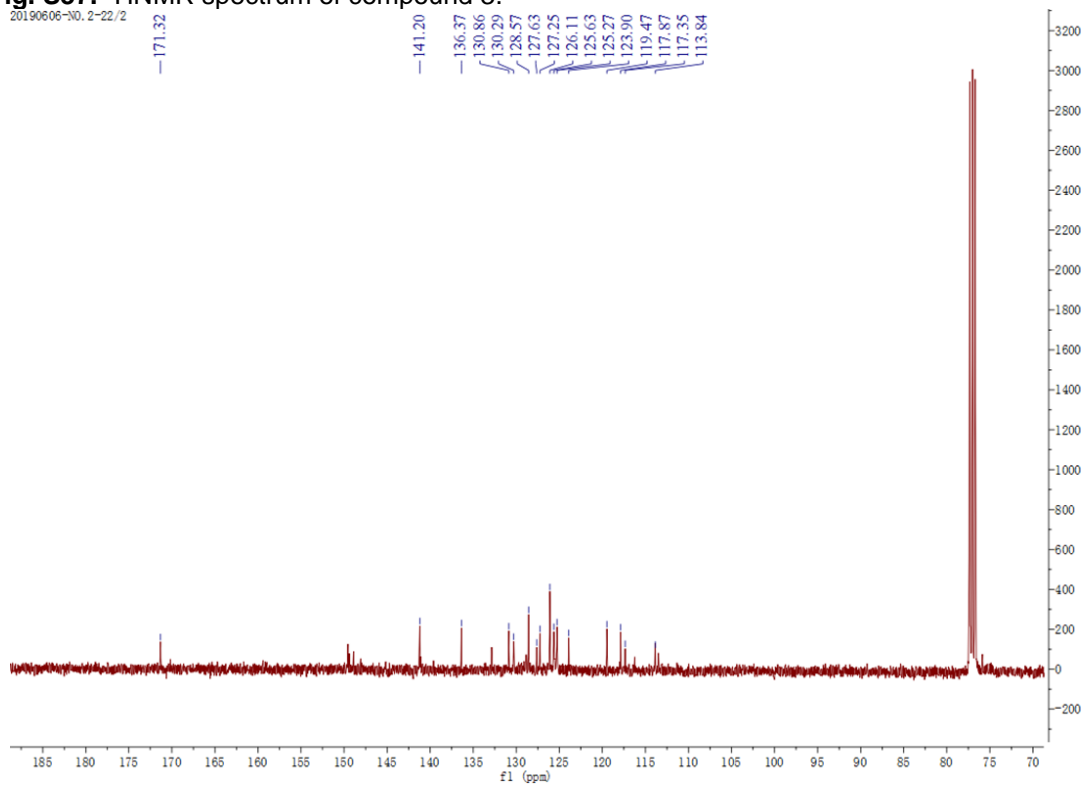


Fig. S38. <sup>13</sup>C NMR spectrum of compound 3.

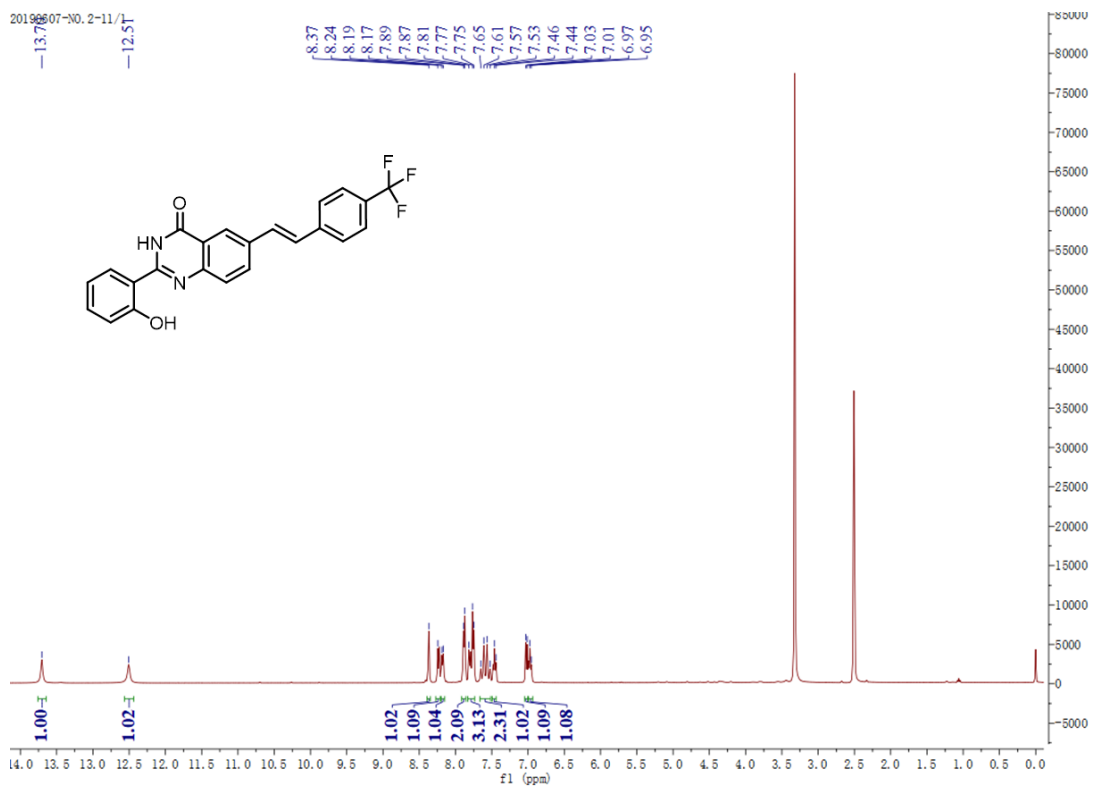


Fig. S39. <sup>1</sup>H NMR spectrum of HPQ1.

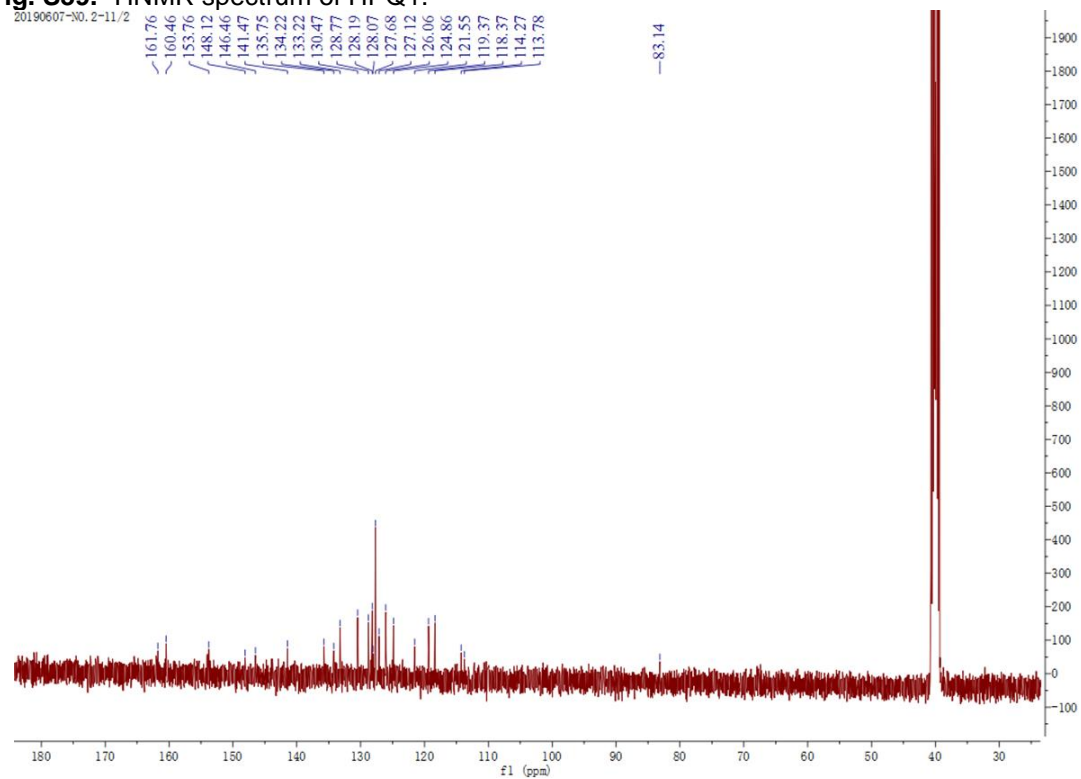


Fig. S40. <sup>13</sup>C NMR spectrum of HPQ1.

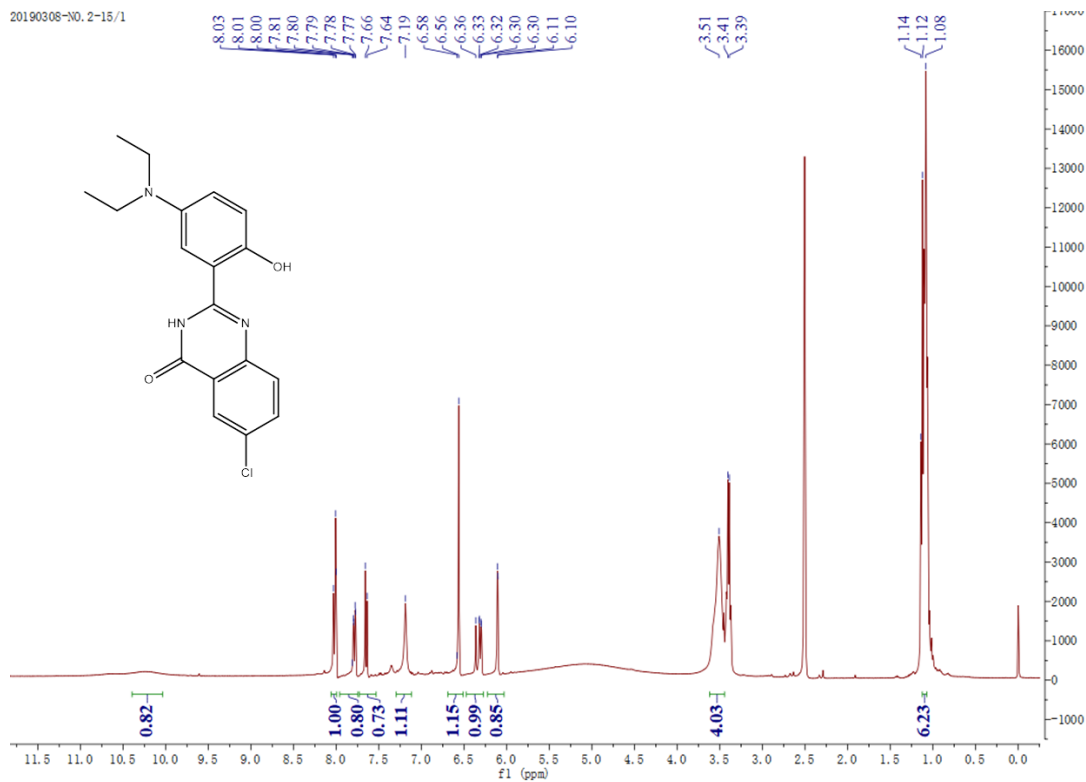


Fig. S41. <sup>1</sup>H NMR spectrum of HPQ2.

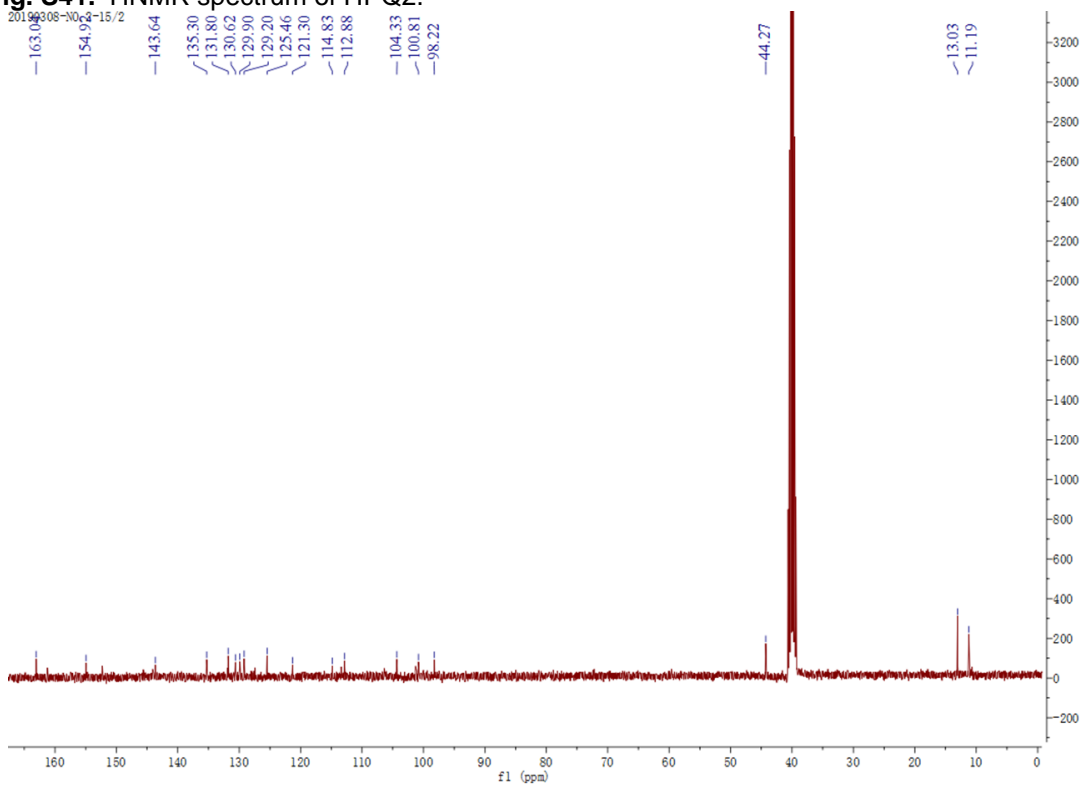


Fig. S42. <sup>13</sup>C NMR spectrum of HPQ2.



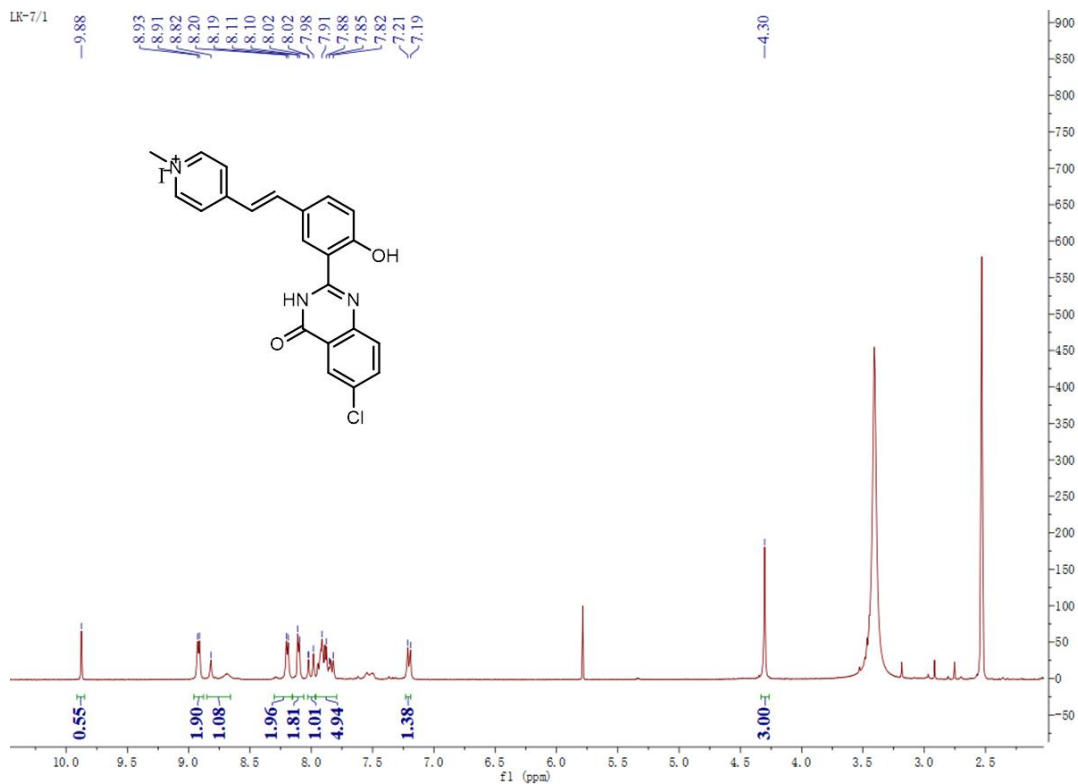


Fig. S43.  $^1\text{H NMR}$  spectrum of HPQ3.

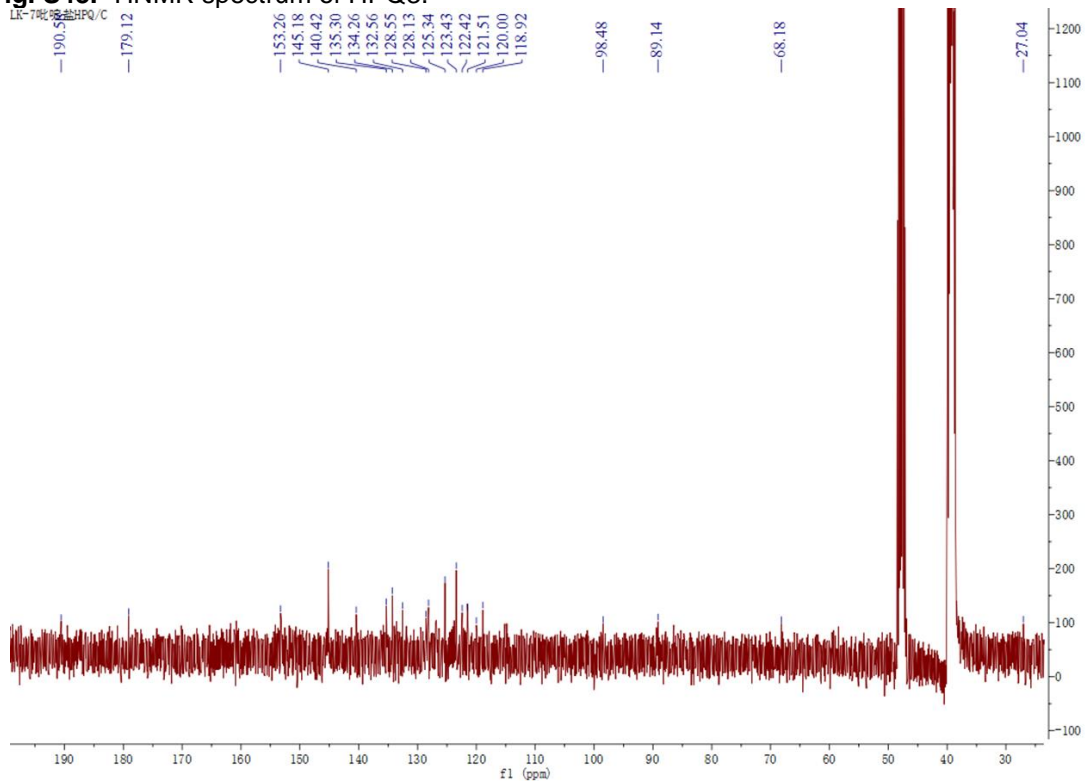


Fig. S44.  $^{13}\text{C NMR}$  spectrum of HPQ3.

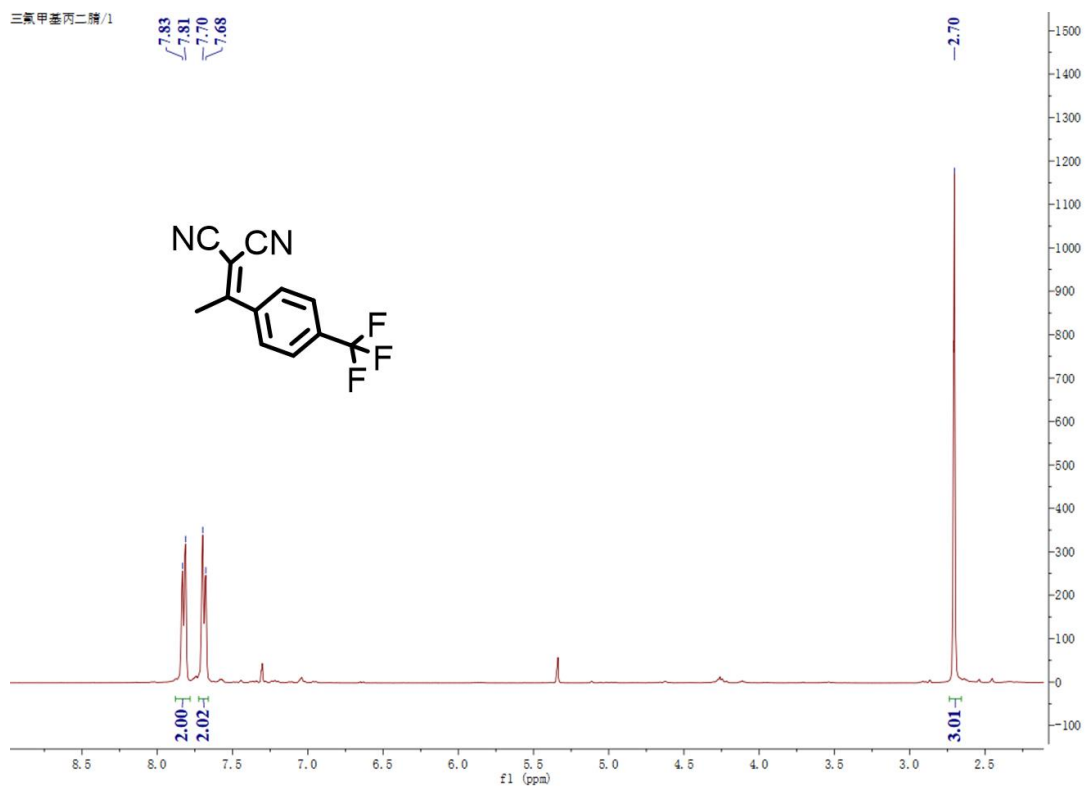


Fig. S45. <sup>1</sup>H NMR spectrum of compound 7.

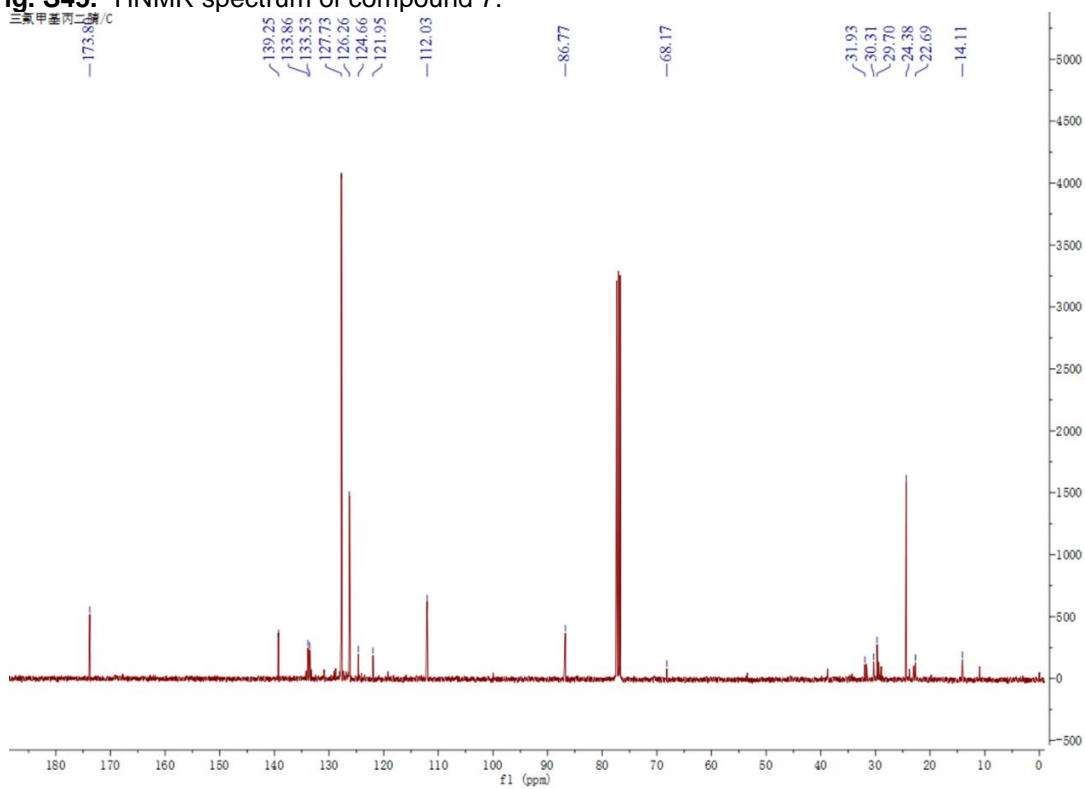


Fig. S46. <sup>13</sup>C NMR spectrum of compound 7.

20190629-NO. 2-1/1

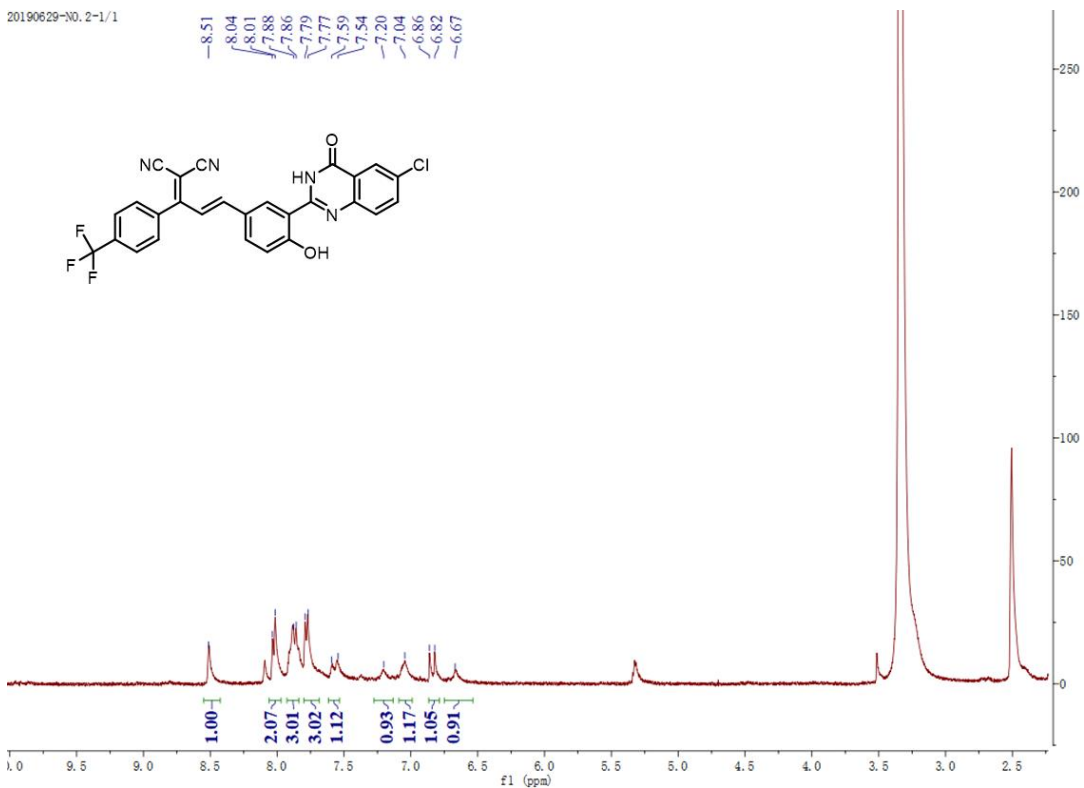


Fig. S47. <sup>1</sup>H NMR spectrum of HPQ4.

20190701-NO. 2-2/1

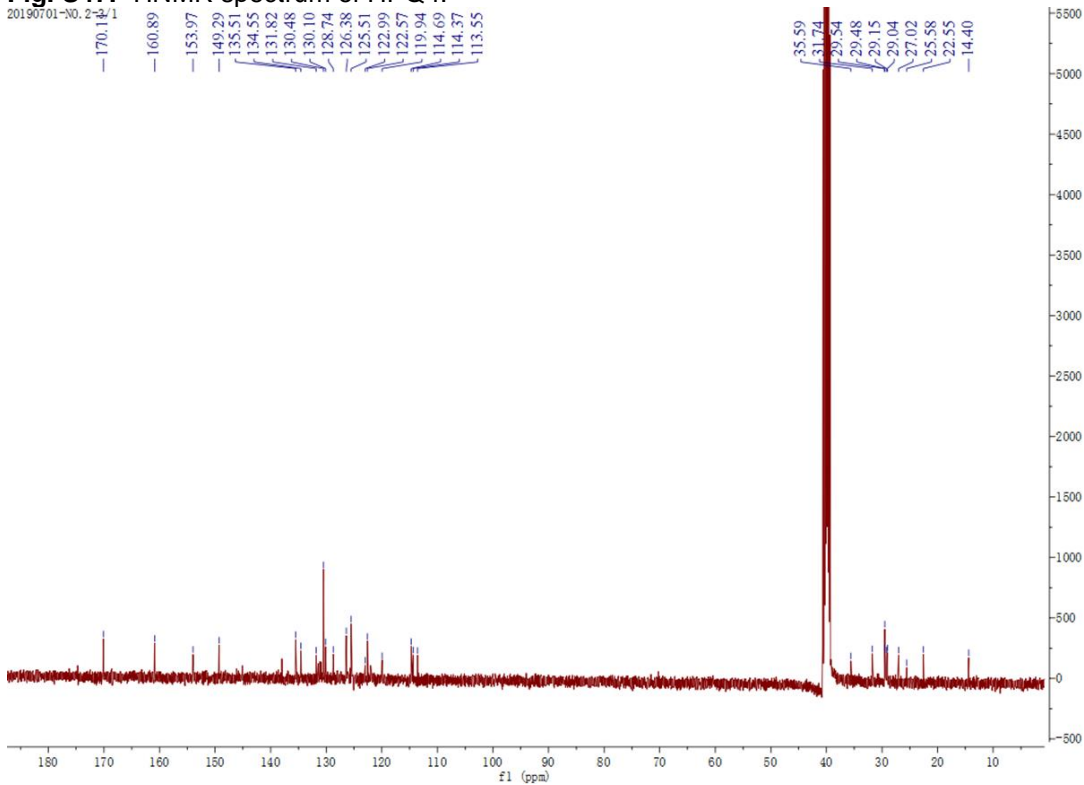


Fig. S48. <sup>13</sup>C NMR spectrum of HPQ4.

20190606-N0.2-23/1

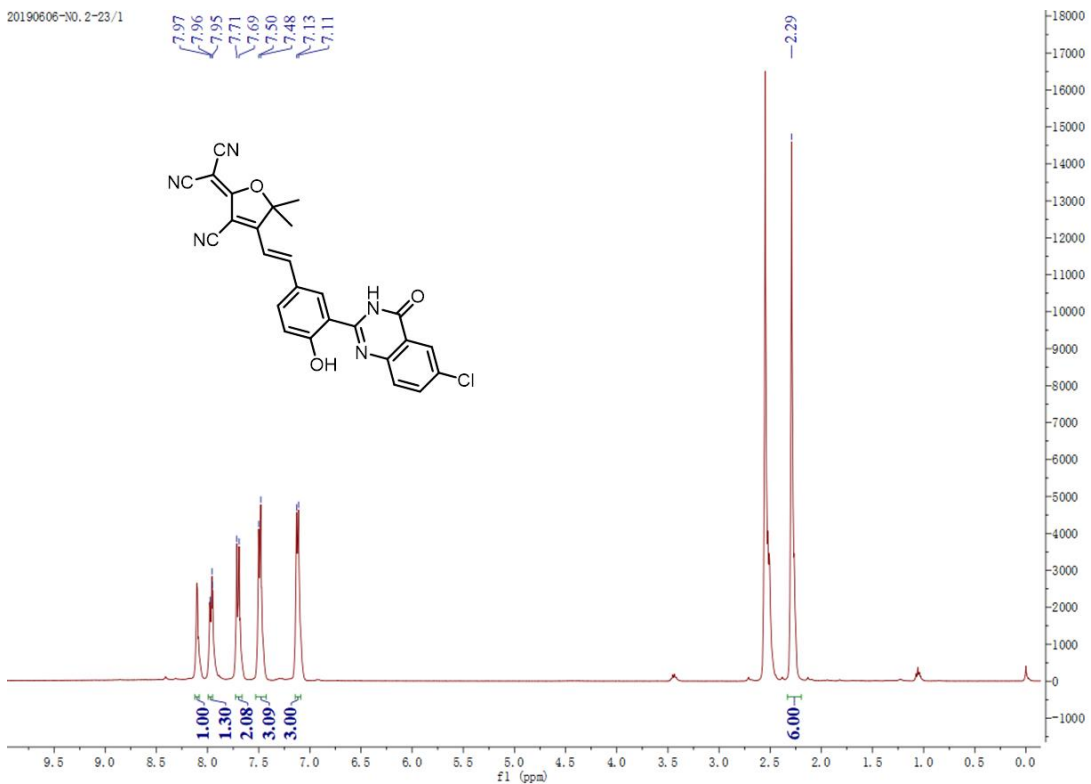


Fig. S49.  $^1\text{H NMR}$  spectrum of HPQ5.

20190606-N0.2-23/2

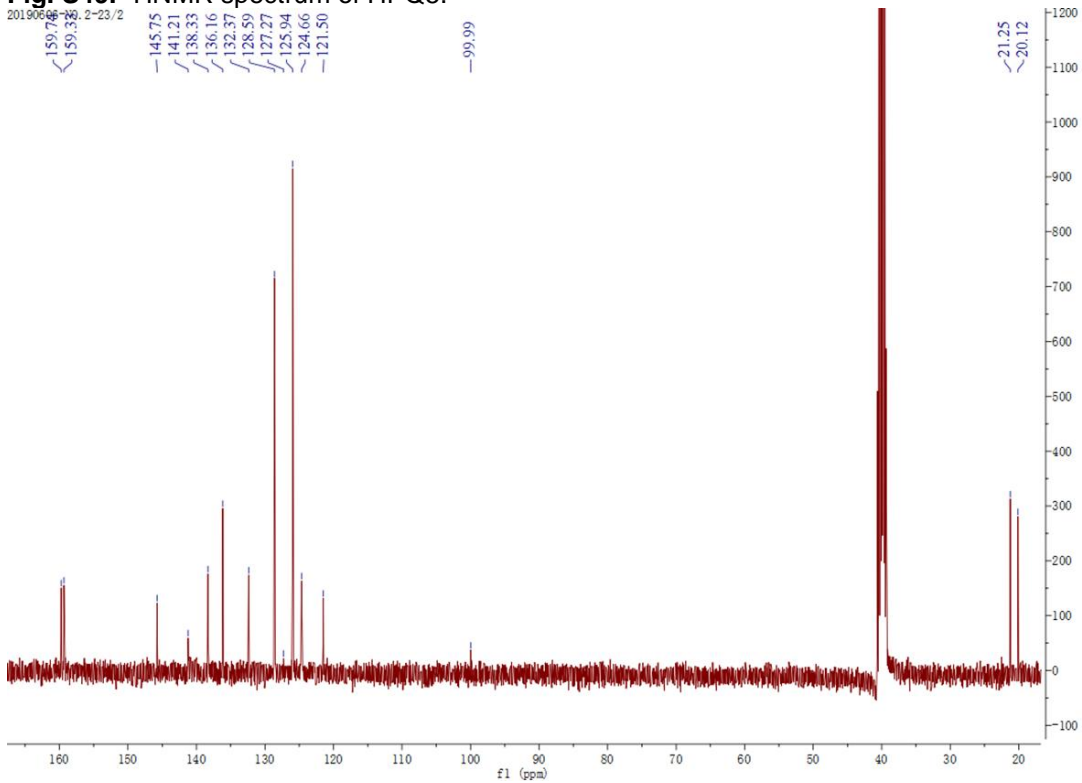


Fig. S50.  $^{13}\text{C NMR}$  spectrum of HPQ5.

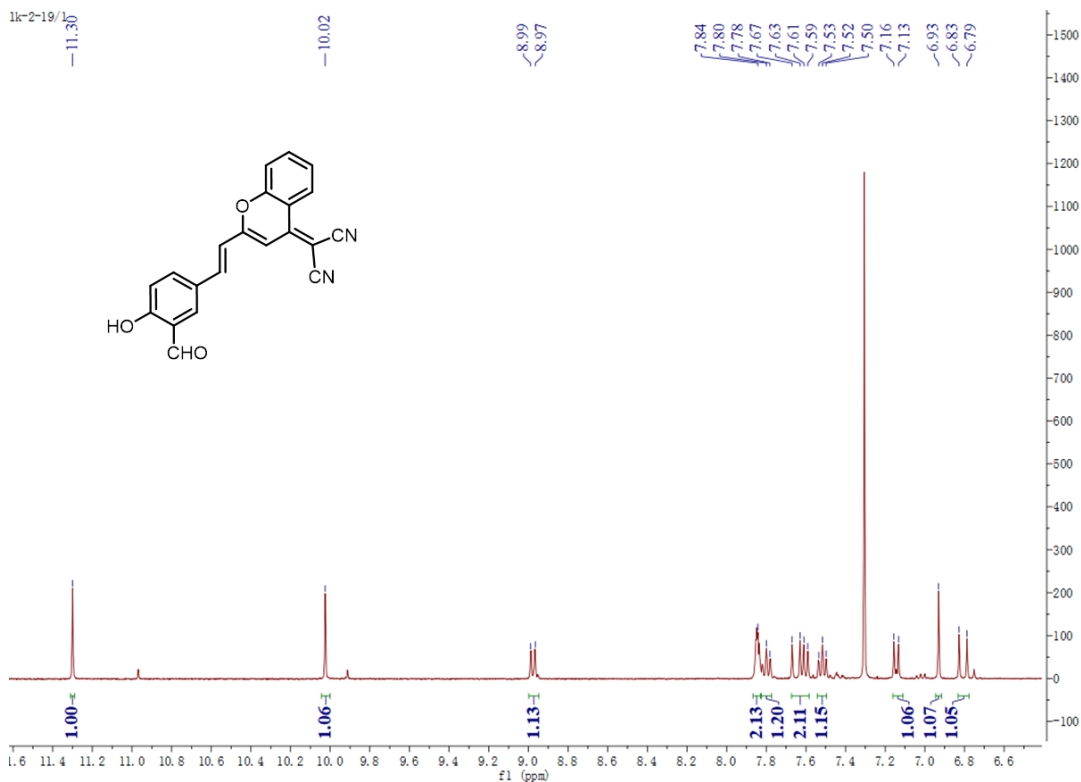


Fig. S51. <sup>1</sup>H NMR spectrum of compound 9.

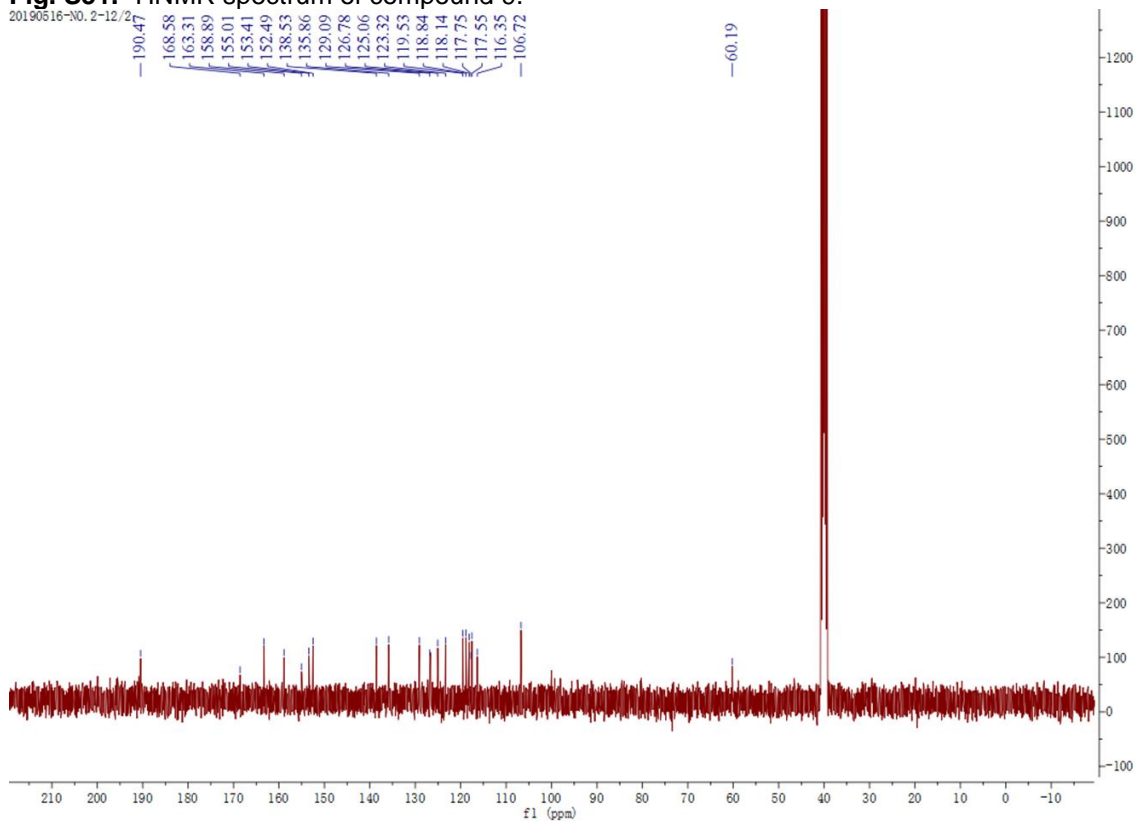


Fig. S52. <sup>13</sup>C NMR spectrum of compound 9.

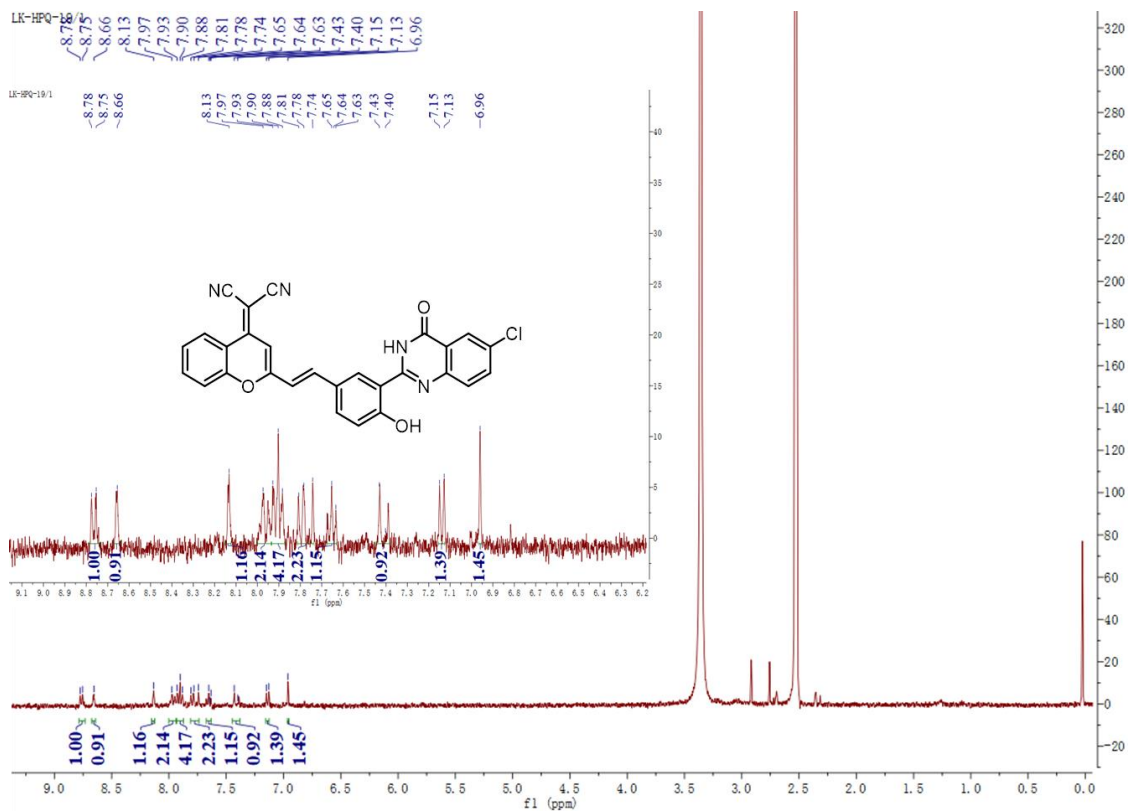


Fig. S53. <sup>1</sup>H NMR spectrum of HYPQ.

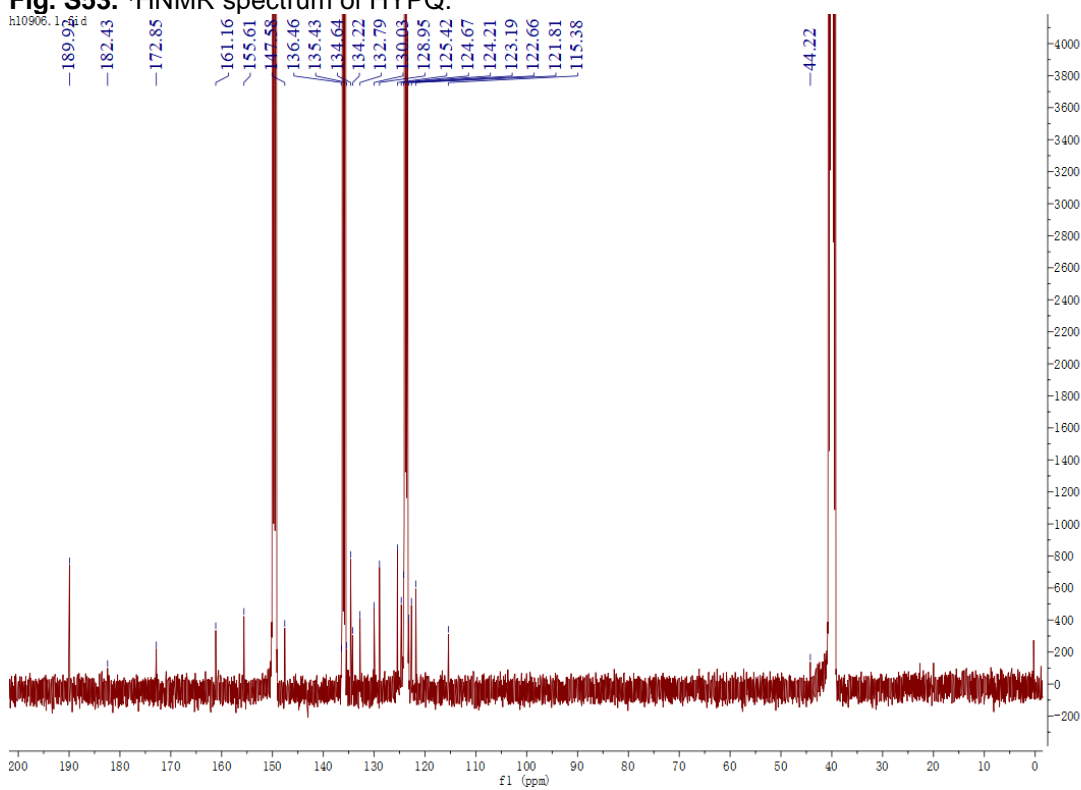


Fig. S54. <sup>13</sup>C NMR spectrum of HYPQ.

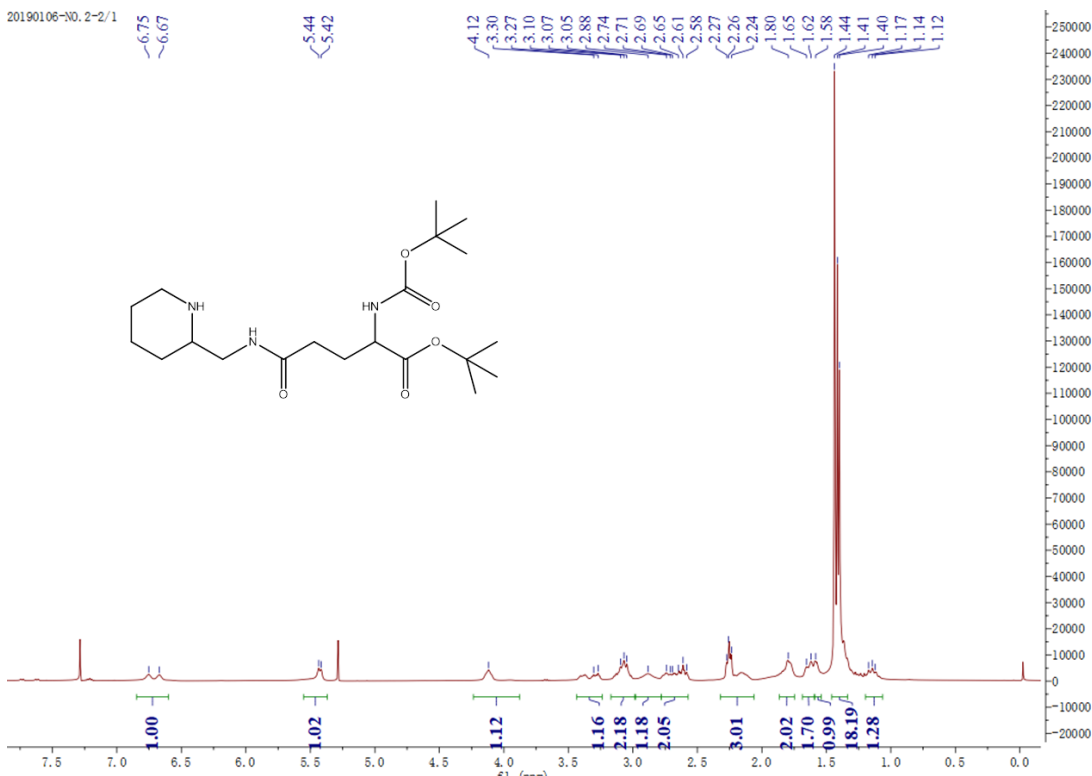


Fig. S55. <sup>1</sup>H NMR spectrum of compound 11.

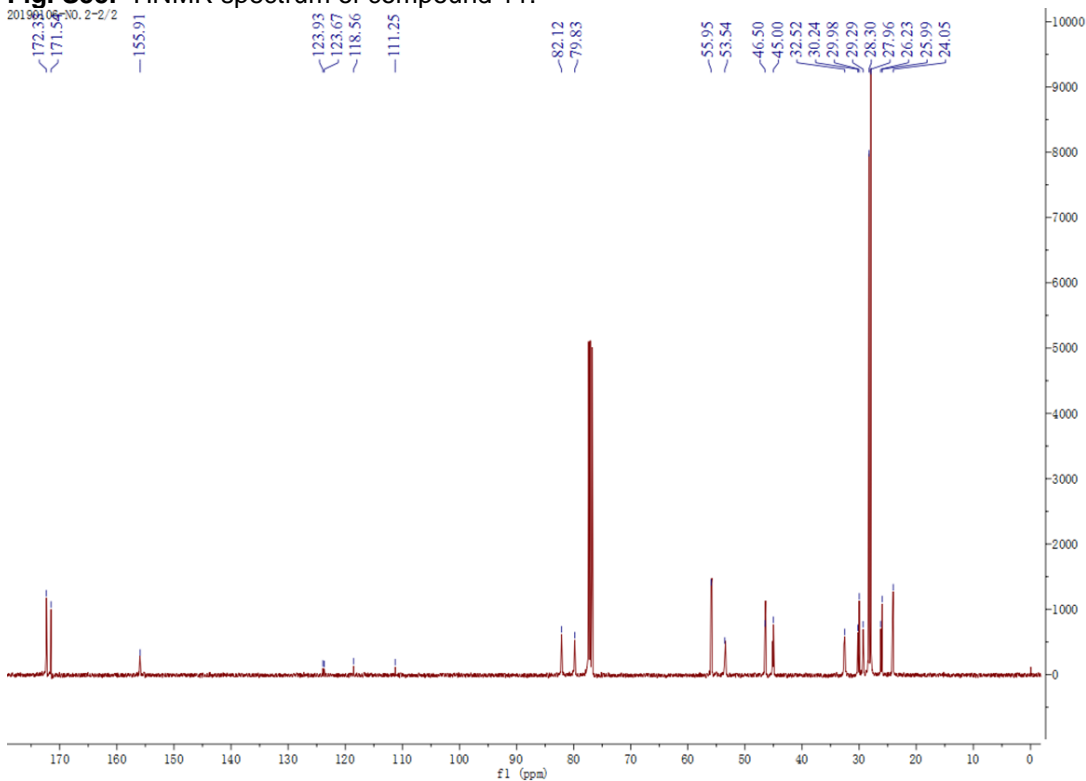
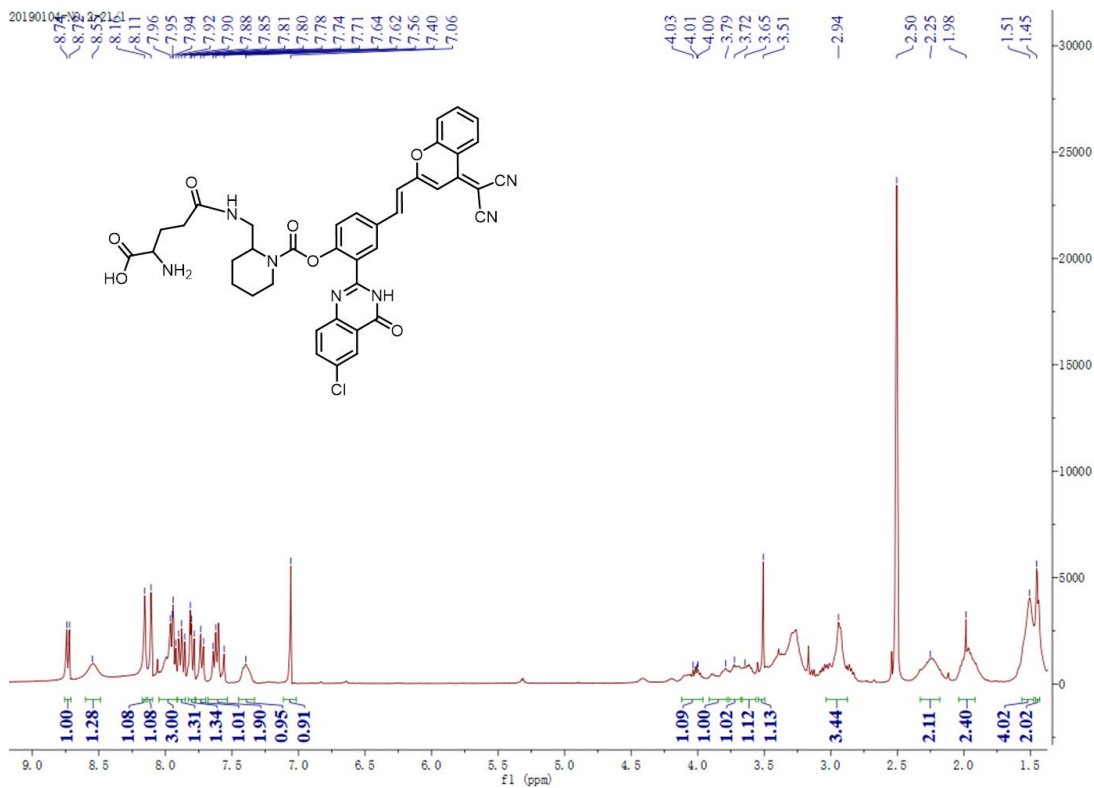
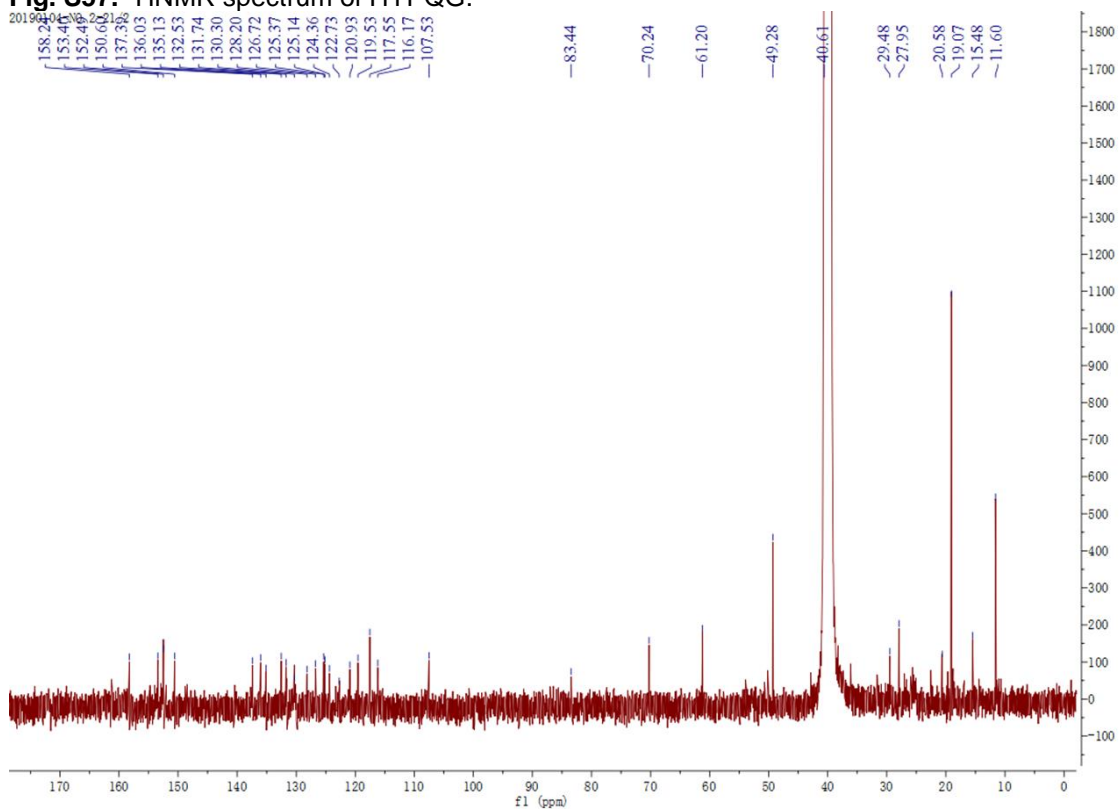


Fig. S56. <sup>13</sup>C NMR spectrum of compound 11.

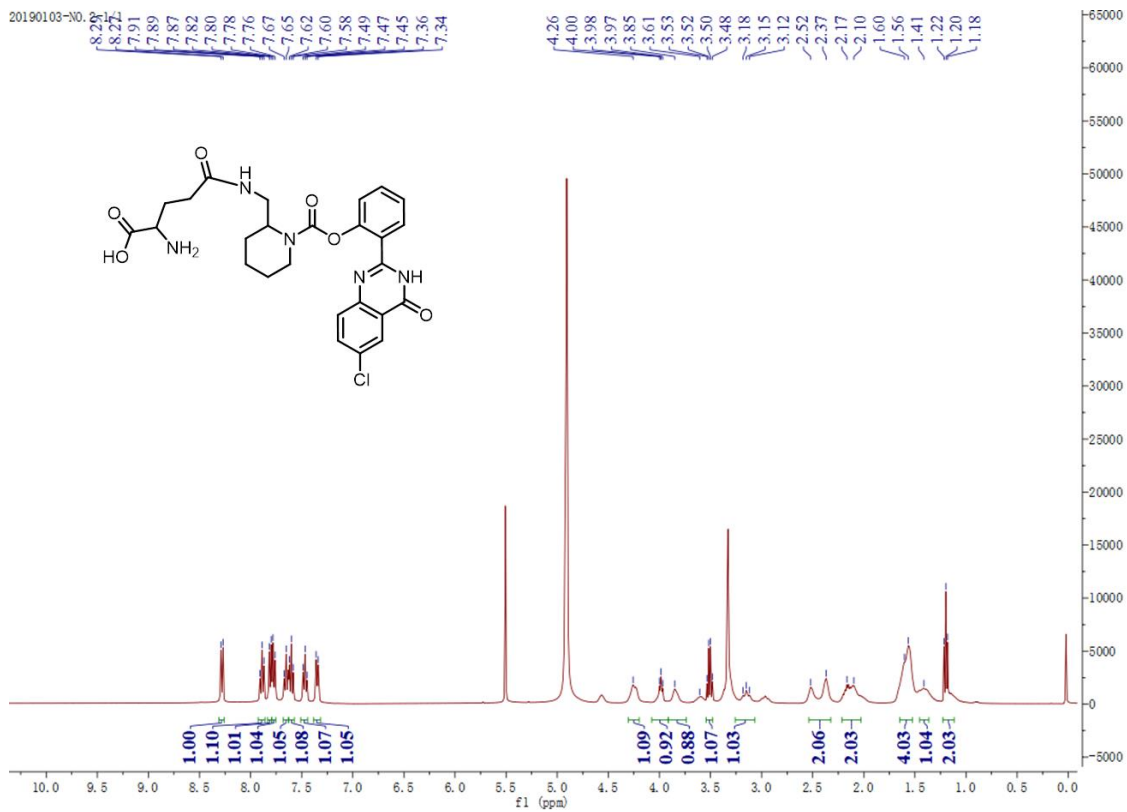


**Fig. S57.**  $^1\text{H}$ NMR spectrum of HYPQG.

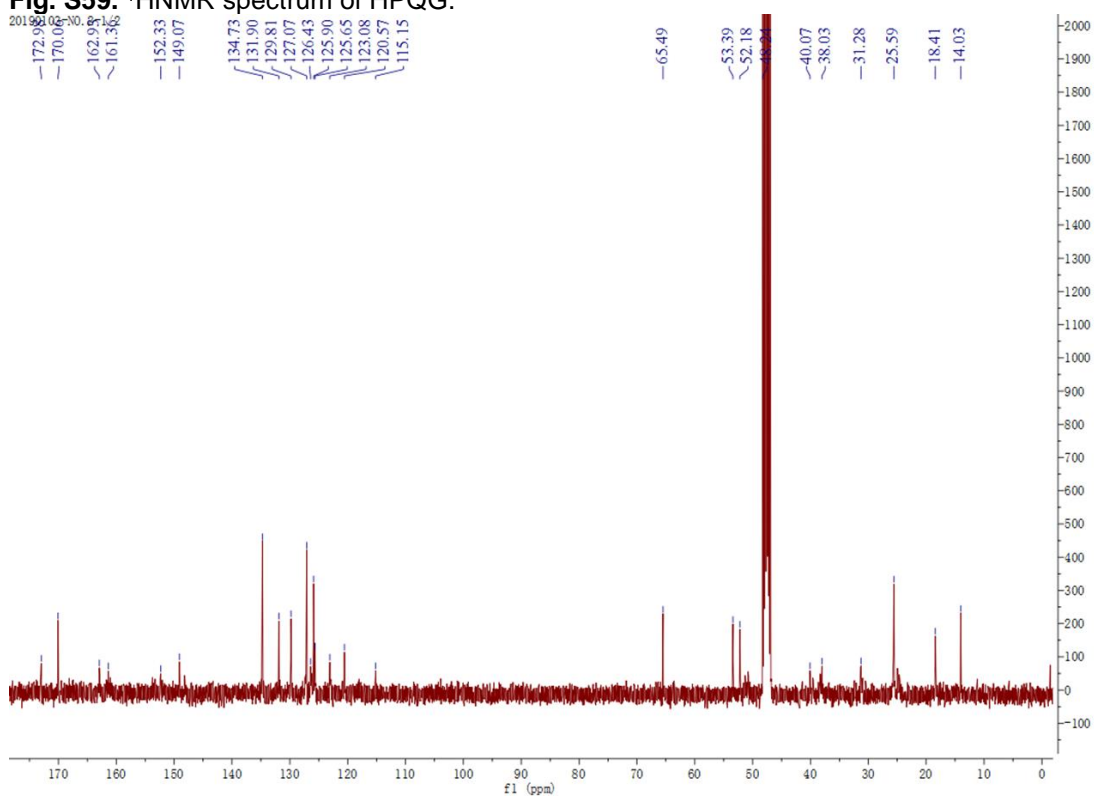


**Fig. S58.**  $^{13}\text{C}$ NMR spectrum of HYPQG.

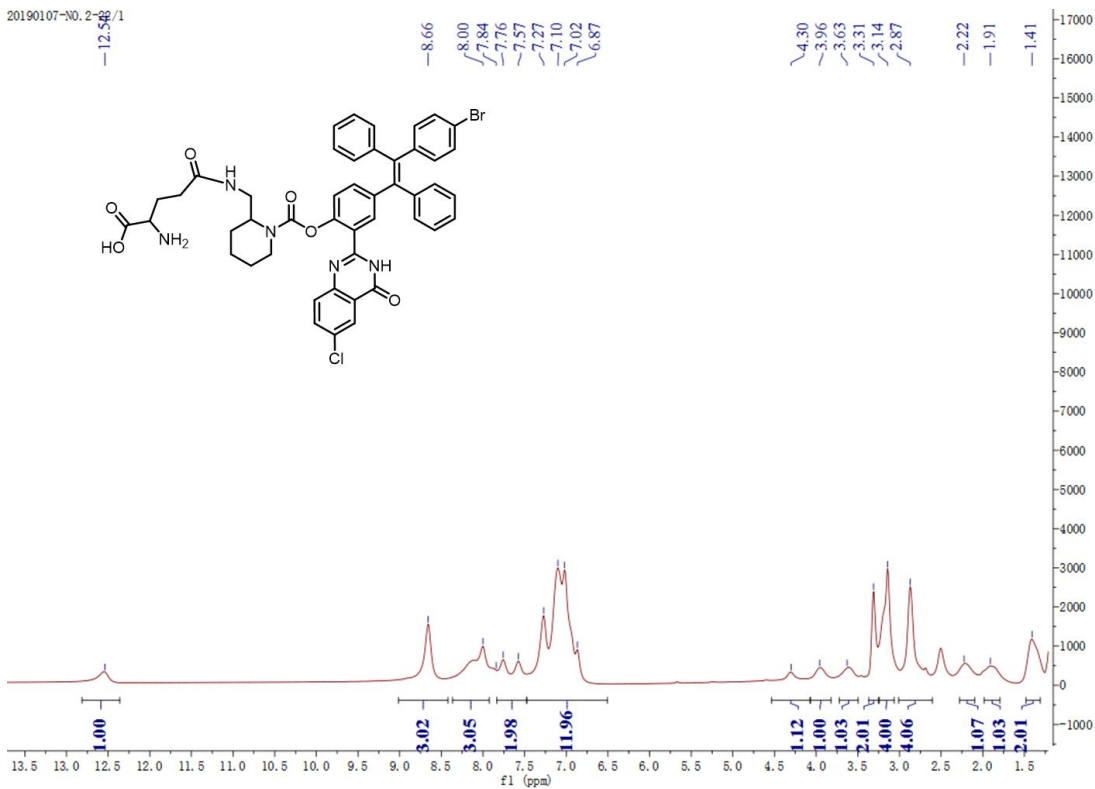




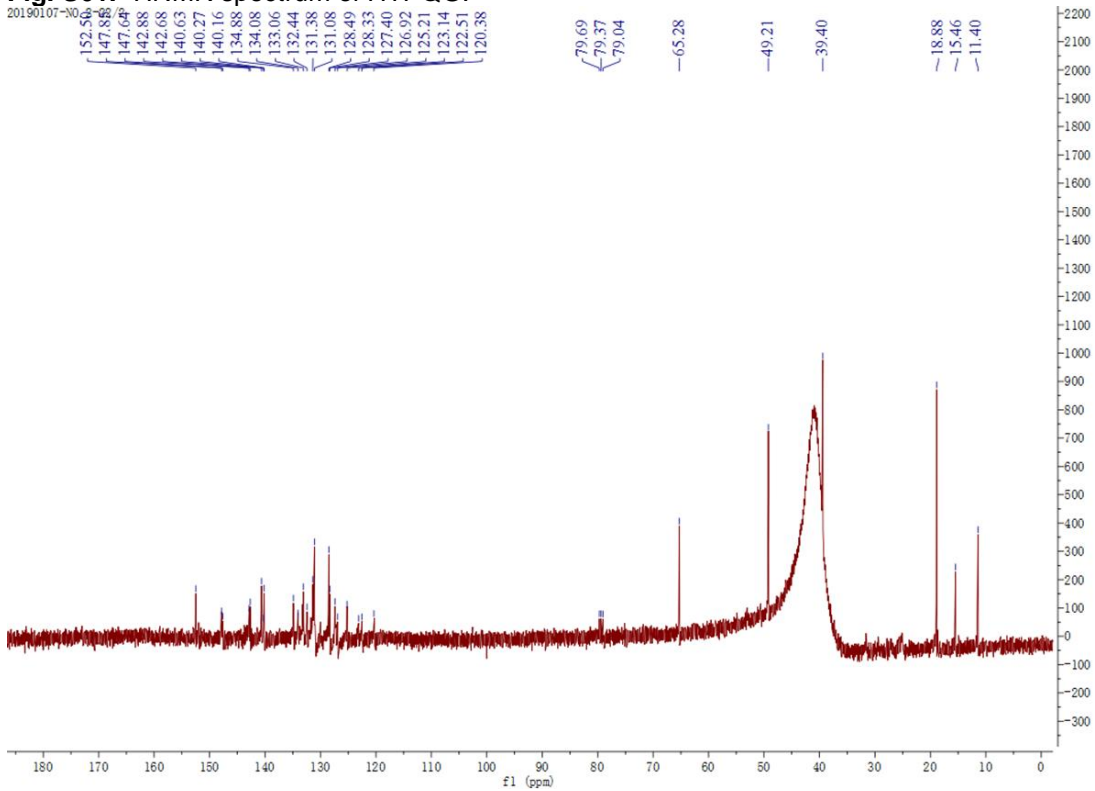
**Fig. S59.**  $^1\text{H}$ NMR spectrum of HPQG.



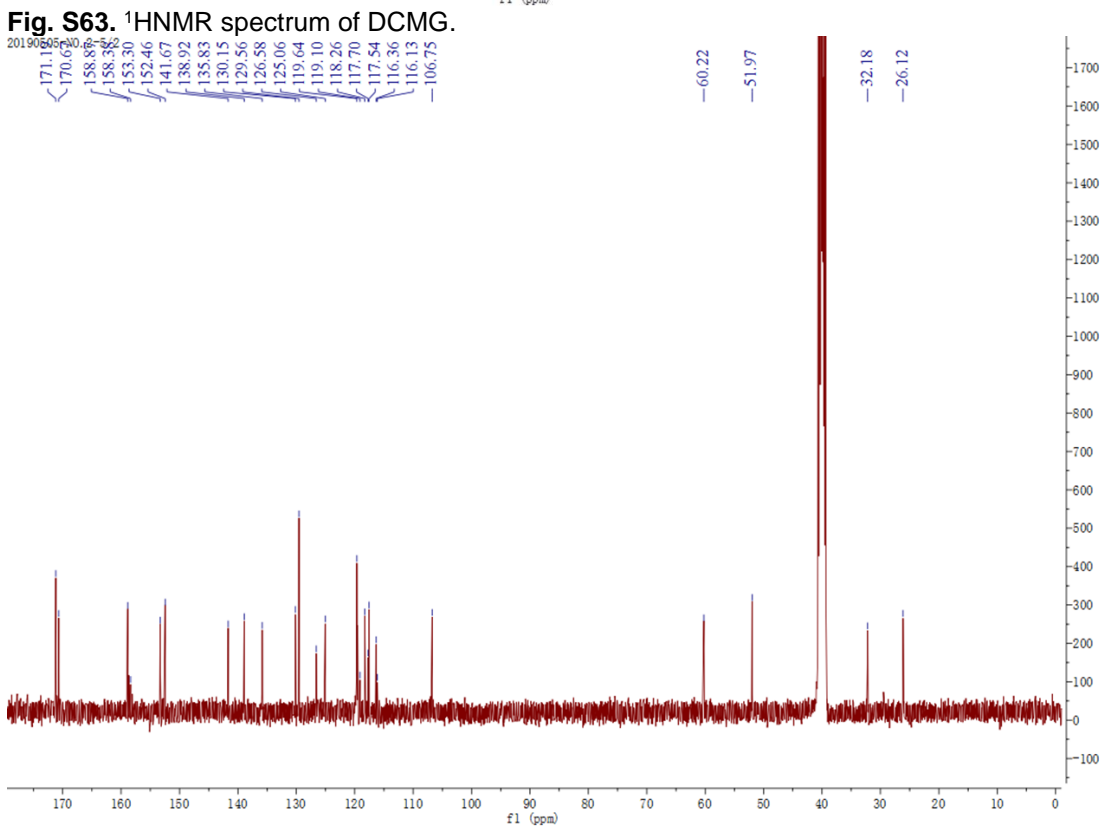
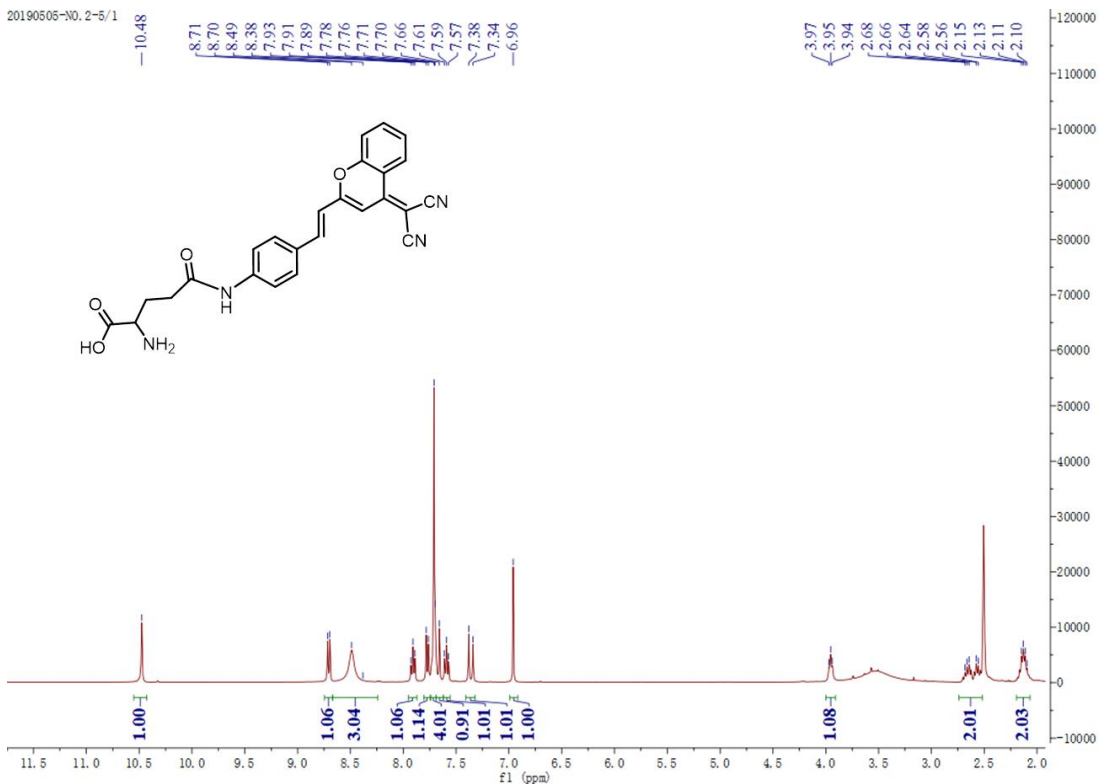
**Fig. S60.**  $^{13}\text{C}$ NMR spectrum of HPQG.



**Fig. S61.**  $^1\text{H}$ NMR spectrum of HTPQG.



**Fig. S62.**  $^{13}\text{C}$ NMR spectrum of HTPQG.



1k-1-13/1

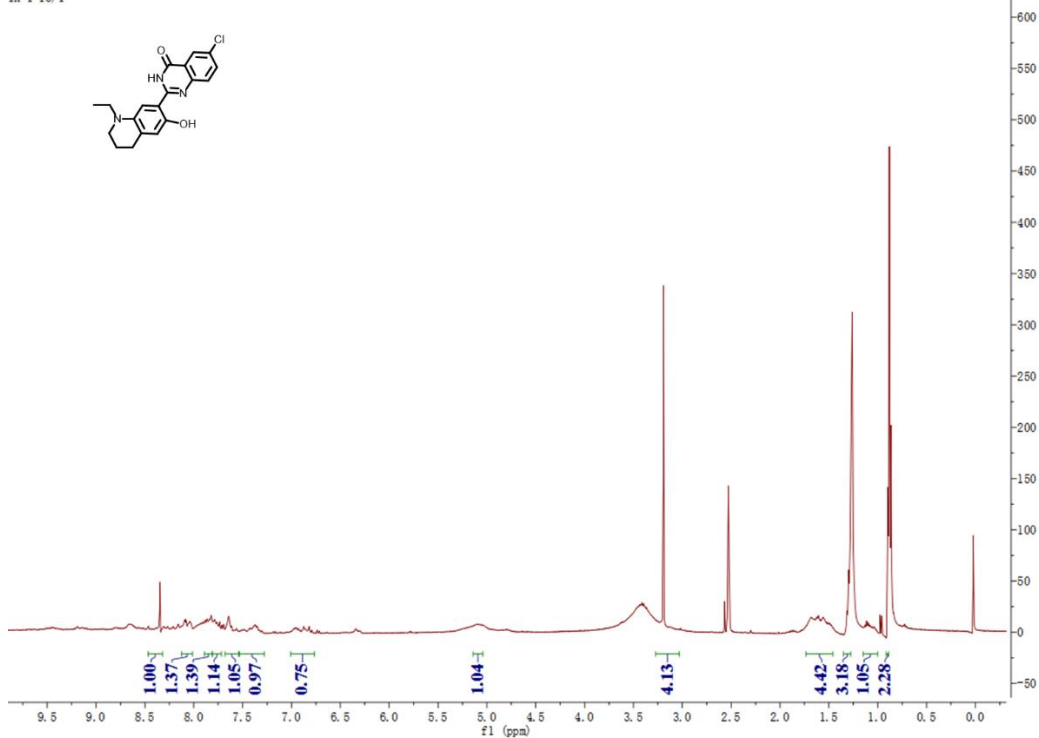


Fig. S65. <sup>1</sup>H NMR spectrum of HPQ-N.

1k1-1/1

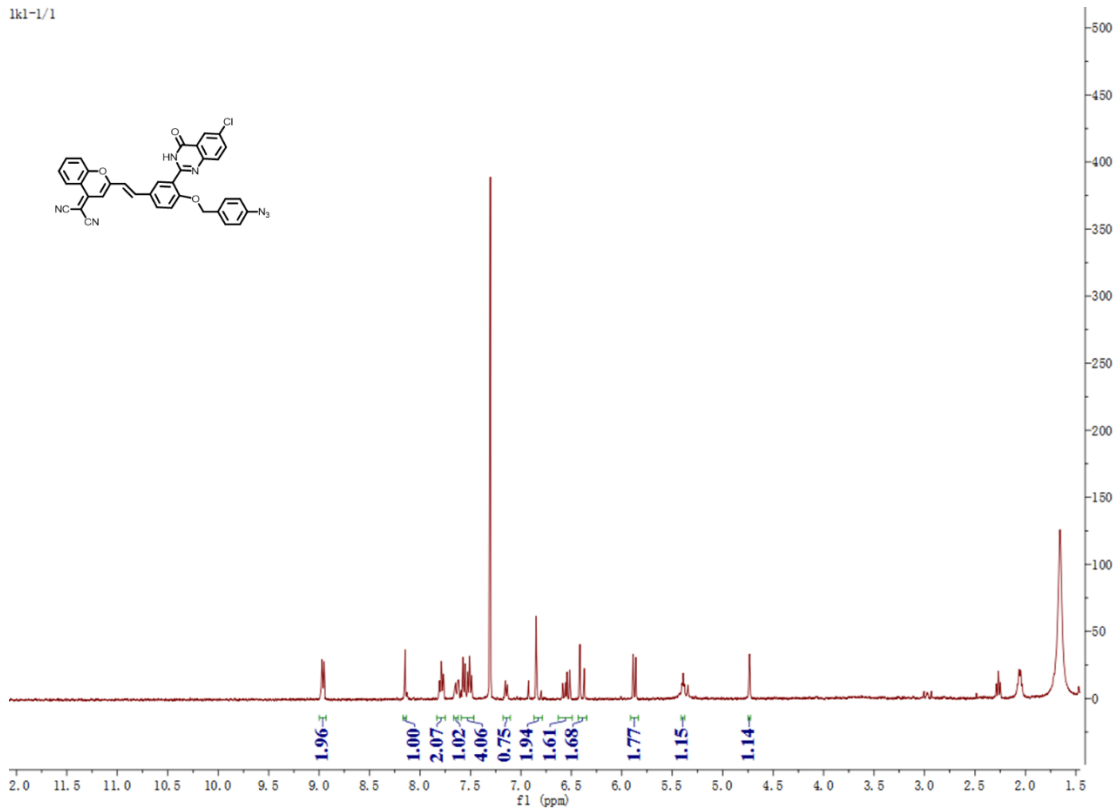


Fig. S66. <sup>1</sup>H NMR spectrum of HYPQ-photoactivatable.

光谱/1

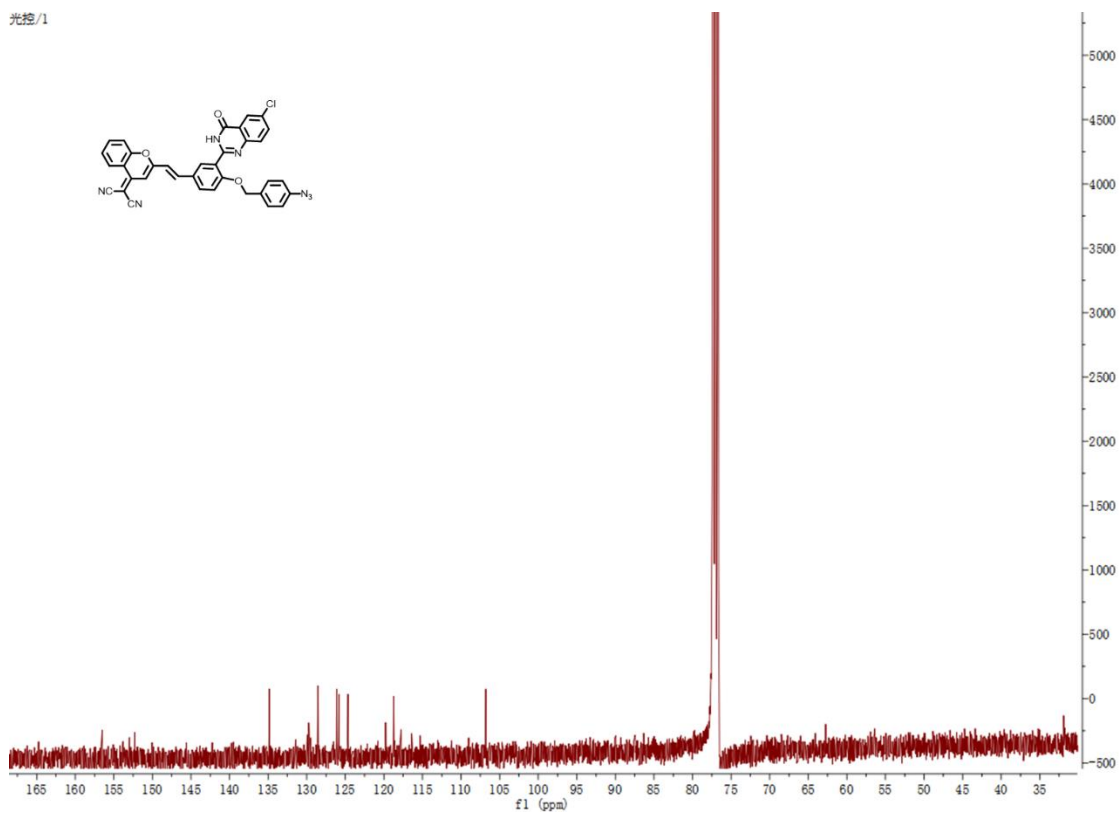


Fig. S67. <sup>13</sup>CNMR spectrum of HYPQ-photoactivatable

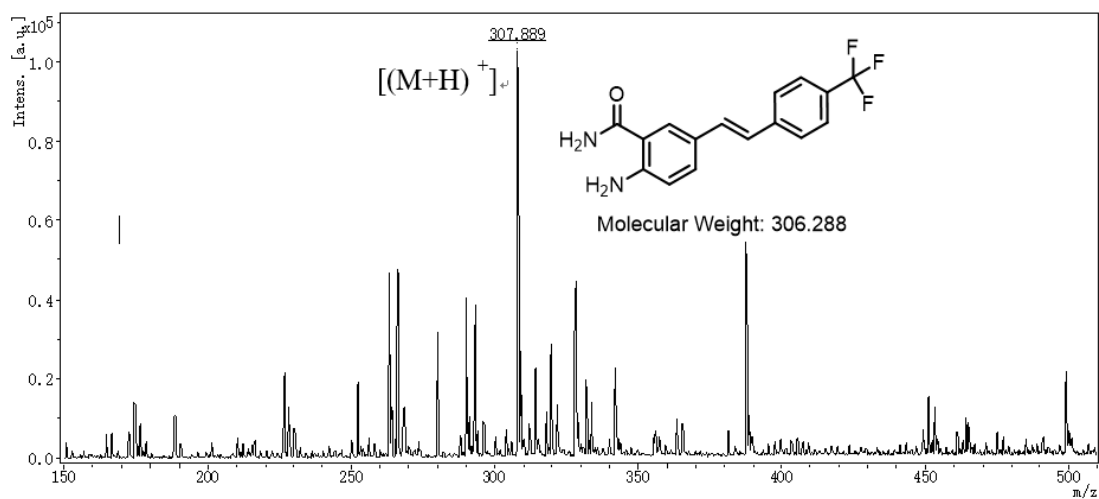
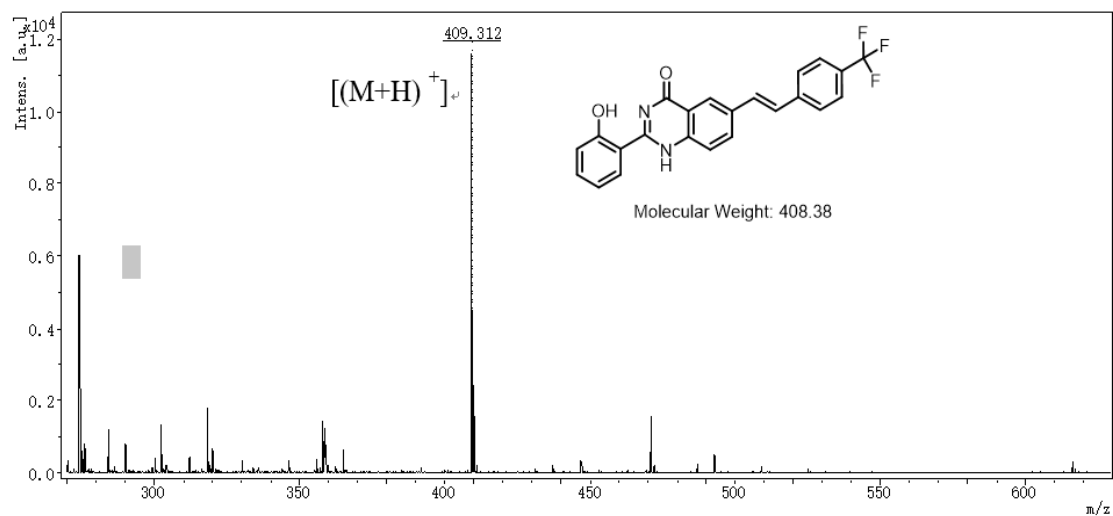
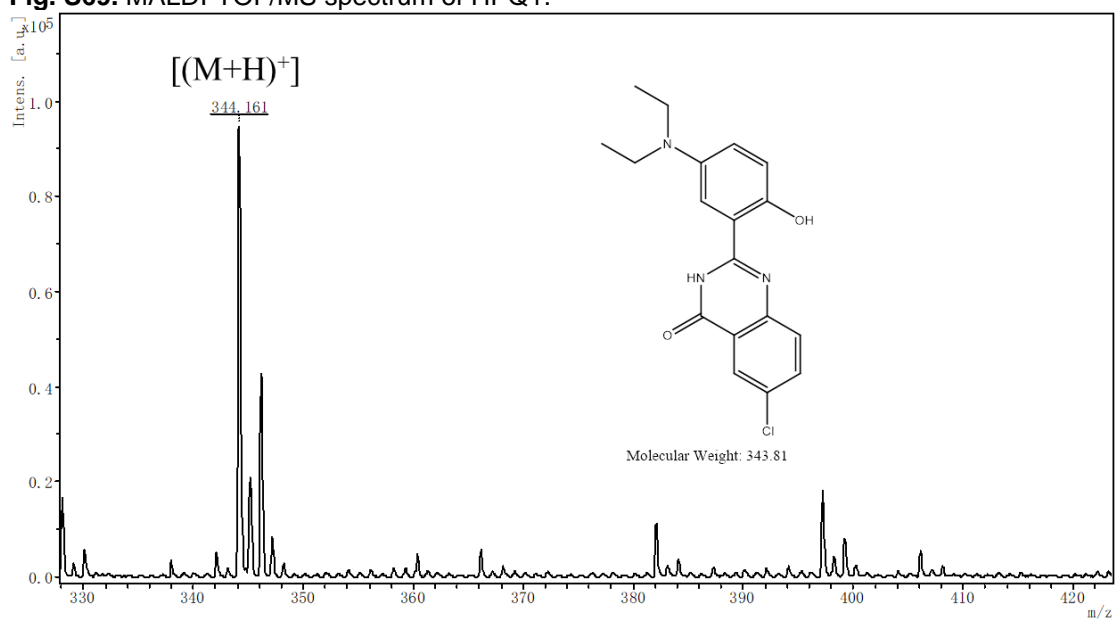


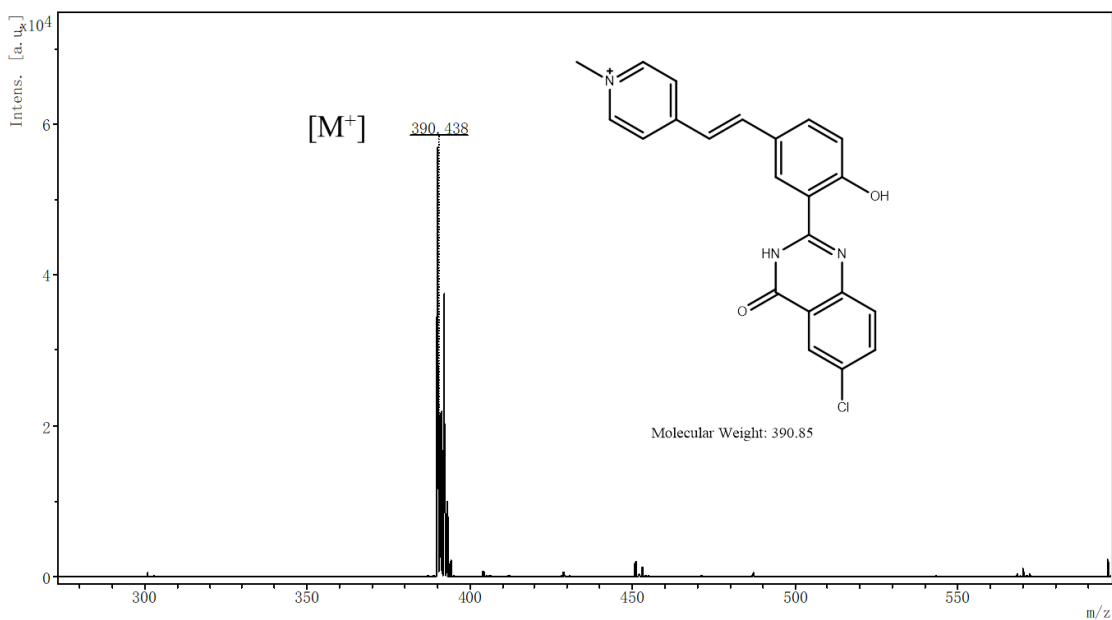
Fig. S68. MALDI-TOF/MS spectrum of compound 3.



**Fig. S69.** MALDI-TOF/MS spectrum of HPQ1.

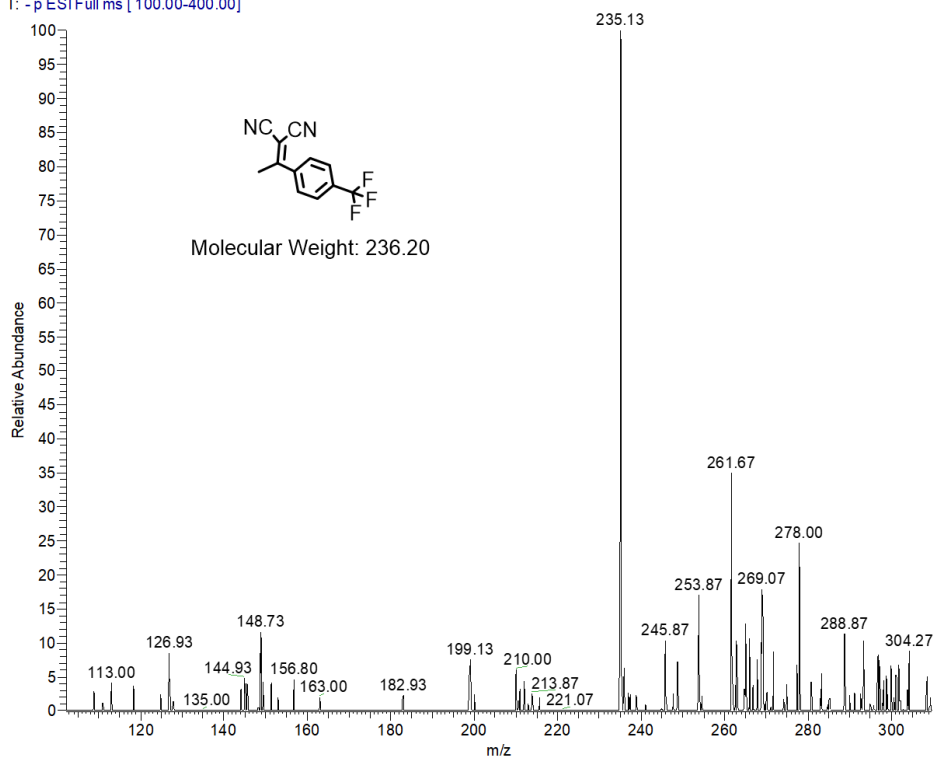


**Fig. S70.** MALDI-TOF/MS spectrum of HPQ2.

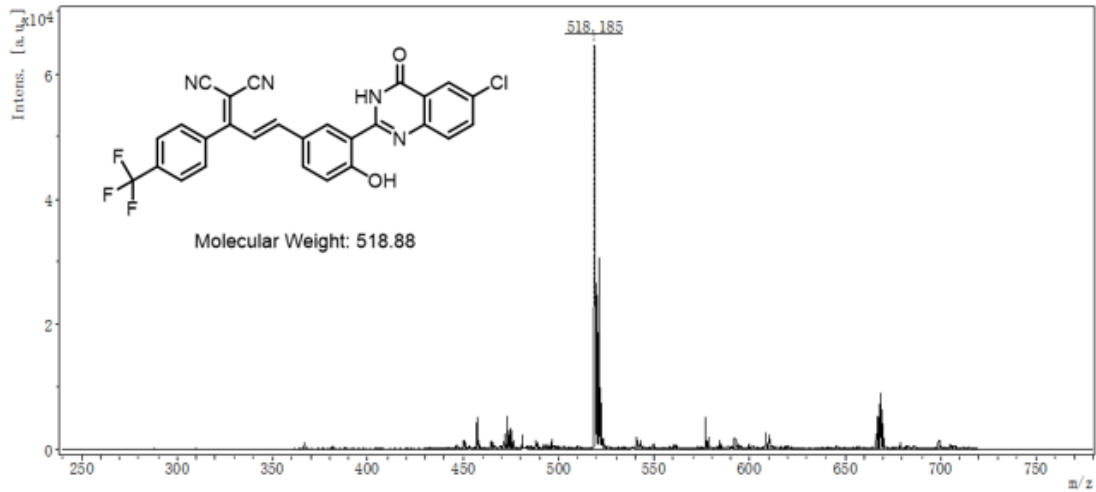


**Fig. S71.** MALDI-TOF/MS spectrum of HPQ3.

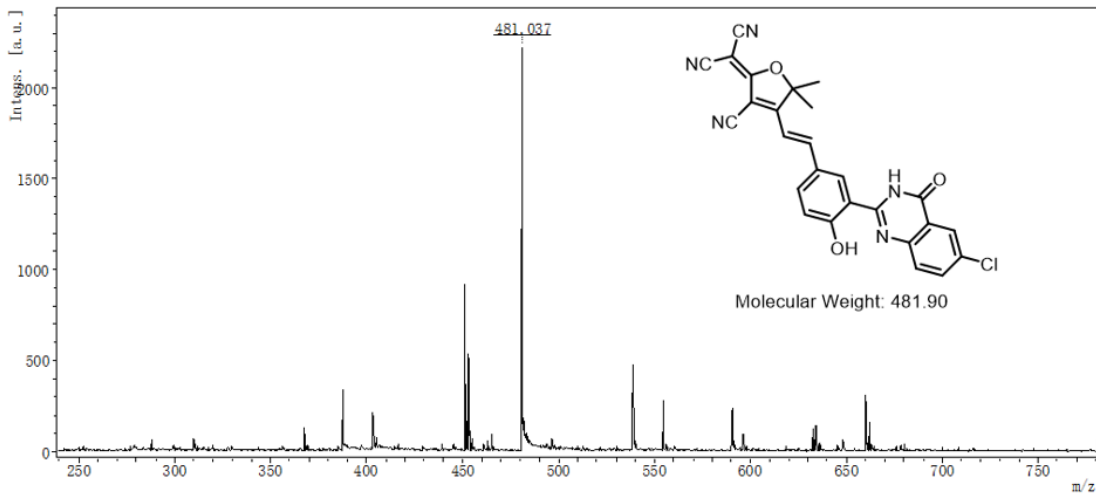
236-1 #189 RT: 1.75 AV: 1 NL: 1.71E5  
T: -p ESI Full ms [100.00-400.00]



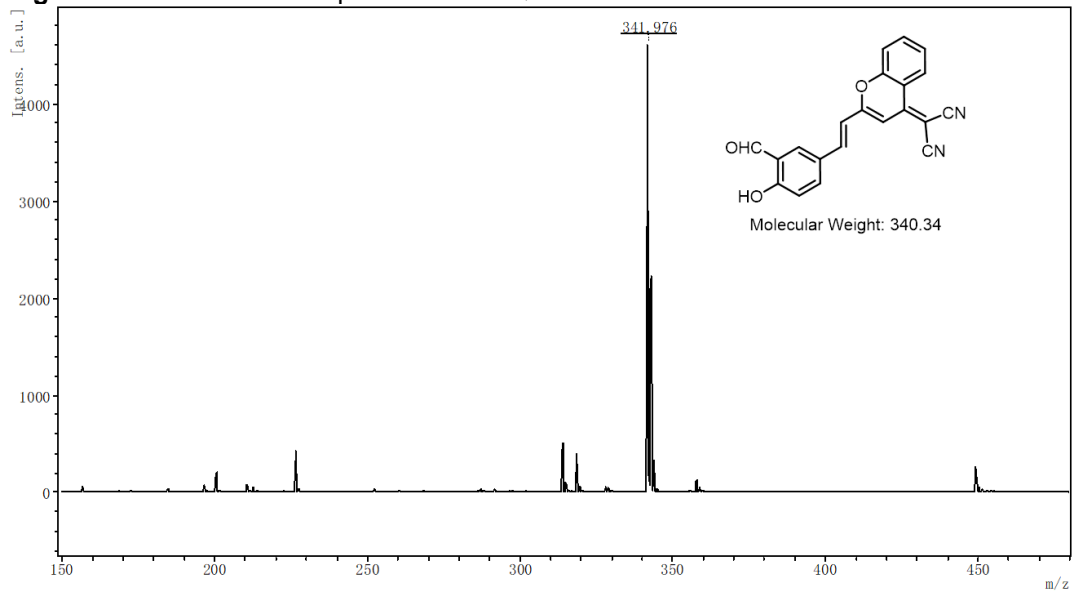
**Fig. S72.** ESI/MS spectrum of compound 7.



**Fig. S73.** MALDI-TOF/MS spectrum of HPQ4.



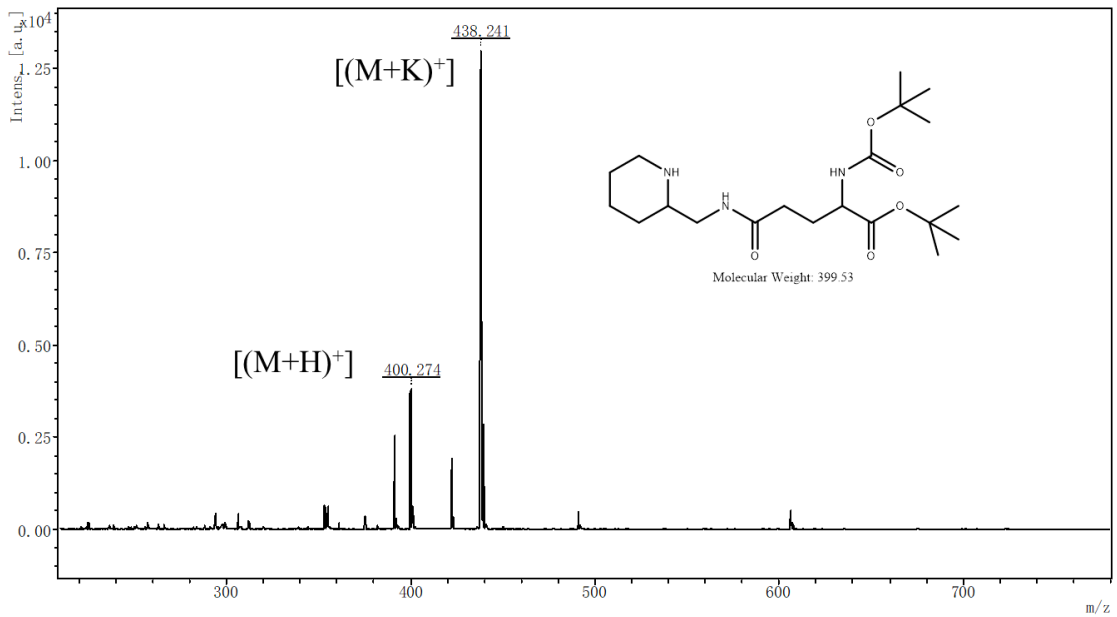
**Fig. S74.** MALDI-TOF/MS spectrum of HPQ5.



**S75.** MALDI-TOF/MS spectrum of compound 9.

**Fig.**

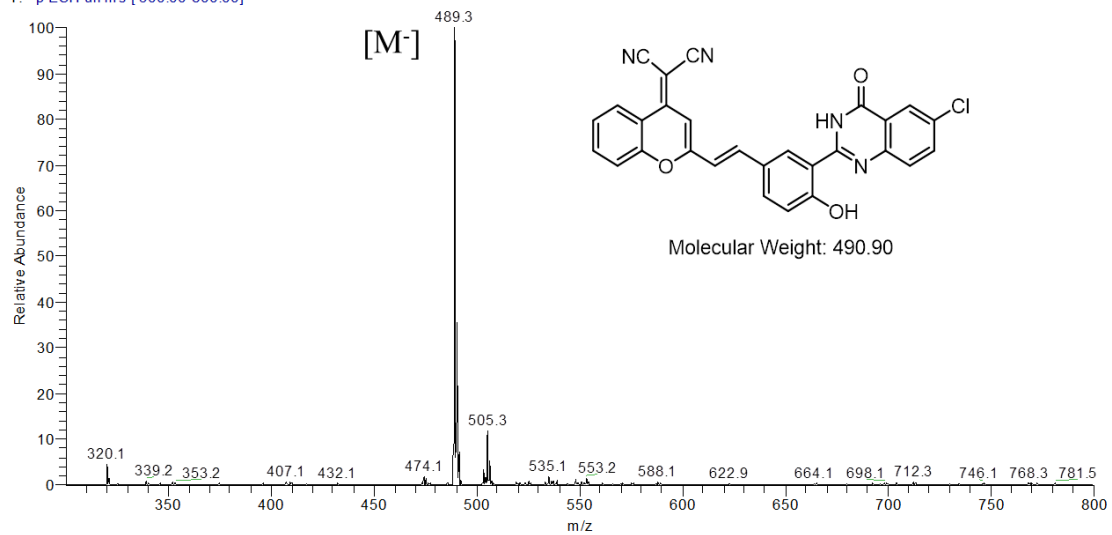




**Fig. S76.** MALDI-TOF/MS spectrum of compound 11.

Ik-490 #26 RT: 0.35 AV: 1 NL: 1.28E6

T: -p ESI Full ms [300.00-800.00]



**Fig. S77.** ESI mass spectrum of compound HYPQ.

LK-2

21-Mar-2019

YL-29 24 (0.414) AM (Cen,4, 80.00, Ht,5000.0,0.00,1.00); Sm (Mn, 2x3.00); Cm (1:38)

TOF MS ES+

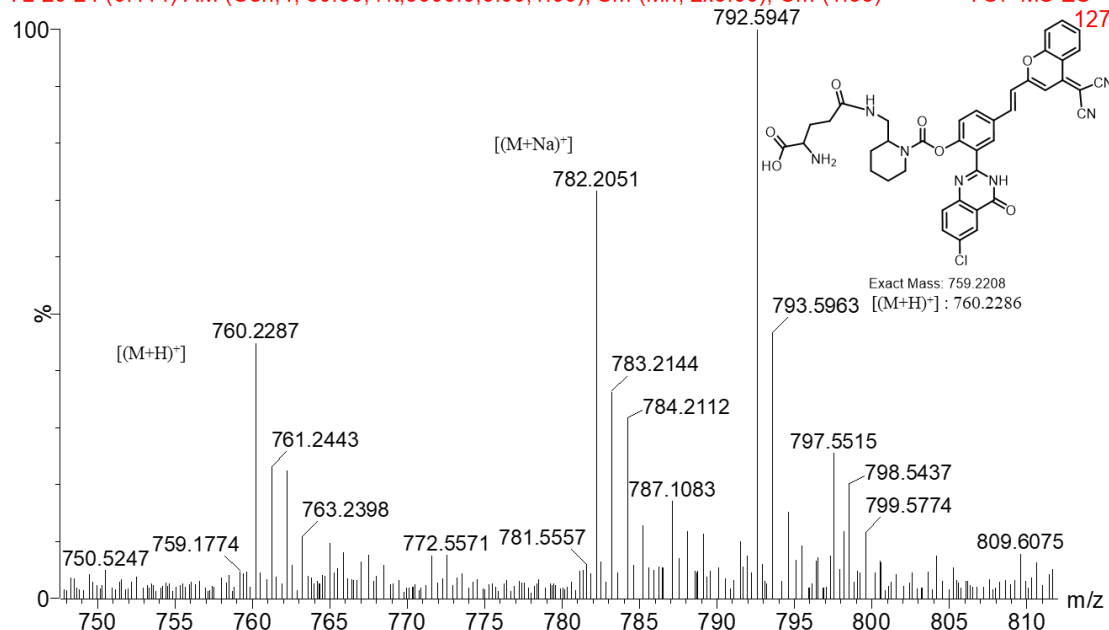


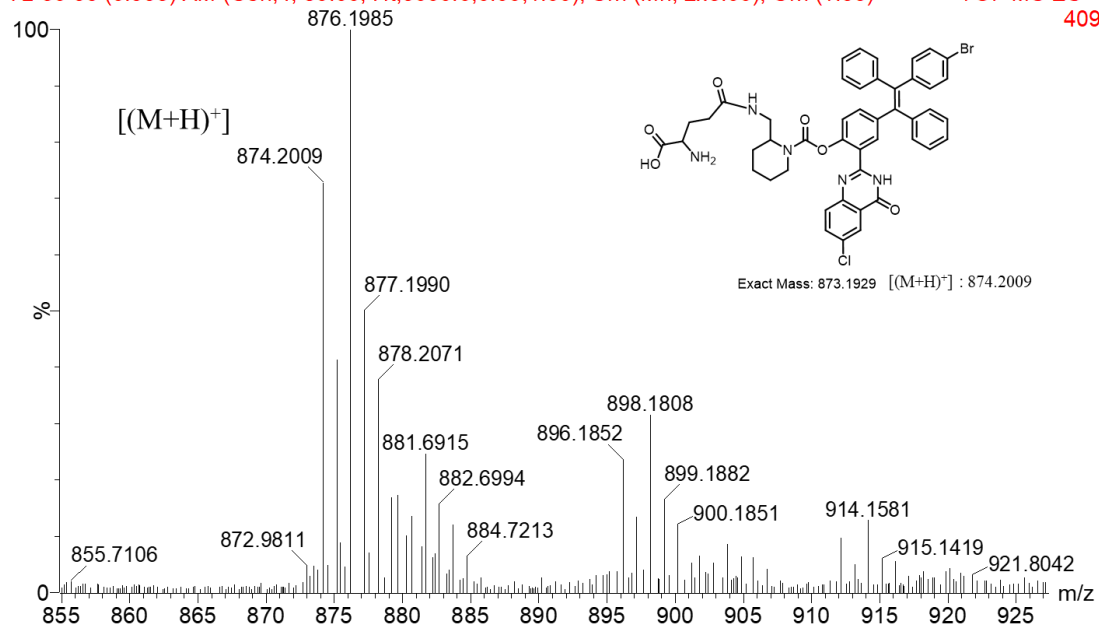
Fig. S78. HRMS mass spectrum of compound HYPQG.

LK-3

21-Mar-2019

YL-30 56 (0.963) AM (Cen,4, 80.00, Ht,5000.0,0.00,1.00); Sm (Mn, 2x3.00); Cm (1:56)

TOF MS ES+



S79. HRMS mass spectrum of compound HTPQG.

Fig.

LK-1

12-Jul-2019

YL-36 2 (0.034) AM (Cen,4, 80.00, Ht,5000.0,0.00,1.00); Sm (Mn, 2x3.00); Cm (1:25)

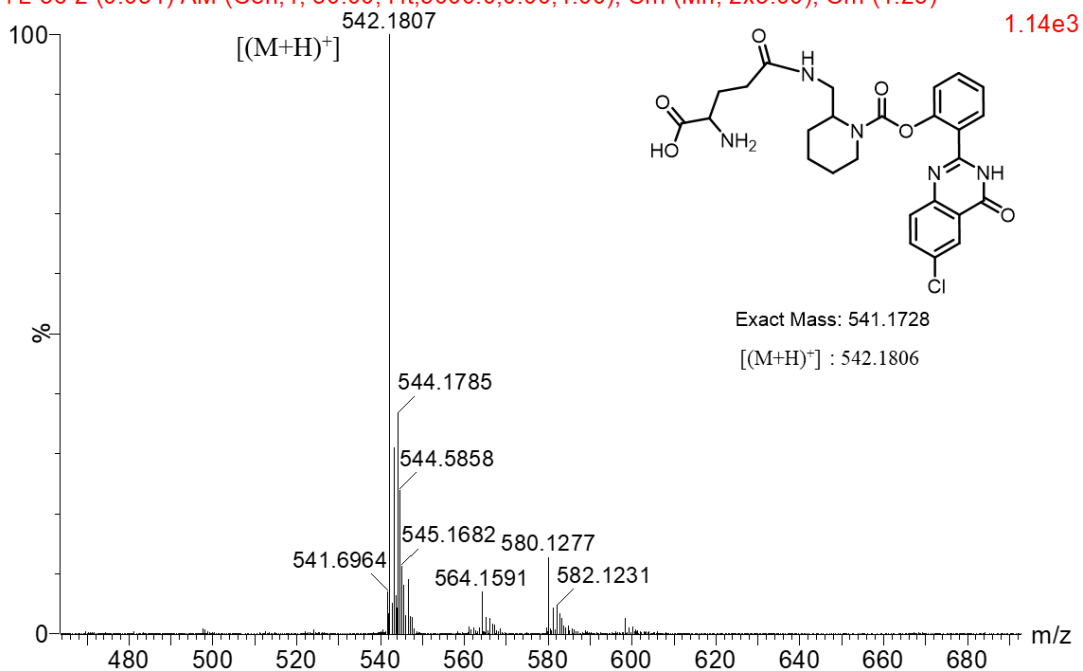


Fig. S80. HRMS mass spectrum of compound HPQG.

LK-2

12-Jul-2019

YL-37 11 (0.190) AM (Cen,4, 80.00, Ht,5000.0,0.00,1.00); Sm (Mn, 2x3.00); Cm (1:23)

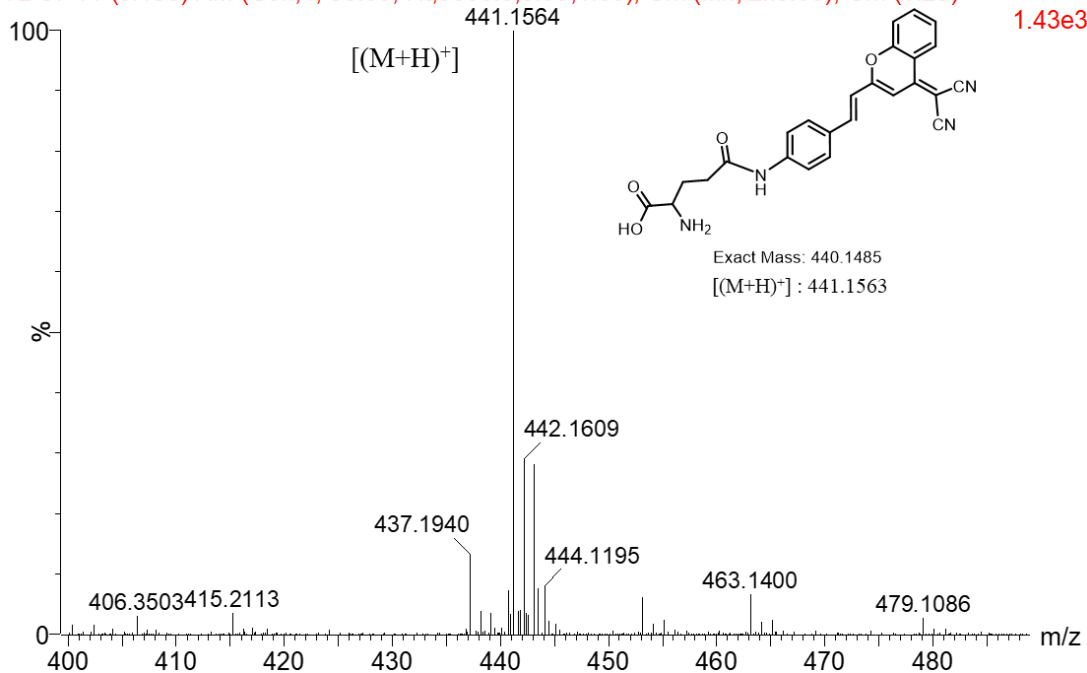
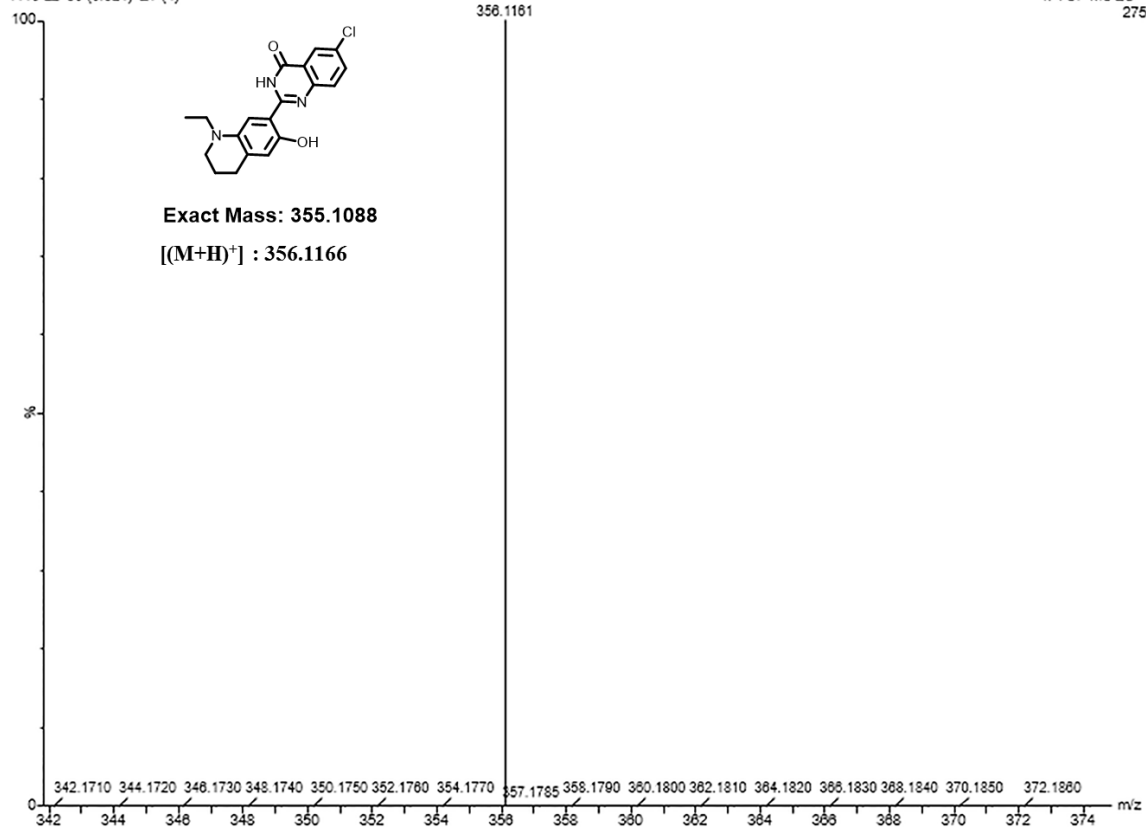


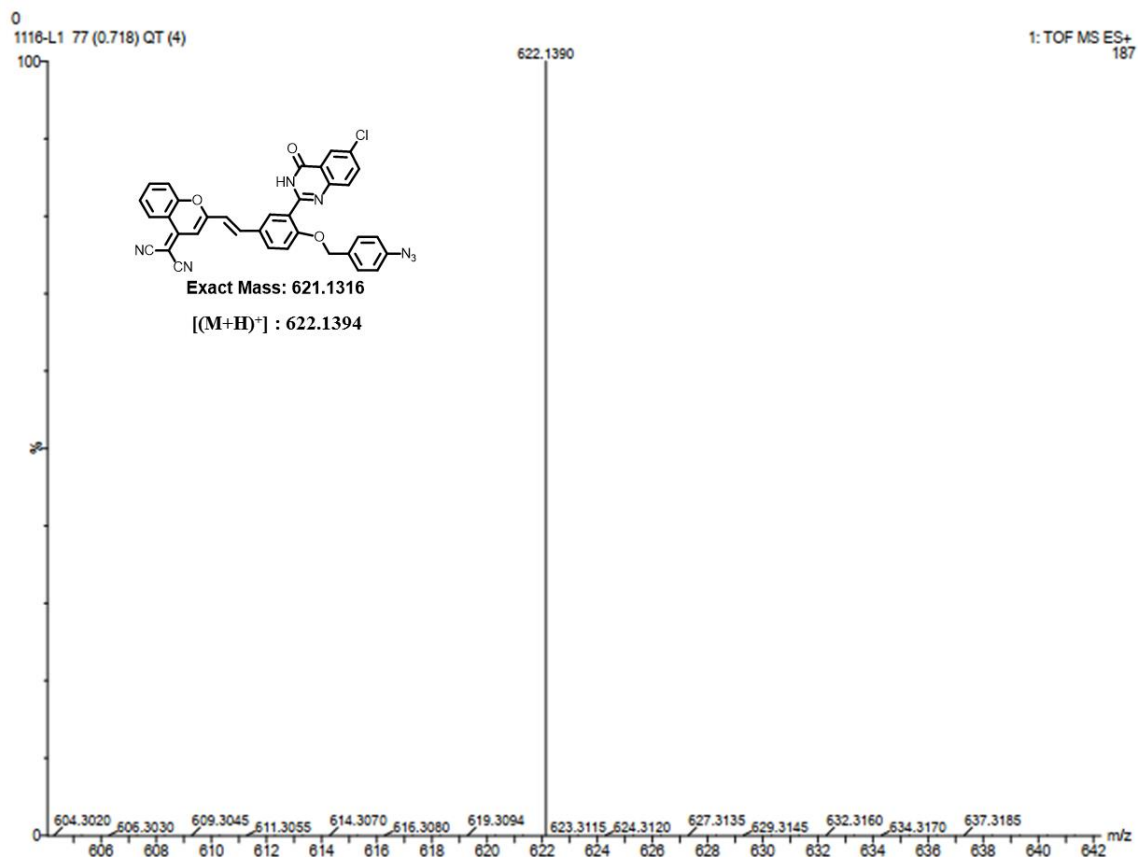
Fig. S81. HRMS mass spectrum of compound DCMG.

1116-L2 89 (0.821) QT (4)

1: TOF MS ES+  
275



**Fig. S82.** HRMS mass spectrum of compound HPQ-N.



**Fig. S83.** HRMS mass spectrum of compound HYPQ-photoactivatable.

## Detail crystallographic data

**Table S7.**

### Crystal data and structure refinement for HPQ. (CCDC: 2045408)

Identification code	HPQ	
Empirical formula	C <sub>14</sub> H <sub>9</sub> Cl N <sub>2</sub> O <sub>2</sub>	
Formula weight	272.68	
Temperature	293(2) K	
Wavelength	1.54184 Å	
Crystal system	Monoclinic	
Space group	P-1	
Unit cell dimensions	a = 7.7209(4) Å	a = 90°.
b = 5.9660(3) Å	b = 96.453(5)°.	
c = 26.5444(10) Å	g = 90°.	
Volume	1214.97(10) Å <sup>3</sup>	
Z	4	
Density (calculated)	1.491 Mg/m <sup>3</sup>	
Absorption coefficient	2.785 mm <sup>-1</sup>	
F(000)	560	
Crystal size	0.1 x 0.05 x 0.05 mm <sup>3</sup>	
Theta range for data collection	3.351 to 66.598°.	
Index ranges	-9 ≤ h ≤ 8, -7 ≤ k ≤ 7, -31 ≤ l ≤ 31	
Reflections collected	13952	
Independent reflections	2145 [R(int) = 0.0461]	
Completeness to theta = 66.598°	100.0 %	
Absorption correction	Semi-empirical from equivalents	
Max. and min. transmission	1.00000 and 0.78632	
Refinement method	Full-matrix least-squares on F <sup>2</sup>	
Data / restraints / parameters	2145 / 0 / 173	
Goodness-of-fit on F <sup>2</sup>	1.040	
Final R indices [I > 2σ(I)]	R1 = 0.0532, wR2 = 0.1600	
R indices (all data)	R1 = 0.0614, wR2 = 0.1683	
Extinction coefficient	n/a	
Largest diff. peak and hole	0.424 and -0.190 e.Å <sup>-3</sup>	

**Table S8. Fractional Atomic Coordinates ( $\times 10^4$ ) and Equivalent Isotropic Displacement Parameters ( $\text{\AA}^2 \times 10^3$ ) for HPQ4.  $U_{\text{eq}}$  is defined as 1/3 of the trace of the orthogonalized  $U_{ij}$  tensor.**

Atom	<i>x</i>	<i>y</i>	<i>z</i>	$U(\text{eq})$
Cl(1)	8037(1)	5710(2)	7358(1)	86(1)
O(1)	5659(2)	9619(3)	5599(1)	54(1)
O(2)	8763(3)	1376(3)	4461(1)	64(1)
N(2)	6504(3)	7305(3)	4993(1)	44(1)
N(1)	8056(3)	3990(3)	5176(1)	46(1)
C(8)	7308(3)	5419(4)	4844(1)	42(1)
C(5)	8032(3)	4417(4)	5688(1)	41(1)
C(9)	7301(3)	4947(4)	4300(1)	43(1)
C(7)	6423(3)	7905(4)	5492(1)	42(1)
C(4)	7267(3)	6358(4)	5859(1)	44(1)
C(10)	6582(3)	6467(4)	3929(1)	48(1)
C(3)	7270(3)	6782(4)	6377(1)	51(1)
C(14)	8004(3)	2927(4)	4136(1)	52(1)
C(6)	8779(3)	2869(4)	6046(1)	54(1)
C(2)	8024(4)	5236(5)	6710(1)	55(1)
C(11)	6535(4)	6012(5)	3421(1)	57(1)
C(13)	7925(4)	2482(5)	3623(1)	61(1)
C(1)	8770(4)	3266(5)	6552(1)	59(1)
C(12)	7211(4)	3982(5)	3268(1)	62(1)

---

**Table S9. Bond Lengths for HPQ.**

Cl(1)-C(2)	1.742(3)
O(1)-C(7)	1.230(3)
O(2)-H(2)	0.8200
O(2)-C(14)	1.354(3)
N(2)-H(2A)	0.8600
N(2)-C(8)	1.365(3)
N(2)-C(7)	1.380(3)
N(1)-C(8)	1.312(3)
N(1)-C(5)	1.386(3)
C(8)-C(9)	1.471(3)
C(5)-C(4)	1.399(3)
C(5)-C(6)	1.401(3)
C(9)-C(10)	1.405(3)
C(9)-C(14)	1.411(3)
C(7)-C(4)	1.444(3)
C(4)-C(3)	1.398(3)
C(10)-H(10)	0.9300
C(10)-C(11)	1.373(4)
C(3)-H(3)	0.9300
C(3)-C(2)	1.362(4)
C(14)-C(13)	1.382(4)
C(6)-H(6)	0.9300
C(6)-C(1)	1.366(4)
C(2)-C(1)	1.394(4)
C(11)-H(11)	0.9300
C(11)-C(12)	1.397(4)
C(13)-H(13)	0.9300
C(13)-C(12)	1.369(4)
C(1)-H(1)	0.9300
C(12)-H(12)	0.9300

**Table S10. Torsion Angles for HPQ.**

C(14)-O(2)-H(2)	109.5
C(8)-N(2)-H(2A)	117.9
C(8)-N(2)-C(7)	124.27(19)
C(7)-N(2)-H(2A)	117.9



C(8)-N(1)-C(5)	119.1(2)
N(2)-C(8)-C(9)	119.4(2)
N(1)-C(8)-N(2)	121.4(2)
N(1)-C(8)-C(9)	119.2(2)
N(1)-C(5)-C(4)	121.6(2)
N(1)-C(5)-C(6)	119.6(2)
C(4)-C(5)-C(6)	118.8(2)
C(10)-C(9)-C(8)	121.4(2)
C(10)-C(9)-C(14)	118.1(2)
C(14)-C(9)-C(8)	120.5(2)
O(1)-C(7)-N(2)	120.9(2)
O(1)-C(7)-C(4)	124.5(2)
N(2)-C(7)-C(4)	114.65(19)
C(5)-C(4)-C(7)	119.0(2)
C(3)-C(4)-C(5)	121.0(2)
C(3)-C(4)-C(7)	120.0(2)
C(9)-C(10)-H(10)	119.2
C(11)-C(10)-C(9)	121.6(2)
C(11)-C(10)-H(10)	119.2
C(4)-C(3)-H(3)	121.0
C(2)-C(3)-C(4)	118.0(2)
C(2)-C(3)-H(3)	121.0
O(2)-C(14)-C(9)	122.7(2)
O(2)-C(14)-C(13)	117.8(2)
C(13)-C(14)-C(9)	119.5(2)
C(5)-C(6)-H(6)	119.8
C(1)-C(6)-C(5)	120.3(2)
C(1)-C(6)-H(6)	119.8
C(3)-C(2)-Cl(1)	119.0(2)
C(3)-C(2)-C(1)	122.5(2)
C(1)-C(2)-Cl(1)	118.5(2)
C(10)-C(11)-H(11)	120.4
C(10)-C(11)-C(12)	119.2(3)
C(12)-C(11)-H(11)	120.4
C(14)-C(13)-H(13)	119.3
C(12)-C(13)-C(14)	121.5(2)

C(12)-C(13)-H(13)	119.3
C(6)-C(1)-C(2)	119.4(2)
C(6)-C(1)-H(1)	120.3
C(2)-C(1)-H(1)	120.3
C(11)-C(12)-H(12)	120.0
C(13)-C(12)-C(11)	120.1(2)
C(13)-C(12)-H(12)	120.0

---

Symmetry transformations used to generate equivalent atoms:

**Table S11. Anisotropic Displacement Parameters ( $\text{\AA}^2 \times 10^3$ ) for HPQ4. The Anisotropic displacement factor exponent takes the form:  $-2\pi^2[h^2a^*U_{11}+2hka^*b^*U_{12}+\dots]$ .**

	U <sup>11</sup>	U <sup>22</sup>	U <sup>33</sup>	U <sup>23</sup>	U <sup>13</sup>	U <sup>12</sup>
—						
Cl(1)	115(1)	94(1)	45(1)	2(1)	-2(1)	12(1)
O(1)	69(1)	45(1)	48(1)	-1(1)	6(1)	19(1)
O(2)	87(1)	46(1)	62(1)	-1(1)	13(1)	21(1)
N(2)	50(1)	38(1)	44(1)	4(1)	6(1)	7(1)
N(1)	48(1)	39(1)	50(1)	2(1)	5(1)	4(1)
C(8)	40(1)	38(1)	48(1)	5(1)	5(1)	-2(1)
C(5)	38(1)	38(1)	47(1)	2(1)	3(1)	0(1)
C(9)	40(1)	38(1)	53(1)	-1(1)	10(1)	0(1)
C(7)	41(1)	37(1)	48(1)	1(1)	7(1)	2(1)
C(4)	41(1)	41(1)	50(1)	2(1)	4(1)	-1(1)
C(10)	51(1)	44(1)	49(1)	2(1)	11(1)	6(1)
C(3)	52(1)	52(1)	48(1)	-3(1)	6(1)	2(1)
C(14)	56(2)	41(1)	59(1)	0(1)	12(1)	2(1)
C(6)	54(1)	46(1)	60(1)	6(1)	-2(1)	7(1)
C(2)	59(2)	61(2)	44(1)	1(1)	-1(1)	-1(1)
C(11)	64(2)	57(2)	50(1)	3(1)	9(1)	3(1)
C(13)	74(2)	47(1)	63(2)	-9(1)	14(1)	4(1)
C(1)	62(2)	57(2)	55(2)	11(1)	-7(1)	4(1)
C(12)	71(2)	69(2)	48(1)	-11(1)	12(1)	-3(1)

—

**Table S12. Hydrogen Atom Coordinates ( $\text{\AA}\times 10^4$ ) and Isotropic Displacement Parameters ( $\text{\AA}^2\times 10^3$ ) for HPQ.**

	x	y	z	U(eq)
H(2)	8726	1804	4754	97
H(2A)	6016	8176	4761	53
H(10)	6126	7815	4031	57
H(3)	6773	8080	6491	61
H(6)	9284	1565	5938	64
H(11)	6060	7042	3181	68
H(13)	8366	1134	3516	73
H(1)	9256	2232	6789	71
H(12)	7176	3649	2925	75

**Table S13. Crystal data and structure refinement for HPQ4. (CCDC: 2045423)**

Identification code	HPQ4
Empirical formula	$\text{C}_{54}\text{H}_{28}\text{Cl}_2\text{F}_6\text{N}_8\text{O}_4$
Formula weight	1037.74
Temperature/K	150.00(10)
Crystal system	triclinic
Space group	P-1
a/ $\text{\AA}$	13.1263(7)
b/ $\text{\AA}$	21.3743(10)
c/ $\text{\AA}$	21.6785(11)
$\alpha/^\circ$	65.178(5)
$\beta/^\circ$	77.671(4)
$\gamma/^\circ$	85.732(4)
Volume/ $\text{\AA}^3$	5392.2(5)
Z	4
$\rho_{\text{calc}}/\text{g/cm}^3$	1.278
$\mu/\text{mm}^{-1}$	1.702
F(000)	2112.0
Crystal size/ $\text{mm}^3$	0.110 $\times$ 0.100 $\times$ 0.080

Radiation	Cu K $\alpha$ ( $\lambda = 1.54184$ )
2 $\theta$ range for data collection/ $^\circ$	4.556 to 147.844
Index ranges	$-16 \leq h \leq 15$ , $-25 \leq k \leq 26$ , $-17 \leq l \leq 26$
Reflections collected	39432
Independent reflections	21154 [ $R_{\text{int}} = 0.0700$ , $R_{\text{sigma}} = 0.0847$ ]
Data/restraints/parameters	21154/70/1393
Goodness-of-fit on $F^2$	1.061
Final R indexes [ $I \geq 2\sigma(I)$ ]	$R_1 = 0.0647$ , $wR_2 = 0.1795$
Final R indexes [all data]	$R_1 = 0.1027$ , $wR_2 = 0.2050$
Largest diff. peak/hole / e $\text{\AA}^{-3}$	0.73/-0.58

### Crystal structure determination of [HPQ4]

**Crystal Data** for  $C_{54}H_{28}Cl_2F_6N_8O_4$  ( $M=1037.74$  g/mol): triclinic, space group P-1 (no. 2),  $a = 13.1263(7)$   $\text{\AA}$ ,  $b = 21.3743(10)$   $\text{\AA}$ ,  $c = 21.6785(11)$   $\text{\AA}$ ,  $\alpha = 65.178(5)^\circ$ ,  $\beta = 77.671(4)^\circ$ ,  $\gamma = 85.732(4)^\circ$ ,  $V = 5392.2(5)$   $\text{\AA}^3$ ,  $Z = 4$ ,  $T = 150.00(10)$  K,  $\mu(\text{Cu K}\alpha) = 1.702$   $\text{mm}^{-1}$ ,  $D_{\text{calc}} = 1.278$   $\text{g/cm}^3$ , 39432 reflections measured ( $4.556^\circ \leq 2\theta \leq 147.844^\circ$ ), 21154 unique ( $R_{\text{int}} = 0.0700$ ,  $R_{\text{sigma}} = 0.0847$ ) which were used in all calculations. The final  $R_1$  was 0.0647 ( $I > 2\sigma(I)$ ) and  $wR_2$  was 0.2050 (all data).

**Table S14 Fractional Atomic Coordinates ( $\times 10^4$ ) and Equivalent Isotropic Displacement Parameters ( $\text{\AA}^2 \times 10^3$ ) for HPQ4.  $U_{\text{eq}}$  is defined as 1/3 of the trace of the orthogonalised  $U_{ij}$  tensor.**

Atom	x	y	z	$U_{\text{eq}}$
Cl1	6710.2(8)	-3545.2(5)	8902.7(5)	39.1(2)
F7	5472(4)	4516(2)	9664(2)	106.0(14)
F8	6834(2)	4990.7(17)	8936(2)	73.9(10)
F9	5297(3)	5335.1(16)	8732(2)	85.7(12)
O1	6528(2)	-758.1(13)	7818.6(12)	34.0(6)
O4	6335(2)	-963.7(12)	10880.0(12)	29.8(5)
N3	6512(2)	-505.2(14)	8738.7(14)	25.5(6)
N4	6406(2)	-1333.6(14)	9879.1(15)	25.0(6)
N7	5099(3)	2036(2)	6867(2)	55.7(10)
N8	5639(5)	4206(2)	6385(3)	81.2(16)
C28	6580(3)	-2879.4(18)	9173.4(19)	28.4(7)
C29	6498(3)	-3047.9(18)	9876(2)	33.8(8)
C30	6428(3)	-2531.1(18)	10107(2)	32.7(8)
C31	6451(3)	-1840.2(17)	9630.4(18)	24.3(7)
C32	6506(3)	-1682.7(17)	8926.0(18)	25.9(7)
C33	6567(3)	-2211.7(18)	8699.8(19)	28.9(7)
C34	6516(3)	-961.7(18)	8440.8(18)	26.1(7)
C35	6425(2)	-688.7(17)	9435.3(17)	23.0(7)
C36	6337(3)	-142.6(17)	9692.3(17)	23.5(7)
C37	6235(3)	548.4(17)	9251.7(18)	26.1(7)
C38	6119(3)	1071.7(17)	9480.0(18)	25.6(7)
C39	6114(3)	884.5(18)	10188(2)	31.0(8)

**Table S14 Fractional Atomic Coordinates ( $\times 10^4$ ) and Equivalent Isotropic Displacement Parameters ( $\text{\AA}^2 \times 10^3$ ) for HPQ4.  $U_{\text{eq}}$  is defined as 1/3 of the trace of the orthogonalised  $U_{ij}$  tensor.**

Atom	x	y	z	U(eq)
C40	6188(3)	209.2(19)	10637.0(19)	28.7(7)
C41	6291(3)	-316.5(18)	10405.7(18)	26.0(7)
C42	5973(3)	1790.4(18)	9029.8(19)	28.9(7)
C43	5853(3)	2034.2(18)	8370(2)	31.3(8)
C44	5734(3)	2747.2(18)	7924.7(19)	27.6(7)
C45	5552(3)	2936(2)	7274(2)	34.4(8)
C46	5582(4)	3642(2)	6781(3)	50.0(11)
C47	5311(3)	2436(2)	7041(2)	39.7(9)
C48	5810(3)	3296.8(17)	8162.8(19)	29.9(7)
C49	4991(3)	3756.5(18)	8143(2)	34.7(8)
C50	5031(3)	4259(2)	8384(2)	42.3(10)
C51	5893(4)	4309(2)	8634(3)	44.5(10)
C52	6718(3)	3867(2)	8637(2)	44.1(10)
C53	6681(3)	3363(2)	8400(2)	38.3(9)
C54	5901(5)	4814(3)	8946(4)	70.1(17)
Cl2	8749.1(12)	3281.6(6)	6807.7(6)	59.4(3)
O2	7151(3)	754.9(14)	7707.9(14)	42.2(7)
O3	6949(2)	1438.0(13)	4578.0(13)	34.5(6)
N1	3915(3)	-4111(2)	7269(2)	54.3(10)
N2	5496(6)	-2747(3)	5136(3)	117(3)
N5	6837(2)	679.8(15)	6752.6(15)	29.5(6)
N6	7089(2)	1609.7(15)	5653.0(16)	30.9(7)
C1	4747(3)	-2392(2)	6592(2)	33.1(8)
C2	5209(3)	-1729(2)	6108(2)	34.6(8)
C3	5417(3)	-1240.8(18)	6306.2(19)	30.0(7)
C4	4723(4)	-2919(2)	6396(2)	43.2(10)
C5	5147(5)	-2830(3)	5692(3)	67.1(16)
C6	4270(4)	-3587(2)	6876(2)	45.0(10)
C7	4256(3)	-2499.2(18)	7319.0(19)	29.5(7)
C8	3423(3)	-2088(2)	7419(2)	40.6(8)
C9	2935(3)	-2177(2)	8081(2)	45.0(8)
C10	3296(3)	-2665(2)	8647(2)	43.1(10)
C11	4128(3)	-3074(2)	8552(2)	42.7(8)
C12	4604(3)	-2990(2)	7886(2)	39.0(8)
C13	2796(5)	-2746(3)	9371(3)	65.0(14)
C14	5866(3)	-558.2(18)	5850.3(19)	28.2(7)
C15	6073(3)	-302.2(19)	5125.9(19)	30.3(8)
C16	6450(3)	353.6(19)	4714.4(19)	31.2(8)
C17	6633(3)	793.0(19)	5017(2)	30.8(8)
C18	6496(3)	539.8(18)	5742.9(18)	27.8(7)
C19	6097(3)	-134.8(18)	6147.5(19)	28.6(7)
C20	6805(3)	970.4(18)	6056.4(19)	28.9(7)
C21	7170(3)	1028.4(18)	7080.4(19)	31.6(8)

**Table S14 Fractional Atomic Coordinates ( $\times 10^4$ ) and Equivalent Isotropic Displacement Parameters ( $\text{\AA}^2 \times 10^3$ ) for HPQ4.  $U_{\text{eq}}$  is defined as 1/3 of the trace of the orthogonalised  $U_{ij}$  tensor.**

Atom	x	y	z	U(eq)
C22	7535(3)	1725.8(18)	6639(2)	32.6(8)
C23	7457(3)	2003.7(18)	5936.8(19)	30.0(7)
C24	7764(4)	2692(2)	5511(2)	39.7(9)
C25	8150(4)	3079(2)	5784(2)	40.3(9)
C26	8236(3)	2786(2)	6483(2)	38.3(9)
C27	7934(3)	2120.5(19)	6911(2)	33.8(8)
F2	2608(9)	-3370(3)	9815(3)	159(4)
F1	1897(6)	-2418(6)	9398(3)	154(4)
F3	3405(17)	-3114(13)	9799(9)	66(2)
F03{	3358(6)	-2478(4)	9627(3)	123(3)
F04C	1914(18)	-3043(14)	9550(11)	68(3)
F14	2650(20)	-2149(10)	9375(10)	63(3)
Cl3	10782.9(8)	7305.9(4)	1315.5(5)	39.1(2)
F10	10601(3)	15884.7(13)	1112.6(15)	69.0(9)
F11	10194(3)	15649.1(14)	2199.3(15)	69.4(9)
F12	9017(3)	15926.2(13)	1601.4(17)	67.6(8)
O6	10366(2)	9176.1(12)	2415.0(12)	34.6(6)
O8	11403(2)	11540.1(12)	-673.3(12)	28.7(5)
N11	11059(2)	10322.9(14)	330.9(14)	23.3(6)
N12	10678(2)	10201.9(14)	1480.8(15)	27.7(6)
N15	8758(3)	10970.5(15)	3550.4(17)	33.9(7)
N16	7919(3)	12885.7(17)	3855.9(18)	43.0(8)
C82	10704(3)	8464.4(18)	1524(2)	29.3(7)
C83	10904(3)	8189.8(18)	1043(2)	29.7(7)
C84	11176(3)	8606.3(18)	329.1(19)	29.1(7)
C85	11229(3)	9312.6(18)	98.3(18)	26.6(7)
C86	11027(2)	9609.6(16)	576.4(17)	22.9(6)
C87	10775(3)	9180.3(17)	1289.3(18)	25.4(7)
C88	10590(3)	9493.3(17)	1779.1(19)	28.2(7)
C89	10882(3)	10597.8(16)	776.6(17)	23.3(7)
C90	10860(3)	11352.6(16)	530.7(17)	23.6(7)
C91	11144(3)	11783.4(17)	-183.5(17)	23.5(7)
C92	11141(3)	12497.6(17)	-402.6(18)	27.5(7)
C93	10848(3)	12785.1(17)	69.5(18)	27.5(7)
C94	10538(3)	12374.2(17)	778.0(17)	26.5(7)
C95	10550(3)	11661.0(17)	993.3(17)	25.4(7)
C96	10190(3)	12688.8(17)	1265.5(17)	26.8(7)
C97	9845(3)	12349.6(17)	1953.7(18)	27.8(7)
C98	9394(3)	12676.5(17)	2417.6(17)	24.9(7)
C99	8871(3)	12298.3(17)	3073.5(17)	25.1(7)
C100	8788(3)	11559.3(17)	3347.6(18)	27.3(7)
C101	8350(3)	12616.2(17)	3522.6(18)	29.4(7)
C102	9511(3)	13432.2(16)	2181.8(17)	25.9(7)

**Table S14 Fractional Atomic Coordinates ( $\times 10^4$ ) and Equivalent Isotropic Displacement Parameters ( $\text{\AA}^2 \times 10^3$ ) for HPQ4.  $U_{\text{eq}}$  is defined as 1/3 of the trace of the orthogonalised  $U_{ij}$  tensor.**

Atom	x	y	z	U(eq)
C103	10509(3)	13724.0(19)	2001(2)	34.1(8)
C104	10621(3)	14418(2)	1841(2)	37.6(9)
C105	9743(3)	14819.5(18)	1851.7(18)	32.9(8)
C106	8756(3)	14540.8(19)	2013.0(19)	34.5(8)
C107	8642(3)	13844.9(18)	2179.7(19)	30.4(7)
C108	9893(4)	15563(2)	1688(2)	44.9(10)
Cl4	12389.3(8)	12458.8(5)	3237.8(5)	41.5(2)
O5	10553(2)	8386.9(13)	5506.2(13)	31.2(5)
O7	10932(2)	10711.5(13)	2425.1(13)	36.7(6)
N9	6763(3)	7396.3(17)	1730.6(17)	37.9(8)
N10	8220(3)	9224.4(16)	1669.4(17)	33.9(7)
N13	10579(2)	9717.1(14)	3393.8(14)	26.8(6)
N14	10815(2)	9586.2(15)	4486.1(14)	24.9(6)
C55	6773(8)	4669(3)	4256(4)	99.1(17)
C56	7052(4)	5416(2)	3932(2)	51.6(12)
C57	7865(5)	5653(2)	3368(3)	66.1(16)
C58	8143(5)	6348(2)	3058(2)	56.7(14)
C60	6804(3)	6553(2)	3881(2)	39.5(9)
C61	6517(4)	5860(2)	4190(2)	47.8(11)
C62	7928(3)	7539.8(19)	2964.6(18)	30.0(7)
C63	7718(3)	7929.6(18)	2322.4(18)	28.1(7)
C64	7190(3)	7636.9(19)	1985.2(19)	30.3(8)
C65	7991(3)	8647.4(19)	1956.6(17)	27.9(7)
C66	8436(3)	7830.6(19)	3314.2(18)	30.6(8)
C67	8655(3)	7467.8(19)	3949.5(19)	33.2(8)
C68	9169(3)	7724.2(19)	4330.6(19)	32.2(8)
C69	9582(3)	8389.6(18)	4040.9(18)	30.1(7)
C70	10080(3)	8631.4(17)	4406.8(17)	25.5(7)
C71	10136(3)	8188.7(18)	5101.8(18)	27.9(7)
C72	9733(3)	7517.5(19)	5389(2)	33.5(8)
C73	9269(3)	7287.2(19)	5014(2)	34.6(8)
C74	10511(3)	9335.9(17)	4096.1(17)	25.1(7)
C75	10916(3)	10392.6(18)	3049.6(18)	27.5(7)
C76	11254(3)	10678.2(18)	3473.6(18)	25.9(7)
C77	11191(3)	10262.0(17)	4179.4(17)	23.9(7)
C78	11618(3)	11357.7(18)	3181.3(19)	29.7(7)
C79	11931(3)	11615.5(18)	3598(2)	31.7(8)
C80	11878(3)	11207.0(18)	4304.7(19)	29.8(7)
C81	11509(3)	10536.6(18)	4598.6(18)	26.4(7)
F13	6340(10)	4508(4)	3847(4)	101(2)
F15	7647(10)	4273(4)	4353(5)	113(2)
F16	6044(10)	4478(4)	4834(5)	107(2)
C59	7614(3)	6795.7(19)	3313.1(19)	33.1(8)



**Table S14 Fractional Atomic Coordinates ( $\times 10^4$ ) and Equivalent Isotropic Displacement Parameters ( $\text{\AA}^2 \times 10^3$ ) for HPQ4.  $U_{\text{eq}}$  is defined as 1/3 of the trace of the orthogonalised  $U_{ij}$  tensor.**

Atom	x	y	z	$U(\text{eq})$
F4	5769(11)	4536(5)	4338(7)	123(3)
F5	7228(12)	4294(5)	3959(8)	131(6)
F6	6879(12)	4363(4)	4908(5)	108(2)

**Table S15 Anisotropic Displacement Parameters ( $\text{\AA}^2 \times 10^3$ ) for HPQ4. The Anisotropic displacement factor exponent takes the form:  $-2\pi^2[h^2a^*U_{11}+2hka^*b^*U_{12}+\dots]$ .**

Atom	$U_{11}$	$U_{22}$	$U_{33}$	$U_{23}$	$U_{13}$	$U_{12}$
Cl1	51.7(6)	25.2(4)	51.1(6)	-24.1(4)	-15.4(4)	3.5(4)
F7	139(4)	106(3)	102(3)	-79(3)	-3(3)	-10(3)
F8	64.9(19)	70(2)	124(3)	-71(2)	-24.3(19)	-5.0(15)
F9	96(3)	56.4(19)	148(3)	-74(2)	-55(2)	25.4(18)
O1	55.2(17)	25.5(12)	22.4(13)	-11.0(10)	-7.5(11)	0.4(11)
O4	40.6(14)	25.4(12)	29.0(13)	-15.4(10)	-10.9(11)	3.6(10)
N3	36.4(16)	18.7(13)	22.6(14)	-11.4(11)	-2.1(12)	-0.3(11)
N4	26.7(14)	21.9(14)	31.2(15)	-14.9(12)	-7.1(12)	0.7(11)
N7	58(2)	63(3)	69(3)	-46(2)	-24(2)	10(2)
N8	130(5)	48(3)	58(3)	-2(2)	-40(3)	-10(3)
C28	33.0(18)	22.5(16)	37(2)	-18.3(15)	-9.1(15)	0.6(14)
C29	44(2)	19.1(16)	41(2)	-11.5(15)	-15.3(17)	2.7(15)
C30	42(2)	24.2(17)	37(2)	-13.7(16)	-15.7(17)	2.7(15)
C31	28.3(17)	22.4(16)	28.8(17)	-17.0(14)	-6.2(14)	1.6(13)
C32	30.1(17)	19.6(16)	30.5(18)	-12.3(14)	-7.1(14)	0.4(13)
C33	33.7(19)	25.0(17)	33.0(19)	-15.9(15)	-8.2(15)	-0.5(14)
C34	30.7(18)	24.9(17)	25.2(17)	-14.0(14)	-2.6(14)	-0.4(13)
C35	22.8(16)	22.7(16)	29.0(17)	-15.8(14)	-5.6(13)	1.2(12)
C36	24.4(16)	24.5(16)	26.8(17)	-17.3(14)	-2.0(13)	0.7(13)
C37	26.4(17)	26.6(17)	28.8(18)	-16.6(15)	-1.3(14)	-1.3(13)
C38	24.7(16)	25.2(17)	28.7(18)	-13.7(14)	-2.6(13)	-2.0(13)
C39	29.5(18)	28.4(18)	46(2)	-24.6(17)	-11.9(16)	2.5(14)
C40	31.7(18)	32.1(18)	31.2(19)	-20.8(16)	-8.8(15)	1.6(14)
C41	24.1(16)	25.7(17)	33.4(19)	-15.8(15)	-9.2(14)	2.5(13)
C42	28.8(17)	23.6(17)	39(2)	-18.5(15)	-5.0(15)	-1.2(13)
C43	32.9(19)	23.2(17)	44(2)	-19.7(16)	-7.0(16)	-0.7(14)
C44	27.2(17)	25.9(17)	31.9(19)	-15.5(15)	-2.5(14)	-1.1(13)
C45	33.7(19)	33.3(19)	41(2)	-18.7(17)	-10.9(16)	3.0(15)
C46	60(3)	43(3)	49(3)	-15(2)	-23(2)	-2(2)
C47	36(2)	46(2)	46(2)	-27(2)	-11.6(18)	5.2(18)
C48	36.6(19)	19.7(16)	34.7(19)	-12.0(15)	-6.8(15)	-2.8(14)

**Table S15 Anisotropic Displacement Parameters ( $\text{\AA}^2 \times 10^3$ ) for HPQ4. The Anisotropic displacement factor exponent takes the form:  $-2\pi^2[h^2a^*2U_{11}+2hka^*b^*U_{12}+\dots]$ .**

Atom	$U_{11}$	$U_{22}$	$U_{33}$	$U_{23}$	$U_{13}$	$U_{12}$
C49	38(2)	23.3(17)	47(2)	-15.1(16)	-14.2(17)	1.1(15)
C50	41(2)	27.9(19)	67(3)	-26(2)	-18(2)	6.1(16)
C51	46(2)	32(2)	67(3)	-31(2)	-14(2)	0.3(18)
C52	45(2)	35(2)	66(3)	-29(2)	-23(2)	0.9(18)
C53	38(2)	27.3(19)	55(3)	-20.4(18)	-14.1(18)	3.0(16)
C54	65(3)	59(3)	122(5)	-64(4)	-38(4)	11(3)
Cl2	93.6(10)	36.6(5)	51.4(7)	-17.2(5)	-15.9(6)	-21.1(6)
O2	67(2)	28.9(14)	27.8(14)	-8.6(11)	-6.0(13)	-10.9(13)
O3	42.4(15)	28.2(13)	29.2(13)	-7.4(11)	-8.0(11)	-3.1(11)
N1	61(3)	35(2)	70(3)	-23(2)	-14(2)	-2.9(18)
N2	178(7)	104(5)	76(4)	-65(4)	32(4)	-36(5)
N5	38.2(17)	20.7(14)	25.5(15)	-7.9(12)	-1.1(13)	-2.2(12)
N6	37.8(17)	23.6(15)	30.4(16)	-11.7(13)	-4.3(13)	1.1(12)
C1	36(2)	32.1(19)	36(2)	-18.7(17)	-8.9(16)	4.0(15)
C2	39(2)	32.9(19)	34(2)	-15.8(16)	-6.3(16)	0.3(16)
C3	31.5(18)	28.2(18)	31.3(19)	-12.6(15)	-8.0(15)	1.8(14)
C4	49(2)	38(2)	48(3)	-25(2)	-4(2)	-0.5(18)
C5	94(4)	60(3)	56(3)	-41(3)	11(3)	-18(3)
C6	51(3)	37(2)	57(3)	-29(2)	-11(2)	2.2(19)
C7	31.6(18)	25.6(17)	31.5(19)	-12.0(15)	-5.4(15)	-3.3(14)
C8	37.0(17)	41.5(18)	48(2)	-23.5(16)	-8.9(15)	8.1(15)
C9	39.4(18)	43.8(18)	54(2)	-24.4(16)	-7.8(15)	10.0(15)
C10	44(2)	48(2)	45(2)	-28(2)	-1.1(19)	-4.4(19)
C11	45.3(19)	39.1(18)	41.8(18)	-14.4(15)	-10.4(15)	2.2(15)
C12	43.4(18)	36.4(17)	37.8(17)	-16.7(15)	-7.7(15)	4.6(14)
C13	79(4)	73(3)	46(3)	-36(3)	4(2)	3(3)
C14	27.0(17)	25.9(17)	31.9(19)	-12.1(15)	-6.2(14)	1.5(14)
C15	27.7(18)	33.6(19)	33.5(19)	-16.2(16)	-10.4(15)	4.1(15)
C16	30.3(18)	35.9(19)	28.9(18)	-13.0(16)	-9.9(15)	1.3(15)
C17	25.4(17)	28.3(18)	37(2)	-11.2(16)	-8.7(15)	2.6(14)
C18	28.9(17)	27.3(17)	27.3(18)	-11.6(14)	-6.3(14)	2.8(14)
C19	29.2(18)	27.4(17)	26.6(18)	-9.9(14)	-3.9(14)	2.7(14)
C20	31.5(18)	25.1(17)	29.1(18)	-10.7(15)	-7.1(14)	6.2(14)
C21	38(2)	24.6(17)	29.2(19)	-10.1(15)	-3.3(15)	0.3(15)
C22	34.3(19)	23.7(17)	39(2)	-13.1(16)	-5.1(16)	1.3(14)
C23	36.9(19)	25.6(17)	27.4(18)	-13.1(15)	-2.5(15)	3.2(14)
C24	57(3)	26.7(19)	33(2)	-12.1(16)	-4.9(18)	-1.1(17)
C25	60(3)	24.4(18)	33(2)	-9.3(16)	-5.1(19)	-5.9(18)
C26	49(2)	29.6(19)	39(2)	-17.4(17)	-4.6(18)	-3.5(17)
C27	42(2)	26.9(18)	29.8(19)	-10.3(15)	-3.0(16)	-2.4(15)
F2	298(12)	81(4)	62(3)	-39(3)	81(5)	-64(5)
F1	101(5)	297(11)	105(5)	-135(6)	-16(4)	79(6)
F3	80(4)	75(4)	46(3)	-34(3)	4(3)	3(3)
F03{	148(6)	184(7)	71(3)	-86(4)	5(3)	-67(5)

**Table S15 Anisotropic Displacement Parameters ( $\text{\AA}^2 \times 10^3$ ) for HPQ4. The Anisotropic displacement factor exponent takes the form:  $-2\pi^2[h^2a^*2U_{11}+2hka^*b^*U_{12}+\dots]$ .**

Atom	$U_{11}$	$U_{22}$	$U_{33}$	$U_{23}$	$U_{13}$	$U_{12}$
F04C	75(5)	75(5)	45(4)	-27(4)	13(4)	3(4)
F14	81(5)	72(5)	43(4)	-39(4)	6(4)	6(4)
Cl3	48.1(5)	21.1(4)	57.0(6)	-20.2(4)	-21.3(5)	3.0(4)
F10	107(3)	29.1(13)	54.4(17)	-15.0(12)	21.6(16)	-26.4(15)
F11	127(3)	34.7(14)	62.3(18)	-26.4(13)	-35.4(18)	-4.4(16)
F12	89(2)	23.7(12)	86(2)	-18.2(13)	-20.0(18)	9.9(13)
O6	60.1(18)	20.6(12)	19.7(13)	-5.1(10)	-5.9(11)	-5.2(11)
O8	38.8(14)	20.9(11)	26.9(13)	-11.3(10)	-4.4(10)	-0.3(10)
N11	28.6(14)	20.5(13)	23.9(14)	-11.9(11)	-5.2(11)	-0.1(11)
N12	44.1(18)	16.7(13)	24.4(15)	-9.2(12)	-9.4(13)	-0.5(12)
N15	43.1(18)	23.4(16)	35.7(17)	-11.7(13)	-8.7(14)	-2.4(13)
N16	66(2)	27.3(16)	33.0(18)	-10.8(15)	-10.4(17)	9.9(16)
C82	31.6(18)	22.6(17)	36(2)	-12.3(15)	-11.2(15)	-1.0(14)
C83	27.0(17)	23.0(17)	44(2)	-16.5(16)	-12.3(15)	0.6(13)
C84	30.4(18)	28.7(18)	38(2)	-23.1(16)	-9.2(15)	3.5(14)
C85	28.1(17)	27.0(17)	27.7(18)	-15.4(15)	-3.2(14)	0.7(13)
C86	22.1(15)	20.2(15)	26.7(17)	-10.6(13)	-3.3(13)	-0.6(12)
C87	30.5(17)	20.5(16)	27.4(17)	-10.3(14)	-8.7(14)	-1.9(13)
C88	34.7(19)	19.5(16)	31.7(19)	-10.4(14)	-8.9(15)	-1.7(14)
C89	25.3(16)	17.7(15)	26.0(17)	-7.3(13)	-6.5(13)	-1.3(12)
C90	29.3(17)	17.7(15)	24.8(17)	-8.2(13)	-8.4(13)	0.0(13)
C91	27.6(17)	21.9(16)	22.2(16)	-10.7(13)	-3.8(13)	-0.2(13)
C92	32.1(18)	20.5(16)	25.7(17)	-6.4(14)	-4.0(14)	-0.1(13)
C93	37.8(19)	18.2(15)	25.9(17)	-8.1(13)	-7.0(14)	0.0(14)
C94	37.5(19)	20.1(16)	22.2(17)	-8.3(13)	-8.5(14)	1.9(14)
C95	36.2(19)	18.6(15)	21.1(16)	-8.2(13)	-5.4(14)	1.2(13)
C96	38.6(19)	17.6(15)	22.4(17)	-7.7(13)	-4.5(14)	1.3(13)
C97	40(2)	17.4(15)	28.1(18)	-10.9(14)	-7.8(15)	1.7(14)
C98	34.3(18)	18.6(15)	22.7(16)	-8.5(13)	-7.9(14)	1.9(13)
C99	32.6(18)	21.4(16)	24.1(17)	-10.9(13)	-8.2(14)	0.8(13)
C100	33.7(18)	22.9(18)	26.4(17)	-10.1(14)	-8.1(14)	-1.9(14)
C101	41(2)	19.1(16)	25.5(18)	-6.7(14)	-7.8(15)	0.1(14)
C102	37.6(19)	17.1(15)	22.4(16)	-8.4(13)	-3.9(14)	-0.2(13)
C103	37(2)	25.1(18)	41(2)	-15.2(16)	-6.2(17)	1.0(15)
C104	47(2)	28.9(19)	33(2)	-11.4(16)	0.8(17)	-9.7(17)
C105	55(2)	19.0(17)	21.8(17)	-7.1(14)	-3.8(16)	-0.5(16)
C106	46(2)	22.9(17)	29.9(19)	-9.2(15)	-4.3(16)	6.8(16)
C107	35.7(19)	23.1(17)	28.6(18)	-7.9(14)	-4.6(15)	0.4(14)
C108	73(3)	23.6(19)	40(2)	-14.6(17)	-12(2)	-2.7(19)
Cl4	49.8(6)	27.3(4)	50.4(6)	-15.6(4)	-14.7(5)	-6.4(4)
O5	43.1(15)	26.9(13)	27.3(13)	-10.7(10)	-15.6(11)	0.1(11)
O7	62.0(18)	23.5(12)	26.8(14)	-8.3(11)	-17.0(12)	-2.0(12)
N9	42.7(19)	38.8(18)	33.6(17)	-16.8(15)	-2.3(14)	-11.7(15)
N10	43.4(18)	27.2(16)	35.0(17)	-15.5(14)	-10.2(14)	0.0(13)

**Table S15 Anisotropic Displacement Parameters ( $\text{\AA}^2 \times 10^3$ ) for HPQ4. The Anisotropic displacement factor exponent takes the form:  $-2\pi^2[h^2a^*2U_{11}+2hka^*b^*U_{12}+\dots]$ .**

Atom	$U_{11}$	$U_{22}$	$U_{33}$	$U_{23}$	$U_{13}$	$U_{12}$
N13	39.9(17)	20.4(14)	24.0(14)	-9.7(12)	-13.3(12)	1.1(12)
N14	28.2(14)	26.3(14)	22.1(14)	-11.1(12)	-7.2(11)	2.2(11)
C55	182(5)	36.8(19)	74(2)	-8.9(19)	-32(3)	-35(2)
C56	88(4)	29(2)	36(2)	-9.9(18)	-12(2)	-12(2)
C57	117(5)	30(2)	47(3)	-20(2)	3(3)	-3(3)
C58	95(4)	31(2)	34(2)	-14.4(19)	11(2)	-6(2)
C60	49(2)	36(2)	36(2)	-17.5(18)	-5.8(18)	-7.5(18)
C61	60(3)	40(2)	39(2)	-13.4(19)	0(2)	-18(2)
C62	37.6(19)	28.3(18)	25.9(18)	-13.9(15)	-3.0(15)	-3.0(15)
C63	35.8(19)	26.2(17)	25.9(17)	-14.2(14)	-4.6(14)	-4.5(14)
C64	34.6(19)	28.6(18)	30.1(19)	-15.2(15)	-3.5(15)	-4.4(15)
C65	34.4(19)	32.8(19)	21.4(16)	-15.2(15)	-7.2(14)	1.3(15)
C66	43(2)	25.7(17)	24.7(18)	-12.5(14)	-4.8(15)	-5.3(15)
C67	45(2)	26.4(18)	29.6(19)	-13.2(15)	-5.6(16)	-6.1(16)
C68	43(2)	25.5(17)	29.5(19)	-9.8(15)	-12.6(16)	-4.5(15)
C69	40(2)	26.3(17)	24.3(18)	-9.1(14)	-10.2(15)	-1.8(15)
C70	32.9(18)	20.5(16)	23.5(17)	-8.4(13)	-8.4(14)	1.9(13)
C71	33.7(18)	24.9(17)	29.3(18)	-12.8(14)	-13.1(15)	4.6(14)
C72	43(2)	25.6(18)	30.3(19)	-6.1(15)	-14.6(16)	1.0(15)
C73	49(2)	21.5(17)	32(2)	-7.0(15)	-11.8(17)	-5.0(16)
C74	27.4(17)	24.1(16)	24.6(17)	-10.5(14)	-7.0(13)	3.8(13)
C75	35.5(19)	24.3(17)	24.7(17)	-10.4(14)	-10.6(14)	4.2(14)
C76	26.9(17)	27.5(17)	28.0(18)	-15.8(14)	-7.2(14)	4.3(13)
C77	24.1(16)	27.3(17)	23.4(17)	-13.5(14)	-5.6(13)	3.7(13)
C78	34.6(19)	23.0(17)	31.0(19)	-8.5(14)	-11.4(15)	1.3(14)
C79	31.6(18)	24.9(17)	42(2)	-15.3(16)	-12.6(16)	1.5(14)
C80	31.2(18)	29.1(18)	35(2)	-16.7(16)	-12.6(15)	1.5(14)
C81	25.1(16)	31.1(18)	25.6(17)	-13.4(15)	-7.9(14)	3.7(14)
F13	193(6)	43(3)	72(3)	-16(3)	-37(4)	-47(3)
F15	187(6)	32(3)	96(4)	3(3)	-34(4)	-19(3)
F16	188(6)	45(3)	69(3)	-9(3)	-2(4)	-42(4)
C59	51(2)	25.2(18)	25.7(18)	-12.1(15)	-8.5(16)	-4.6(16)
F4	182(6)	50(3)	103(4)	5(4)	-26(5)	-37(4)
F5	178(13)	45(5)	158(11)	-67(7)	55(10)	-24(7)
F6	187(6)	41(3)	74(4)	10(3)	-42(4)	-27(4)

**Table S16. Bond Lengths for HPQ4.**

Atom Atom	Length/ $\text{\AA}$	Atom Atom	Length/ $\text{\AA}$
Cl1 C28	1.738(3)	Cl3 C83	1.735(3)
F7 C54	1.411(8)	F10 C108	1.331(5)
F8 C54	1.300(6)	F11 C108	1.338(5)
F9 C54	1.295(6)	F12 C108	1.340(6)

**Table S16. Bond Lengths for HPQ4.**

Atom	Atom	Length/Å	Atom	Atom	Length/Å
O1	C34	1.228(4)	O6	C88	1.232(4)
O4	C41	1.339(4)	O8	C91	1.340(4)
N3	C34	1.377(4)	N11	C86	1.389(4)
N3	C35	1.372(4)	N11	C89	1.301(4)
N4	C31	1.391(4)	N12	C88	1.377(4)
N4	C35	1.307(4)	N12	C89	1.376(4)
N7	C47	1.140(5)	N15	C100	1.146(5)
N8	C46	1.146(6)	N16	C101	1.140(5)
C28	C29	1.391(5)	C82	C83	1.371(5)
C28	C33	1.366(5)	C82	C87	1.398(5)
C29	C30	1.381(5)	C83	C84	1.403(5)
C30	C31	1.400(5)	C84	C85	1.379(5)
C31	C32	1.405(5)	C85	C86	1.399(4)
C32	C33	1.400(4)	C86	C87	1.406(5)
C32	C34	1.455(5)	C87	C88	1.448(5)
C35	C36	1.478(4)	C89	C90	1.472(4)
C36	C37	1.397(5)	C90	C91	1.411(5)
C36	C41	1.419(5)	C90	C95	1.395(5)
C37	C38	1.388(4)	C91	C92	1.395(5)
C38	C39	1.412(5)	C92	C93	1.378(5)
C38	C42	1.458(5)	C93	C94	1.396(5)
C39	C40	1.371(5)	C94	C95	1.394(4)
C40	C41	1.398(5)	C94	C96	1.457(5)
C42	C43	1.342(5)	C96	C97	1.345(5)
C43	C44	1.439(5)	C97	C98	1.458(5)
C44	C45	1.365(5)	C98	C99	1.359(5)
C44	C48	1.485(5)	C98	C102	1.485(4)
C45	C46	1.433(6)	C99	C100	1.439(5)
C45	C47	1.439(5)	C99	C101	1.442(5)
C48	C49	1.397(5)	C102	C103	1.398(5)
C48	C53	1.389(5)	C102	C107	1.389(5)
C49	C50	1.386(5)	C103	C104	1.386(5)
C50	C51	1.383(6)	C104	C105	1.387(6)
C51	C52	1.383(6)	C105	C106	1.379(6)
C51	C54	1.498(6)	C105	C108	1.495(5)
C52	C53	1.380(5)	C106	C107	1.387(5)
Cl2	C26	1.734(4)	Cl4	C79	1.732(4)
O2	C21	1.230(5)	O5	C71	1.342(4)
O3	C17	1.339(4)	O7	C75	1.230(4)
N1	C6	1.142(6)	N9	C64	1.139(5)
N2	C5	1.136(7)	N10	C65	1.153(5)
N5	C20	1.379(5)	N13	C74	1.379(4)
N5	C21	1.370(5)	N13	C75	1.374(4)
N6	C20	1.305(5)	N14	C74	1.309(4)
N6	C23	1.394(5)	N14	C77	1.390(4)

**Table S16. Bond Lengths for HPQ4.**

Atom	Atom	Length/Å	Atom	Atom	Length/Å
C1	C2	1.443(5)	C55	C56	1.487(7)
C1	C4	1.365(5)	C55	F13	1.315(10)
C1	C7	1.496(5)	C55	F15	1.375(14)
C2	C3	1.348(5)	C55	F16	1.329(13)
C3	C14	1.457(5)	C55	F4	1.328(15)
C4	C5	1.443(7)	C55	F5	1.271(12)
C4	C6	1.445(6)	C55	F6	1.318(12)
C7	C8	1.389(5)	C56	C57	1.375(7)
C7	C12	1.380(5)	C56	C61	1.372(7)
C8	C9	1.380(6)	C57	C58	1.389(6)
C9	C10	1.385(7)	C58	C59	1.373(6)
C10	C11	1.382(6)	C60	C61	1.388(6)
C10	C13	1.508(6)	C60	C59	1.379(6)
C11	C12	1.387(6)	C62	C63	1.366(5)
C13	F2	1.279(8)	C62	C66	1.442(5)
C13	F1	1.330(9)	C62	C59	1.492(5)
C13	F3	1.31(2)	C63	C64	1.439(5)
C13	F03{	1.298(8)	C63	C65	1.432(5)
C13	F04C	1.27(2)	C66	C67	1.349(5)
C13	F14	1.280(19)	C67	C68	1.453(5)
C14	C15	1.399(5)	C68	C69	1.390(5)
C14	C19	1.393(5)	C68	C73	1.410(5)
C15	C16	1.368(5)	C69	C70	1.393(5)
C16	C17	1.409(5)	C70	C71	1.418(5)
C17	C18	1.408(5)	C70	C74	1.468(5)
C18	C19	1.406(5)	C71	C72	1.395(5)
C18	C20	1.474(5)	C72	C73	1.367(5)
C21	C22	1.442(5)	C75	C76	1.449(5)
C22	C23	1.407(5)	C76	C77	1.398(5)
C22	C27	1.396(5)	C76	C78	1.393(5)
C23	C24	1.404(5)	C77	C81	1.411(4)
C24	C25	1.375(6)	C78	C79	1.377(5)
C25	C26	1.402(6)	C79	C80	1.399(5)
C26	C27	1.363(5)	C80	C81	1.378(5)
F3	F03{	1.25(2)			

**Table S17. Bond Angles for HPQ4.**

Atom	Atom	Atom	Angle/°	Atom	Atom	Atom	Angle/°
C35	N3	C34	124.9(3)	C89	N11	C86	118.8(3)
C35	N4	C31	118.2(3)	C89	N12	C88	124.1(3)
C29	C28	Cl1	118.3(3)	C83	C82	C87	118.4(3)
C33	C28	Cl1	119.9(3)	C82	C83	Cl3	119.5(3)
C33	C28	C29	121.8(3)	C82	C83	C84	121.8(3)

**Table S17. Bond Angles for HPQ4.**

Atom	Atom	Atom	Angle/°	Atom	Atom	Atom	Angle/°
C30	C29	C28	119.9(3)	C84	C83	Cl3	118.7(3)
C29	C30	C31	119.7(3)	C85	C84	C83	119.7(3)
N4	C31	C30	118.1(3)	C84	C85	C86	119.9(3)
N4	C31	C32	122.5(3)	N11	C86	C85	118.9(3)
C30	C31	C32	119.4(3)	N11	C86	C87	121.9(3)
C31	C32	C34	118.6(3)	C85	C86	C87	119.3(3)
C33	C32	C31	120.3(3)	C82	C87	C86	120.9(3)
C33	C32	C34	121.2(3)	C82	C87	C88	120.4(3)
C28	C33	C32	118.9(3)	C86	C87	C88	118.7(3)
O1	C34	N3	121.2(3)	O6	C88	N12	120.3(3)
O1	C34	C32	124.8(3)	O6	C88	C87	125.1(3)
N3	C34	C32	114.0(3)	N12	C88	C87	114.6(3)
N3	C35	C36	119.1(3)	N11	C89	N12	121.9(3)
N4	C35	N3	121.8(3)	N11	C89	C90	119.9(3)
N4	C35	C36	119.1(3)	N12	C89	C90	118.2(3)
C37	C36	C35	121.1(3)	C91	C90	C89	120.5(3)
C37	C36	C41	118.5(3)	C95	C90	C89	121.2(3)
C41	C36	C35	120.3(3)	C95	C90	C91	118.3(3)
C38	C37	C36	122.7(3)	O8	C91	C90	123.0(3)
C37	C38	C39	117.4(3)	O8	C91	C92	117.5(3)
C37	C38	C42	123.0(3)	C92	C91	C90	119.5(3)
C39	C38	C42	119.5(3)	C93	C92	C91	120.7(3)
C40	C39	C38	121.3(3)	C92	C93	C94	121.3(3)
C39	C40	C41	121.0(3)	C93	C94	C96	120.4(3)
O4	C41	C36	123.6(3)	C95	C94	C93	117.7(3)
O4	C41	C40	117.3(3)	C95	C94	C96	121.9(3)
C40	C41	C36	119.1(3)	C94	C95	C90	122.5(3)
C43	C42	C38	126.2(3)	C97	C96	C94	125.9(3)
C42	C43	C44	125.8(3)	C96	C97	C98	124.7(3)
C43	C44	C48	120.7(3)	C97	C98	C102	120.2(3)
C45	C44	C43	121.0(3)	C99	C98	C97	121.0(3)
C45	C44	C48	118.3(3)	C99	C98	C102	118.8(3)
C44	C45	C46	122.4(4)	C98	C99	C100	121.4(3)
C44	C45	C47	121.7(4)	C98	C99	C101	121.9(3)
C46	C45	C47	115.9(4)	C100	C99	C101	116.7(3)
N8	C46	C45	178.0(6)	N15	C100	C99	177.4(4)
N7	C47	C45	178.4(5)	N16	C101	C99	177.2(4)
C49	C48	C44	119.2(3)	C103	C102	C98	119.4(3)
C53	C48	C44	121.2(3)	C107	C102	C98	120.8(3)
C53	C48	C49	119.6(3)	C107	C102	C103	119.7(3)
C50	C49	C48	120.1(4)	C104	C103	C102	119.7(4)
C51	C50	C49	119.6(4)	C103	C104	C105	119.7(4)
C50	C51	C52	120.4(4)	C104	C105	C108	118.2(4)
C50	C51	C54	119.7(4)	C106	C105	C104	121.0(3)
C52	C51	C54	119.7(4)	C106	C105	C108	120.7(4)

**Table S17. Bond Angles for HPQ4.**

Atom	Atom	Atom	Angle/°	Atom	Atom	Atom	Angle/°
C53	C52	C51	120.2(4)	C105	C106	C107	119.3(4)
C52	C53	C48	120.0(4)	C106	C107	C102	120.5(4)
F7	C54	C51	111.0(5)	F10	C108	F11	106.9(4)
F8	C54	F7	101.8(5)	F10	C108	F12	106.2(4)
F8	C54	C51	113.6(5)	F10	C108	C105	113.1(3)
F9	C54	F7	101.1(5)	F11	C108	F12	104.7(4)
F9	C54	F8	113.2(5)	F11	C108	C105	112.2(3)
F9	C54	C51	114.5(5)	F12	C108	C105	113.1(4)
C21	N5	C20	123.5(3)	C75	N13	C74	123.8(3)
C20	N6	C23	118.5(3)	C74	N14	C77	118.4(3)
C2	C1	C7	119.3(3)	F13	C55	C56	110.7(6)
C4	C1	C2	121.5(4)	F13	C55	F15	106.0(9)
C4	C1	C7	119.1(4)	F13	C55	F16	102.7(10)
C3	C2	C1	123.1(4)	F15	C55	C56	111.0(8)
C2	C3	C14	126.3(4)	F16	C55	C56	114.1(7)
C1	C4	C5	121.0(4)	F16	C55	F15	111.9(8)
C1	C4	C6	122.0(4)	F4	C55	C56	114.3(9)
C6	C4	C5	116.9(4)	F5	C55	C56	118.3(8)
N2	C5	C4	178.3(6)	F5	C55	F4	103.2(10)
N1	C6	C4	178.3(5)	F5	C55	F6	106.5(12)
C8	C7	C1	118.2(3)	F6	C55	C56	112.8(6)
C12	C7	C1	122.1(3)	F6	C55	F4	99.7(10)
C12	C7	C8	119.6(4)	C57	C56	C55	118.5(5)
C9	C8	C7	120.2(4)	C61	C56	C55	120.9(5)
C8	C9	C10	119.8(4)	C61	C56	C57	120.6(4)
C9	C10	C13	120.2(4)	C56	C57	C58	119.6(4)
C11	C10	C9	120.3(4)	C59	C58	C57	120.3(4)
C11	C10	C13	119.5(5)	C59	C60	C61	120.2(4)
C10	C11	C12	119.6(4)	C56	C61	C60	119.6(4)
C7	C12	C11	120.4(4)	C63	C62	C66	121.7(3)
F2	C13	C10	114.7(5)	C63	C62	C59	118.9(3)
F1	C13	C10	112.9(5)	C66	C62	C59	119.4(3)
F3	C13	C10	109.1(9)	C62	C63	C64	121.2(3)
F3	C13	F1	138.0(9)	C62	C63	C65	122.1(3)
F03{	C13	C10	112.7(5)	C65	C63	C64	116.7(3)
F03{	C13	F1	103.4(6)	N9	C64	C63	178.7(4)
F03{	C13	F3	57.2(10)	N10	C65	C63	178.9(4)
F04C	C13	C10	109.5(10)	C67	C66	C62	123.8(3)
F04C	C13	F14	107.7(16)	C66	C67	C68	126.9(3)
F14	C13	C10	109.2(9)	C69	C68	C67	122.1(3)
C15	C14	C3	123.3(3)	C69	C68	C73	118.2(3)
C19	C14	C3	118.6(3)	C73	C68	C67	119.6(3)
C19	C14	C15	118.1(3)	C68	C69	C70	121.9(3)
C16	C15	C14	121.6(3)	C69	C70	C71	118.6(3)
C15	C16	C17	120.1(3)	C69	C70	C74	121.5(3)



**Table S17. Bond Angles for HPQ4.**

Atom	Atom	Atom	Angle/°	Atom	Atom	Atom	Angle/°
O3	C17	C16	116.4(3)	C71	C70	C74	119.9(3)
O3	C17	C18	123.8(3)	O5	C71	C70	122.9(3)
C18	C17	C16	119.8(3)	O5	C71	C72	117.7(3)
C17	C18	C20	119.9(3)	C72	C71	C70	119.4(3)
C19	C18	C17	118.1(3)	C73	C72	C71	120.9(3)
C19	C18	C20	121.9(3)	C72	C73	C68	120.9(3)
C14	C19	C18	122.0(3)	N13	C74	C70	118.2(3)
N5	C20	C18	119.4(3)	N14	C74	N13	121.9(3)
N6	C20	N5	122.2(3)	N14	C74	C70	119.9(3)
N6	C20	C18	118.3(3)	O7	C75	N13	120.7(3)
O2	C21	N5	121.3(3)	O7	C75	C76	124.3(3)
O2	C21	C22	123.4(3)	N13	C75	C76	115.0(3)
N5	C21	C22	115.3(3)	C77	C76	C75	118.6(3)
C23	C22	C21	118.8(3)	C78	C76	C75	120.3(3)
C27	C22	C21	120.3(4)	C78	C76	C77	121.1(3)
C27	C22	C23	120.9(3)	N14	C77	C76	122.2(3)
N6	C23	C22	121.5(3)	N14	C77	C81	118.6(3)
N6	C23	C24	119.2(3)	C76	C77	C81	119.1(3)
C24	C23	C22	119.2(3)	C79	C78	C76	118.9(3)
C25	C24	C23	119.5(4)	C78	C79	Cl4	119.3(3)
C24	C25	C26	120.2(4)	C78	C79	C80	120.9(3)
C25	C26	Cl2	119.0(3)	C80	C79	Cl4	119.8(3)
C27	C26	Cl2	119.3(3)	C81	C80	C79	120.4(3)
C27	C26	C25	121.7(4)	C80	C81	C77	119.5(3)
C26	C27	C22	118.5(4)	C58	C59	C60	119.7(4)
F03{	F3	C13	60.7(11)	C58	C59	C62	118.9(4)
F3	F03{	C13	62.1(10)	C60	C59	C62	121.3(3)

**Table S18. Torsion Angles for HPQ4.**

A	B	C	D	Angle/°	A	B	C	D	Angle/°
Cl1	C28	C29	C30	177.9(3)	F1	C13	F3	F03{	-72.3(18)
Cl1	C28	C33	C32	-177.3(3)	F1	C13	F03{	F3	139.1(11)
N3	C35	C36	C37	6.5(5)	Cl3	C83	C84	C85	177.0(3)
N3	C35	C36	C41	-177.4(3)	O8	C91	C92	C93	177.8(3)
N4	C31	C32	C33	178.9(3)	N11	C86	C87	C82	177.2(3)
N4	C31	C32	C34	-0.1(5)	N11	C86	C87	C88	-2.8(5)
N4	C35	C36	C37	-172.7(3)	N11	C89	C90	C91	-7.1(5)
N4	C35	C36	C41	3.5(5)	N11	C89	C90	C95	172.2(3)
C28	C29	C30	C31	-0.6(6)	N12	C89	C90	C91	175.0(3)
C29	C28	C33	C32	2.3(6)	N12	C89	C90	C95	-5.7(5)
C29	C30	C31	N4	-178.3(3)	C82	C83	C84	C85	-1.2(5)
C29	C30	C31	C32	2.3(5)	C82	C87	C88	O6	0.1(6)
C30	C31	C32	C33	-1.7(5)	C82	C87	C88	N12	-179.6(3)

**Table S18. Torsion Angles for HPQ4.**

A	B	C	D	Angle/°	A	B	C	D	Angle/°
C30	C31	C32	C34	179.2(3)	C83	C82	C87	C86	1.1(5)
C31	N4	C35	N3	-1.6(5)	C83	C82	C87	C88	-178.9(3)
C31	N4	C35	C36	177.6(3)	C83	C84	C85	C86	1.0(5)
C31	C32	C33	C28	-0.6(5)	C84	C85	C86	N11	-178.3(3)
C31	C32	C34	O1	-177.5(3)	C84	C85	C86	C87	0.2(5)
C31	C32	C34	N3	2.6(5)	C85	C86	C87	C82	-1.2(5)
C33	C28	C29	C30	-1.7(6)	C85	C86	C87	C88	178.7(3)
C33	C32	C34	O1	3.5(6)	C86	N11	C89	N12	0.7(5)
C33	C32	C34	N3	-176.4(3)	C86	N11	C89	C90	-177.1(3)
C34	N3	C35	N4	4.6(5)	C86	C87	C88	O6	-179.8(3)
C34	N3	C35	C36	-174.6(3)	C86	C87	C88	N12	0.5(5)
C34	C32	C33	C28	178.5(3)	C87	C82	C83	Cl3	-178.0(3)
C35	N3	C34	O1	175.2(3)	C87	C82	C83	C84	0.2(5)
C35	N3	C34	C32	-4.9(5)	C88	N12	C89	N11	-3.3(5)
C35	N4	C31	C30	-179.9(3)	C88	N12	C89	C90	174.6(3)
C35	N4	C31	C32	-0.5(5)	C89	N11	C86	C85	-179.2(3)
C35	C36	C37	C38	178.0(3)	C89	N11	C86	C87	2.3(5)
C35	C36	C41	O4	0.9(5)	C89	N12	C88	O6	-177.2(3)
C35	C36	C41	C40	-178.8(3)	C89	N12	C88	C87	2.5(5)
C36	C37	C38	C39	0.4(5)	C89	C90	C91	O8	2.8(5)
C36	C37	C38	C42	-177.6(3)	C89	C90	C91	C92	-178.5(3)
C37	C36	C41	O4	177.1(3)	C89	C90	C95	C94	178.9(3)
C37	C36	C41	C40	-2.6(5)	C90	C91	C92	C93	-1.0(5)
C37	C38	C39	C40	-2.0(5)	C91	C90	C95	C94	-1.8(5)
C37	C38	C42	C43	5.3(6)	C91	C92	C93	C94	-0.6(6)
C38	C39	C40	C41	1.2(5)	C92	C93	C94	C95	1.0(5)
C38	C42	C43	C44	-178.4(3)	C92	C93	C94	C96	-177.4(3)
C39	C38	C42	C43	-172.7(4)	C93	C94	C95	C90	0.2(5)
C39	C40	C41	O4	-178.6(3)	C93	C94	C96	C97	177.9(4)
C39	C40	C41	C36	1.1(5)	C94	C96	C97	C98	-172.9(3)
C41	C36	C37	C38	1.8(5)	C95	C90	C91	O8	-176.6(3)
C42	C38	C39	C40	176.1(3)	C95	C90	C91	C92	2.1(5)
C42	C43	C44	C45	-175.9(4)	C95	C94	C96	C97	-0.4(6)
C42	C43	C44	C48	4.2(6)	C96	C94	C95	C90	178.6(3)
C43	C44	C45	C46	-170.6(4)	C96	C97	C98	C99	166.3(4)
C43	C44	C45	C47	9.7(6)	C96	C97	C98	C102	-14.5(6)
C43	C44	C48	C49	-125.2(4)	C97	C98	C99	C100	3.2(5)
C43	C44	C48	C53	55.2(5)	C97	C98	C99	C101	-175.1(3)
C44	C48	C49	C50	177.9(4)	C97	C98	C102	C103	-62.2(5)
C44	C48	C53	C52	-178.2(4)	C97	C98	C102	C107	121.9(4)
C45	C44	C48	C49	54.9(5)	C98	C102	C103	C104	-174.3(3)
C45	C44	C48	C53	-124.7(4)	C98	C102	C107	C106	174.7(3)
C48	C44	C45	C46	9.3(6)	C99	C98	C102	C103	117.1(4)
C48	C44	C45	C47	-170.4(4)	C99	C98	C102	C107	-58.9(5)
C48	C49	C50	C51	0.9(7)	C102	C98	C99	C100	-176.0(3)

**Table S18. Torsion Angles for HPQ4.**

A	B	C	D	Angle/°	A	B	C	D	Angle/°
C49	C48	C53	C52	2.2(6)	C102	C98	C99	C101	5.7(5)
C49	C50	C51	C52	0.8(7)	C102	C103	C104	C105	-0.8(6)
C49	C50	C51	C54	-175.1(5)	C103	C102	C107	C106	-1.2(5)
C50	C51	C52	C53	-1.0(7)	C103	C104	C105	C106	-0.7(6)
C50	C51	C54	F7	88.8(6)	C103	C104	C105	C108	178.9(4)
C50	C51	C54	F8	-157.1(5)	C104	C105	C106	C107	1.3(6)
C50	C51	C54	F9	-24.9(8)	C104	C105	C108	F10	48.8(5)
C51	C52	C53	C48	-0.5(7)	C104	C105	C108	F11	-72.2(5)
C52	C51	C54	F7	-87.1(6)	C104	C105	C108	F12	169.7(4)
C52	C51	C54	F8	27.0(8)	C105	C106	C107	C102	-0.3(6)
C52	C51	C54	F9	159.2(5)	C106	C105	C108	F10	-131.5(4)
C53	C48	C49	C50	-2.4(6)	C106	C105	C108	F11	107.5(5)
C54	C51	C52	C53	174.9(5)	C106	C105	C108	F12	-10.6(5)
C12	C26	C27	C22	-179.2(3)	C107	C102	C103	C104	1.8(6)
O2	C21	C22	C23	-175.8(4)	C108	C105	C106	C107	-178.4(3)
O2	C21	C22	C27	2.7(6)	C14	C79	C80	C81	179.6(3)
O3	C17	C18	C19	176.0(3)	O5	C71	C72	C73	178.0(4)
O3	C17	C18	C20	-6.2(5)	O7	C75	C76	C77	179.6(3)
N5	C21	C22	C23	4.2(5)	O7	C75	C76	C78	0.7(6)
N5	C21	C22	C27	-177.3(3)	N13	C75	C76	C77	-1.4(5)
N6	C23	C24	C25	-178.5(4)	N13	C75	C76	C78	179.7(3)
C1	C2	C3	C14	-179.0(4)	N14	C77	C81	C80	-179.6(3)
C1	C7	C8	C9	178.8(4)	C55	C56	C57	C58	-179.7(6)
C1	C7	C12	C11	-179.9(4)	C55	C56	C61	C60	179.3(6)
C2	C1	C4	C5	-1.0(7)	C56	C57	C58	C59	0.2(9)
C2	C1	C4	C6	179.5(4)	C57	C56	C61	C60	-0.3(8)
C2	C1	C7	C8	60.5(5)	C57	C58	C59	C60	0.2(8)
C2	C1	C7	C12	-119.6(4)	C57	C58	C59	C62	-179.5(5)
C2	C3	C14	C15	4.9(6)	C61	C56	C57	C58	-0.1(9)
C2	C3	C14	C19	-175.6(4)	C61	C60	C59	C58	-0.6(7)
C3	C14	C15	C16	176.9(3)	C61	C60	C59	C62	179.1(4)
C3	C14	C19	C18	-177.7(3)	C62	C66	C67	C68	179.6(4)
C4	C1	C2	C3	-167.7(4)	C63	C62	C66	C67	179.6(4)
C4	C1	C7	C8	-117.9(4)	C63	C62	C59	C58	70.8(6)
C4	C1	C7	C12	62.0(5)	C63	C62	C59	C60	-108.9(4)
C7	C1	C2	C3	14.0(6)	C66	C62	C63	C64	-178.6(3)
C7	C1	C4	C5	177.4(5)	C66	C62	C63	C65	0.3(6)
C7	C1	C4	C6	-2.2(6)	C66	C62	C59	C58	-109.8(5)
C7	C8	C9	C10	1.8(7)	C66	C62	C59	C60	70.5(5)
C8	C7	C12	C11	0.0(6)	C66	C67	C68	C69	-5.5(7)
C8	C9	C10	C11	-1.4(7)	C66	C67	C68	C73	175.3(4)
C8	C9	C10	C13	177.5(5)	C67	C68	C69	C70	-179.6(4)
C9	C10	C11	C12	0.3(7)	C67	C68	C73	C72	-179.0(4)
C9	C10	C13	F2	134.8(8)	C68	C69	C70	C71	-1.9(6)
C9	C10	C13	F1	12.7(9)	C68	C69	C70	C74	-179.9(3)

**Table S18. Torsion Angles for HPQ4.**

A	B	C	D	Angle/°	A	B	C	D	Angle/°
C9	C10	C13	F3	-165.5(13)	C69	C68	C73	C72	1.8(6)
C9	C10	C13	F03{	-104.0(7)	C69	C70	C71	O5	-176.6(3)
C9	C10	C13	F04C	73.9(15)	C69	C70	C71	C72	2.7(5)
C9	C10	C13	F14	-43.8(16)	C69	C70	C74	N13	-11.2(5)
C10	C11	C12	C7	0.4(6)	C69	C70	C74	N14	168.5(3)
C10	C13	F3	F03{	105.3(7)	C70	C71	C72	C73	-1.3(6)
C10	C13	F03{	F3	-98.7(11)	C71	C70	C74	N13	170.8(3)
C11	C10	C13	F2	-46.3(10)	C71	C70	C74	N14	-9.5(5)
C11	C10	C13	F1	-168.4(7)	C71	C72	C73	C68	-1.0(6)
C11	C10	C13	F3	13.4(14)	C73	C68	C69	C70	-0.4(6)
C11	C10	C13	F03{	74.9(8)	C74	N13	C75	O7	-178.0(3)
C11	C10	C13	F04C	-107.2(14)	C74	N13	C75	C76	3.0(5)
C11	C10	C13	F14	135.1(15)	C74	N14	C77	C76	0.0(5)
C12	C7	C8	C9	-1.1(6)	C74	N14	C77	C81	179.4(3)
C13	C10	C11	C12	-178.6(4)	C74	C70	C71	O5	1.4(5)
C14	C15	C16	C17	-0.5(5)	C74	C70	C71	C72	-179.3(3)
C15	C14	C19	C18	1.9(5)	C75	N13	C74	N14	-3.3(5)
C15	C16	C17	O3	-176.5(3)	C75	N13	C74	C70	176.4(3)
C15	C16	C17	C18	4.5(5)	C75	C76	C77	N14	0.0(5)
C16	C17	C18	C19	-5.1(5)	C75	C76	C77	C81	-179.4(3)
C16	C17	C18	C20	172.7(3)	C75	C76	C78	C79	179.8(3)
C17	C18	C19	C14	1.9(5)	C76	C77	C81	C80	-0.2(5)
C17	C18	C20	N5	-169.0(3)	C76	C78	C79	C14	179.7(3)
C17	C18	C20	N6	7.7(5)	C76	C78	C79	C80	-0.6(6)
C19	C14	C15	C16	-2.6(5)	C77	N14	C74	N13	1.6(5)
C19	C18	C20	N5	8.8(5)	C77	N14	C74	C70	-178.1(3)
C19	C18	C20	N6	-174.5(3)	C77	C76	C78	C79	0.8(5)
C20	N5	C21	O2	177.5(4)	C78	C76	C77	N14	178.9(3)
C20	N5	C21	C22	-2.5(5)	C78	C76	C77	C81	-0.5(5)
C20	N6	C23	C22	0.6(5)	C78	C79	C80	C81	-0.1(6)
C20	N6	C23	C24	-179.8(4)	C79	C80	C81	C77	0.5(5)
C20	C18	C19	C14	-175.9(3)	F13	C55	C56	C57	-70.7(12)
C21	N5	C20	N6	-0.4(6)	F13	C55	C56	C61	109.7(10)
C21	N5	C20	C18	176.2(3)	F15	C55	C56	C57	46.7(9)
C21	C22	C23	N6	-3.5(5)	F15	C55	C56	C61	-133.0(8)
C21	C22	C23	C24	177.0(4)	F16	C55	C56	C57	174.1(9)
C21	C22	C27	C26	-177.6(4)	F16	C55	C56	C61	-5.5(12)
C22	C23	C24	C25	1.1(6)	C59	C60	C61	C56	0.7(7)
C23	N6	C20	N5	1.4(5)	C59	C62	C63	C64	0.8(6)
C23	N6	C20	C18	-175.2(3)	C59	C62	C63	C65	179.7(3)
C23	C22	C27	C26	0.8(6)	C59	C62	C66	C67	0.2(6)
C23	C24	C25	C26	-0.1(7)	F4	C55	C56	C57	-128.6(10)
C24	C25	C26	C12	178.8(4)	F4	C55	C56	C61	51.7(11)
C24	C25	C26	C27	-0.7(7)	F5	C55	C56	C57	-6.7(16)
C25	C26	C27	C22	0.3(6)	F5	C55	C56	C61	173.6(13)

**Table S18. Torsion Angles for HPQ4.**

A	B	C	D	Angle/°	A	B	C	D	Angle/°
C27	C22	C23	N6	178.1(4)	F6	C55	C56	C57	118.4(11)
C27	C22	C23	C24	-1.5(6)	F6	C55	C56	C61	-61.2(13)

**Table S19. Hydrogen Atom Coordinates ( $\text{\AA}\times 10^4$ ) and Isotropic Displacement Parameters ( $\text{\AA}^2\times 10^3$ ) for HPQ4.**

Atom	x	y	z	U(eq)
H4	6390.78	-1230.6	10692.38	45
H3B	6567.28	-72.99	8468.16	31
H29	6490.3	-3507.43	10189.37	41
H30	6366.21	-2641.62	10576.26	39
H33	6598.08	-2109.99	8234.78	35
H37	6245.16	662.37	8786.57	31
H39	6059.16	1225.86	10352.49	37
H40	6169.17	99.42	11102.32	34
H42	5961.62	2110.47	9218.06	35
H43	5845.19	1714.21	8183.88	38
H49	4417.55	3725.19	7968.55	42
H50	4481.49	4561.37	8377.41	51
H52	7298.99	3908.86	8799.24	53
H53	7239.28	3068.91	8400.14	46
H3	7017.61	1657.52	4799.42	52
H5	6636.51	256.8	6994.13	35
H2	5371.55	-1635.07	5638.51	41
H3A	5258.6	-1350.15	6779.37	36
H8	3193.89	-1751.77	7037.8	49
H9	2365.75	-1910.35	8147.16	54
H11	4366.83	-3402.94	8932.66	51
H12	5161.7	-3265.48	7820.22	47
H15	5951	-585	4919.05	36
H16	6586.66	509.85	4234.18	37
H19	5983.32	-303.35	6628.32	34
H24	7706.05	2886.12	5047.62	48
H25	8355.27	3535.18	5504.83	48
H27	7991.93	1933.66	7374.43	41
H8A	11355.73	11118.08	-490.9	43
H12A	10599.65	10409.85	1751.63	33
H82	10526.47	8181.73	1995.86	35
H84	11319.79	8406.83	13.1	35
H85	11399.25	9591.26	-374.59	32
H92	11337.8	12782.44	-872.32	33
H93	10857.65	13262.23	-86.72	33
H95	10343.63	11380.02	1463.36	31
H96	10208.32	13167.72	1084.38	32

**Table S19. Hydrogen Atom Coordinates ( $\text{\AA}\times 10^4$ ) and Isotropic Displacement Parameters ( $\text{\AA}^2\times 10^3$ ) for HPQ4.**

Atom	x	y	z	U(eq)
H97	9897.76	11872.06	2147.48	33
H103	11095.12	13453.43	1989.51	41
H104	11282.12	14613.91	1725.88	45
H106	8172.62	14816.51	2009.91	41
H107	7978.14	13653.17	2290.93	36
H5A	10722.06	8795.99	5296.96	47
H13	10400.3	9520.67	3157.82	32
H57	8224.94	5350.37	3196	79
H58	8691.17	6510.75	2676.28	68
H60	6448.08	6854.07	4057.05	47
H61	5965.93	5696.74	4569.92	57
H66	8623.65	8295.72	3088.57	37
H67	8455.71	7004.61	4166.4	40
H69	9524.24	8681.96	3589.55	36
H72	9782.21	7223.03	5841.32	40
H73	9014.75	6835.9	5212.33	42
H78	11649.58	11632.88	2712.29	36
H80	12092.82	11389.16	4578.24	36
H81	11469.3	10267.33	5069.56	32

**Table S20. Atomic Occupancy for HPQ4.**

Atom	Occupancy	Atom	Occupancy	Atom	Occupancy
F2	0.823(7)	F1	0.823(7)	F3	0.177(7)
F03{	0.823(7)	F04C	0.177(7)	F14	0.177(7)
F13	0.534(7)	F15	0.534(7)	F16	0.534(7)
F4	0.466(7)	F5	0.466(7)	F6	0.466(7)

**Table S21. Solvent masks information for HPQ4.**

Number	X	Y	Z	Volume	Electron count	Content
1	0.000	0.500	0.500	453.3	130.6	
2	0.000	0.500	0.000	225.0	52.1	
3	0.318	0.015	0.717	204.8	62.0	
4	0.682	0.985	0.283	204.8	62.0	

## SI References

1. S. Terzyan *et al.*, Human  $\gamma$ -glutamyl transpeptidase 1: structures of the free enzyme, inhibitor-bound tetrahedral transition states, and glutamate-bound enzyme reveal novel movement within the active site during catalysis. *J. Bio. Chem.* **290**,17576-17586 (2015).
2. E. Bobyr *et al.*, High-Resolution Analysis of  $Zn^{2+}$  Coordination in the Alkaline Phosphatase Superfamily by EXAFS and X-ray Crystallography. *J. Mol. Biol.* **415**, 102-117 (2012).
3. H. Liu, F. Liu, F. Wang, R. Q. Yu, J. H. Jiang, A novel mitochondrial-targeting near-infrared fluorescent probe for imaging  $\gamma$ -glutamyl transpeptidase activity in living cells. *Analyst* **143**, 5530-5535 (2018).
4. L. Zhou *et al.*, A high-resolution mitochondria-targeting ratiometric fluorescent probe for detection of the endogenous hypochlorous acid. *Spectrochimica Acta Part A* **166**, 129-134 (2016).
5. P. Gopalan *et al.*, Star-shaped azo-based dipolar chromophores: design, synthesis, matrix compatibility, and electro-optic activity. *J. Am. Chem. Soc.* **126**, 1741-1747 (2004).
6. J. Wang *et al.*, Two-photon near infrared fluorescent turn-on probe toward cysteine and its imaging applications. *ACS Sens.* **1**, 882-887 (2016).
7. K. Li *et al.*, *In situ* imaging of furin activity with a highly stable probe by releasing of precipitating fluorochrome. *Anal. chem.* **90**, 11680-11687 (2018).
8. M. Prost, L. Canaple, J. Samarut, J. Hasserodt, Tagging live cells that express specific peptidase activity with solid-state fluorescence. *Chembiochem* **15**, 1413-1417 (2014).
9. H. W. Liu *et al.*, *In situ* localization of enzyme activity in live cells by a molecular probe releasing a precipitating fluorochrome. *Angew. Chem. Int. Ed.* **56**, 11788-11792 (2017).
10. P. Zhang *et al.*, A two-photon fluorescent sensor revealing drug-induced liver injury via tracking gamma-glutamyltranspeptidase (GGT) level in vivo. *Biomaterials* **80**, 46-56 (2016).
11. L. Li, W. Shi, Z. Wang, Q. Gong, H. Ma, Sensitive fluorescence probe with long analytical wavelengths for gamma-glutamyl transpeptidase detection in human serum and living cells. *Anal. Chem.* **87**, 8353-8359 (2015).
12. P. Wang *et al.*, An efficient two-photon fluorescent probe for measuring gamma-glutamyltranspeptidase activity during the oxidative stress process in tumor cells and tissues. *Analyst* **142**, 1813-1820 (2017).